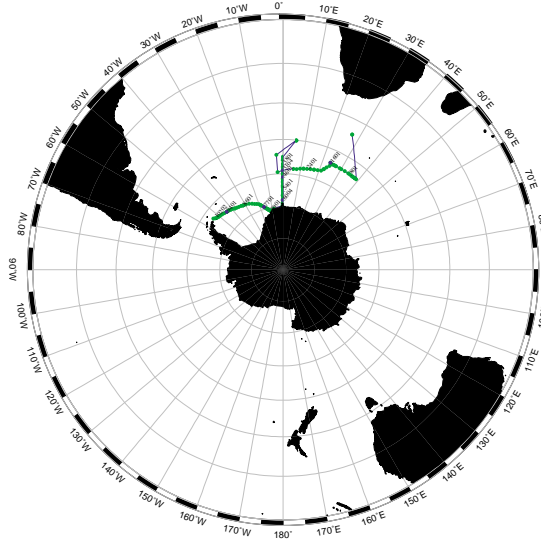


CRUISE NARRATIVE (S04A, SR04)

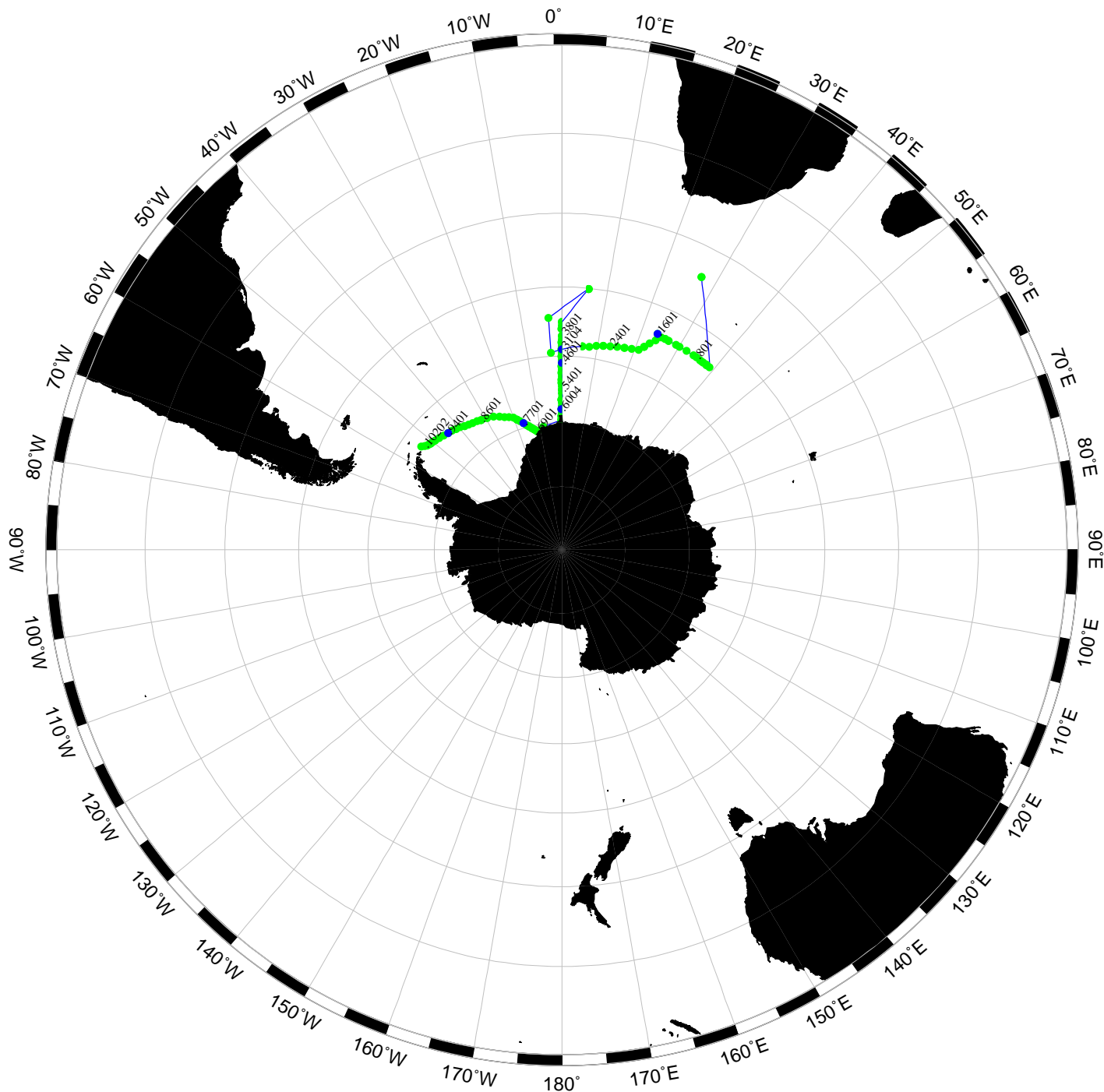


Highlights

WHP Cruise Summary Information

WOCE section designation	S04A, SR04	
Expedition designation (ExpoCode)	06AQANTXIII_4	
Chief Scientist and affiliation	Eberhard Fahrbach/AWI	
	Stiftung Alfred-Wegener-Institut für Polar und Meeresforschung	
	Fachbereich Klimasystem	
	Postfach 120161, D-27515 Bremerhaven, GER.	
	Phone: (+49) (0)471 4831-1820	
	FAX: (+49) (0)471 4831-1797	
	email: efahrbach@awi-bremerhaven.de	
	Office: Bussestr. 24	
	http://www.awi-bremerhaven.de	
Dates	1996.MAR.17 - 1996.MAY.20	
Ship	RV Polarstern	
Ports of call	Cape Town, S Africa to Punta Arenas, Chile to Bremerhaven, Germany	
Number of stations	104	
Stations' Geographic boundaries	44° 0.35' S 53° 37.44' W	38° 59.81' E 71° 1.30' S
Floats and drifters deployed	0	
Moorings deployed or recovered	3 recovered; 14 deployed	

Station locations for S04A & SR04: Polarstern, 1996



Contributing Authors:

Matthias Alpers/IAPR	Andreas Hansjosten/AWI	Erika Mutschke/UMAG
MarcoAntonio/UACH	Josef Hbffner/IAPR	Jochen Nowaczyk/AWI
Wolf Arntz/AWI	Elisabeth Helmke/AWI	Martin Rauschert/AWIP
Karl Bakker/NIOZ	Miriam de las Heras/AWI	Carlos Rios/UMAG
Anke Bittkau/AWI	Josepf Höffner/IAPR	Gerd Rohardt/AWI
Harald Bohlmann/AWI	Mario Hoppema/AWI	Harald Rohr/AWI
Klaus Bulsiewicz/IUPB	Mario Hopperna/AWI	Malte Runge/IUPB
Alexander Buschmann/AWI	Uta Horstmann/AWI	Björn Schlenker/IUPB
Lardies Carrasco/UACH	Markus Jochum/AWI	Michael Schröder/AWI
Nicola Jane Debenham/NHM	Ulla Klauke/AWI	Hiltrud Sieverding/IUPB
Corinna Dubischar/AWI	Edmund Knuth/DWD	Vassili Spiridonov/ZMMU
Erich Dunker/AWI	Herbert Köhler/DWD	Michel Stoll/NIOZ
Joachim England/DWD	Leif Kolb/AWI	Birgit Strohscher/AWI
Veit Eska/IAPR	Peter Albert Lamont/SAMS	Giok Nio Tan/AWI
Eberhard Fahrbach/AWI	Katrin Linse/IPO	Tanja Winterrath/AWI
Timothy John Ferrero/NHM	Pedro Martinez-Arbizu/FBZO	Andreas Wisotzki/AWI
Gerhard Fraas/IUPB	Ralf Meyer/AWI	Hannelore Witte/AWI
Kai Horst George/FBZO	Anneke MOhlebach/AWI	Rebecca Woodgate/AWI
Dieter Gerdes/AWI	Hans-Joachim Möller/DWD	Ulf von Zahn/IAPR
Janja Gorny/AWI	Americo Montiel/UMAG	Andreas Zimmermann/AWI
Matthias Gorny/AWI	Gisela Silveira Moura/FBZO	

1.1 Summary and Itinerary

The Polarstern-cruise ANT XIII/4 started on March 17th, 1996 in Cape Town. The first part of the cruise consisted of multidisciplinary work with a focus on physical oceanography in the Weddell Sea, during the second part logistic tasks were carried out at King George Island and a benthological programme was performed in the Drake Passage. During the whole cruise, temperature measurements were made with a newly developed potassium temperature lidar, which was designed to measure the natural variations in temperature of the mesopause at different geographical locations and in different seasons. The high temporal and vertical resolution of the lidar together with the simultaneous observations of the potassium layer allowed better insight into dynamic processes in the upper atmosphere.

A major part of the deep and bottom waters of the global ocean are ventilated by the injection of waters from the Weddell Sea. Cooling in winter and sea ice formation, as well as the interaction between the ocean and the ice shelves, induce water mass modifications which generate water masses on the shelf which are dense enough to sink to the bottom of the Weddell basin. During their descent, they mix with ambient water masses and are carried with the cyclonic Weddell gyre circulation to the north. The formation of bottom and deep water determines the exchange of atmospheric carbon dioxide (CO₂) between the ocean and the atmosphere. Through the upwelling of CO₂-rich deep-water, CO₂ can be given up to the atmosphere, a process which counteracts the CO₂ flux due to cooling and biological processes at the surface. Thus the components of

the CO₂ system were measured to determine whether the Weddell Sea is a source or a sink for atmospheric CO₂. The physical oceanography measurements of the cruise contribute to the World Ocean Circulation Experiment, (WOCE). The hydrographical sections are referred in the WOCE code as the repeat sections SR2 and SR4 and the Atlantic part of the S4-section. In order to better understand the processes and effects which are important in this area, the programme consisted of four components.

1. To determine the inflow from the Antarctic Circumpolar Current into the eastern Weddell Sea, a hydrographical section was worked from 24°41'E to 39°E, using a CTD-probe (Conductivity-Temperature with Depth) in connection with water samplers and an ADCP (Acoustic Doppler Current Profiler).
2. The outflow of the bottom water from the east into the western Weddell Sea was measured by a zonal hydrographical section along the eastward current in the north of the Weddell gyre from 0° to 24°41 E.
3. The exchange between the eastern and western Weddell Sea was measured on a meridional hydrographical section through the Weddell gyre along the Greenwich Meridian. Here, in addition to the use of the CTD-sensor, water samplers and ADCP, moorings were also recovered and deployed.
4. To determine the inflow into the southern Weddell Sea from the east and the outflow in the north-west, a hydrographical section was performed through the southern Weddell Sea and moorings were deployed near Joinville Island.

Among other uses, these measurements will be used to validate models which simulate the circulation and water mass formation in the Weddell Sea. The isotopes of oxygen, including ¹⁸O, nutrients and the tracers Freon-11, Freon-12, Freon-113 and CCl₄, as well as Tritium, ³He, He and Ne give information about the water mass formation and spreading. Samples of the stable carbon isotope ¹³C were taken for paleo-oceanographic studies.

The marine organic chemistry group concentrated on the autumn distribution of dissolved and particulate phytosterols in the Weddell Sea to understand the fate of phytosterols and other trace organic compounds in the ocean starting with biosynthesis and input into the euphotic zone and ending with the possible final deposition into the bottom sediments of the deep sea.

Planktological studies focused on the distribution of some dominant zooplankton and micronekton species such as *Calanoides acutus* and *Rhincalanus gigas* (the two dominant Copepodes of the Antarctic), which show a clear dependence on the oceanographic structure of the Weddell gyre. These species very probably do not reproduce in the western Weddell Sea. Thus the population is maintained by the advection of individuals who have over-wintered in the Warm Deep Water and by local recruitment in the eastern Weddell gyre. The presence of Antarctic krill, *Euphausia superba*, in the eastern Weddell gyre seems to play an important role in the maintaining of the krill population in the Atlantic sector of the southern polar seas. Krill can be brought into the Weddell Sea by the

advection of krill- larvae with the inflow of Warm Deep Water, although adult krill are usually found at shallower depths. On this cruise, the formation of the over-wintering population of the larger calanoid Copepods and the abundance of the krill-larvae in the Warm Deep Water was measured using the Acoustic Doppler Current Profiler (ADCP) and an Optical Plankton Counter (OPC) in combination with conventional net sampling. The Chlorophyll-concentration at different depths along all the sections was measured and combined qualitatively with the phytoplankton determined from the water samples. Investigations of the Antarctic zooplankton ecology focused on the completion of the reproductive periods of various species which shows a strong geographical variation. The transition of several dominant zooplankton species to over-wintering was studied in different areas of the Weddell Sea. Using the Multinet catches, the vertical distribution of the different stages of development of the Copepodes was determined.

The second part of the cruise concentrated on the investigation of the ecological relationship between the marine fauna of the Antarctic Peninsular and the southern-most part of South America. South America is the closest present- day land mass to Antarctica. Thus it is assumed that the exchange between South America and Antarctica has been longer and more intense than with the other continents. Due to bad weather, the benthological group were unable to fly to King George Island. Also the collection of material from the Dallmann laboratory, which is connected to the Argentinean Jubany-Station, could only be completed to a limited extent. The unfavourable weather conditions meant the activities planned for King George Island were cancelled and the work concentrated instead on the continental slope south of Terra del Fuego. During the "Joint Magellan VICTOR HENSEN Campaign 1994", a large number of samples were collected in shallow and deep water in the Magellan Straits (to a depth of 650 m), in the northwestern part of the Beagle Canal and from the eastern exit of the Beagle Canal to Cape Horn. On this cruise, along a section on the northern continental slope of Drake Passage, at different depths samples were taken with the Multicorer, the Multibox Corer, the Dredge and the underwater-camera to study the macro and meiozoobenthic structure, and to complete the available benthic samples with material obtained from greater depths. In addition, samples were taken for physiological, biological reproduction and population dynamic experiments. Finally, observations were made of behaviour patterns and material was gathered for genetic work. It appeared that the transition to the Antarctic is rather of a gradual nature than abrupt. Despite this fact, considerable differences remain between the Antarctic and this southernmost part of the Magellan region. This indicates that 20 million years of separation and isolation, despite some glacial periods of 'increased interchange, have led to rather distinct separation of two neighbouring marine ecosystems which originally had an identical fauna. Supporting hydrographic data was acquired with the CTD. The cruise ended in Punta Arenas on May 20th, 1996. The cruise track is displayed in [Figure 1](#).

2. Scientific programmes

2.1 Investigations of the atmosphere

2.1.1 Weather Conditions

(Hans-Joachim Möller, Herbert Köhler/DWD)

The passage from Cape Town to 54°S 39°E was dominated by a subtropical high with moderate winds but many clouds. South of 50°S, the first frontal troughs were crossed. The following westward passage was characterized by the alternation of deep lows and small wedges of high pressure. Westerly winds between 25 and 35 knots were most frequent. While passing through gale centres and frontal troughs the wind increased up to Force 9 for a short time, but also decreased to Force 4 when passing through the wedges. The passage to the northeast to the mooring position in the oceanic Polar Front was favoured by a meridional trough, followed by a strong wedge of high pressure.

On the way to the meridional hydrographic section on the Greenwich Meridian the strong westerly wind regime prevailed. The following passage south was dominated by a large polar low, filled with cold air. For many days, showers with snow and soft hail occurred. At the beginning of the second part of April, a cold air flow in the middle troposphere formed a meridional trough, which reached far north to the coast of Uruguay. This trough moved south-eastward, carrying cold antarctic air in its back, The corresponding surface low deepened rapidly to a gale with its centre between Bouvet Island and the Antarctic coast. The minimum pressure at the centre was less than 950 hPa, with RV "Polarstern" situated south of the it. For 36 hours, northeasterly to easterly winds of about 35 knots were observed with a heavy swell.

The first pancake ice was encountered at 69°09'S on April 21th about 30 nm north of the ice shelf edge. Before this time, only isolated icebergs had been passed, but now many bergs and growlers, frosted in the pack ice were observed. The wedge of a high pressure system, situated at the western Weddell Sea, extended more and more to the east. On April 24th, when we reached the Atka Bight, the finest calmy and sunny weather was experienced. For the next days, this high pressure zone influenced the Weddell Sea. At the end of April, a gale centre was formed in the Scotia Sea and consequently the southeasterly winds increased to gale force for a short time. The rising pressure, resulting from the following wedge, calmed the weather down rapidly.

Further lows were encountered during the passage through the ice of the southern Weddell Sea. A southeasterly to southwesterly airflow was at their back, whilst northeasterly to northwesterly winds dominated at their front. The situation during May 4th/5th can serve as an example: Over the western Weddell Sea, a trough was generated. Warm air was advected southward at its front with northwesterly winds Force 6. The air temperature rose continuously, from -170 C in the morning until it reached its maximum of +1°C at 23.00 UTC. The warm air flow brought a high humidity, low stratus clouds and poor visibility. The passage of the trough at 00.00 UTC was accompanied by a decreasing westerly wind, but not by a change in temperature. The strongly backing, southwest wind

caused a powerful cold air advection. The temperature dropped to -7°C in one hour, and after 12.00 UTC of May 5th to below -21°C , in spite of continual sunshine.

In the northern part of the Weddell Sea, mostly young ice up to 30 cm thick was observed. West of 50OW however, large first-year or multiyear ice floes with thickness between 3 and 5 m reduced the ship's speed considerably. The ice edge had been shifted far west-northwest by continuous southeasterly winds with a speed up to Force 8. Wind and tides exerted a strong pressure on the ice, restricting seriously the progress of the cruise. The ice edge was reached on May 11th at 18 UTC near $62.2^{\circ}\text{ S } 57^{\circ}\text{W}$. At this position in Bransfield Strait a chain of icebergs lined up the ice edge like a barrier.

The crossing of the Drake Passage was favoured by a zone of high pressure, which extended from Argentina via the Magellan region and the Drake Passage to the southern part of the Antarctic Peninsula. The high pressure system moved east only very slowly and dominated by weak winds until the middle of May. Then, a more cyclonic westerly situation developed, but strong westerly winds were not encountered until the very end of the cruise, because the pressure difference between the subtropical high and the polar trough was rather weak.

Westerly to northwesterly winds accounted for more than 40% of the hourly observations of ANT XIII/4. Wind forces 5, 6 and 7 were each recorded 20% of the time. Gales occurred only 7% of the time, although the climatological value is nearly 20%. The frequency distributions of wind speed and direction is displayed in [Figure 2](#).

2.1.2 Temperature observations in the mesopause

(Josepf Höffner, Veit Eska/IAPR)

Objectives

The major task of the IAPR-group was to test the new potassium temperature lidar of the Institute of Atmospheric Research at the Rostock university and to make first measurements. Routine observations were planned to take place on ANT XIII/5 when better weather conditions were expected. Therefore we planned to build up a stable configuration for our untested lidar system.

The main part of our temperature lidar is a new high energy, narrow band, tuneable and pulsed alexandrite laser. The laser pulses are used for resonance scattering from free potassium atoms in the mesopause region. The backscattered photons are collected by a telescope and recorded by a photomultiplier. The scattering altitude is calculated from the time-of-flight of the light. It is possible to measure the Doppler broadening of the K(D1) fine structure by continuous spectral tuning of the alexandrite laser. This method allows an absolute air temperature determination in the scattering volume. Vertical wind velocities within the potassium layer are measured by Doppler shifted frequencies of the fine structure. A combination of Rayleigh backscattering and resonance scattering allows temperature measurements in the mesosphere and stratosphere down to 30 km.

Potassium acts as a tracer for our temperature measurements. Up till now, potassium measurements have been made with only three lidar systems. All took place in the northern hemisphere. Our measurements of the potassium layer are the first with a potassium temperature lidar in the southern hemisphere. The southernmost other temperature measurements in the mesopause at an altitude of 80 to 110 km, we are aware of, occurred at 31°S in Australia. Our first measurements indicated, that enough potassium is present in the southern atmosphere for temperature measurements from somewhat less than 80 km up to 110 km height. This altitude range is the coldest in the whole atmosphere and thus very interesting. With our lidar system, we are able to continuously measure these temperatures. This is only possible with a ground/ship based lidar system.

Preliminary results

Observations of the potassium layer have been performed for 16 nights during the entire cruise. Eleven nights were suitable for temperature measurements in the mesopause. Temperature measurements require nearly 30 minutes, whereas the potassium density can be determined in a few minutes. Several nights allowed us measurements of up to 12 hours and it was possible to observe changes in the temperatures on one night. These observations are the longest made with this lidar system.

The measured structure of the potassium layer is very similar to the that observed on the Isle Ruegen in spring 1995. It is a broad layer and extends from 78 km up to 120 km height. The density maximum is nearly 20 atoms/cm³. At a height of 120 km the potassium density is only 0.01 atoms/cm³. The column density is nearly 20 Mio. atoms/cm². We have not observed significant monthly differences in column density of potassium in April and May. On one of the first measured nights, we observed a peak in the potassium layer density. This could be a sporadic potassium layer, seen as a sudden rise in density. The extent of this layer is very small. The measurements were too short to observe this previously unknown phenomenon because of cloudy weather this night.

A measured backscattered profile collected during the night from May 2th to 3th is shown in [Figure 3](#) (left) and a temperature profile up to 106 km height in the same night in [Figure 3](#) (right). The mesopause temperature was distinctly higher than that of the reference atmosphere CIRA '89. Measurements on the other nights showed similar results. A second local minimum lies in 83 km height. The backscattered signal ([Figure 3](#), right) shows a Rayleigh backscattering within the potassium layer, which helps to determine temperatures down to 35 km in the stratosphere.

The dynamic variability of the potassium layer during one night is displayed in [Figure 4](#). The lower boundary of the layer moves up and down more than once during the night. The reason is probably wave activity. The shape and location of the layer change continuously. The density maximum of the layer is higher at the end of the night than at the beginning. Similar tendencies also exist on the other measured nights. For more detailed analysis, we must improve and expand our software.

2.2 Physical Oceanography

2.2.1 Deep and Bottom Water Formation in the Weddell Sea

(Eberhard Fahrback, Janja Gorny, Andreas Hansjosten, Miriam de las Heras, Uta Horstmann, Markus Jochum, Leif Kolb, Ralf Meyer, Gerd Rohardt, Harald Rohr, Michael Schröder, Giok Nio Tan, Tanja Winterrath, Andreas Wisotzki, Hannelore Witte, Rebecca Woodgate/AWI).

Objectives

A major part of the deep and bottom waters of the global ocean are ventilated by an injection of waters from the Weddell Sea. Cooling in winter and sea ice formation, as well as the interaction between the ocean and the ice shelves, induce water mass modifications which form water masses on the shelf which are dense enough to sink to the bottom of the Weddell basin. During their descent, they mix with ambient water masses and are carried with the cyclonic Weddell gyre circulation to the north where they partly leave the Weddell Sea towards the Antarctic Circumpolar Current and partly recirculate, steered by topographic features.

The increase in density due to cooling in the Weddell Sea counteracts the decrease in salinity due to precipitation and melting of ice shelf or icebergs. This increase in freshwater can similarly be compensated by the inflow of salty, deep water from the Antarctic Circumpolar Current, a process which takes place predominantly in the eastern Weddell gyre. This water mass is observed as Warm Deep Water. During its path through the cyclonic gyre, it constantly loses heat and salt. The warm regime is typified by the relatively warm conditions in the southeast of the gyre, which are determined by the close proximity of the inflow in the eastern Weddell Sea. The cold regime in the northeast is created by the cooling of the Warm Deep Water in the course of its circulation through the gyre. The inflow is subject to intense fluctuations which are partly generated by the interaction of the flow with the bottom topography. The kinematics and dynamics of the fluctuations will be investigated to understand the variations of the inflow. In the Weddell Sea, these fluctuations are of importance because of their effect on the vertical stability and consequently vertical mixing in the open ocean. This can affect the sea ice cover to the extent of the generation of open ocean polynyas and the possibility of the formation of deep water.

To quantify these processes, measurements were carried out of the water mass characteristics and transport of the inflow in the eastern Weddell Sea, the exchanges between the eastern and the western Weddell gyre and the outflow into the Weddell-Scotia Confluence. The geostrophic transport determination will be optimized by quasi-synoptic measurements at various locations. The ageostrophic parts of the current field will be assessed by direct current measurements. To estimate the relevance of the results obtained, long-term measurements of the inflow, the mixing depth and the characteristics of the deep water were initiated. Because of the impact of the sea ice formation on the water mass modification, it is planned to measure the variations of the meridional profile of the sea ice thickness and concentration with moored instruments to identify possible interactions between sea ice and mixing variability. The measurements on the section will

be repeated in part several times, to ascertain the longer time scale variations in the properties and distribution of the water masses.

The measurements will be used to validate models of the Weddell gyre circulation and the water mass formation. For this purpose, long time series of oceanic currents and water mass characteristics, as well as of the atmospheric forcing and the sea ice cover, are required to investigate the response of the system to variations of the forcing conditions. The measurements of the physical oceanography programme are a contribution to the World Ocean Circulation Experiment (WOCE). The hydrographic sections represent a contribution to the WOCE-section S4 and the repeatsections SR4 and SR2. The moorings in the western Weddell Sea are part of the international DOVETAIL (Deep Ocean VEntilation Through Antarctic Intermediate Layers) Project, which is part of the iAnzone Programme. Through these international projects, instruments are also provided from the Universitat Politecnica de Catalunya in Barcelona, Spain.

Work at sea

The programme consists of measurements from ship, using the CTD-probe (Conductivity and Temperature with Depth) connected to a water sampler, XBTs (eXpendable Bathythermographs) and both ship-borne and lowered ADCP (Acoustic Doppler Current Profiler). In addition, 3 moorings were recovered and 14 moorings deployed. The investigation is split into four geographical regions.

1. To determine the inflow from the Antarctic Circumpolar Current into the eastern Weddell Sea, a hydrographical section, consisting of 14 CTD and water sample casts, was performed from 39°E to 24°41'E (Figures 5 and 6).
2. To determine the intensity of eddy activity in the transition region between the Antarctic Circumpolar Current and the Weddell gyre, time series are collected over many years. To this aim, moorings were recovered and re-deployed (see Figure 5, Table 1 and 2) and XBTs were used to measure between the CTD stations (Figures 10 -12).
3. The exchange between the eastern and western Weddell Sea will be derived from a zonal hydrographical section along the eastward current in the north of the Weddell gyre from 00 to 24041E consisting of 15 stations and a perpendicular meridional hydrographical section of 32 stations through the Weddell gyre along the Greenwich Meridian from 55°S to the ice-shelf edge at 69°38.5'S (Figures 5, 7 and 8). The Greenwich Meridian section was already sampled once in 1992. In addition, 8 moorings were deployed (Figures 5 and 13, Table 1).
4. To determine the inflow into the southern Weddell Sea from the east and the outflow in the north-west, a hydrographical section of 36 stations was performed through the southern Weddell Sea (Figures 5 and 9). This was the fourth repeat of this section since 1989. Six moorings were deployed near Joinville Island (Figures 5 and 13, Table 3).

Table 1: Moorings deployed on the Greenwich Meridian.

Mooring	Latitude	Date	Water Depth (m)	Type	SN	Depth (m)
	Longitude	Time (UTC)				
B06	54° 20.6'S	07.04.96	2677	AVTP	9763	250
	03° 17.0'W	12:09		AVTPC	9193	399
				ACM-CTD	1391	400
				AVTP	9182	1493
				ST	890109	2280
AW1228-1	57° 00.0'S	13.04.96	3857	AVT	9186	2685
	00° 00.2'W	15:30		AVTP	11887	434
				ACM-CTD	1389	795
				AVT	9768	2090
AW1227-3	59° 01.8'S	04.04.96	4605	ACM-CTD	1387	3812
	00° 00.0'W	19:00		ULS	10	156
				AVTP	9201	262
				AVTP	9211	698
				SC	1978	699
				ACM-CTD	1392	700
				AVT	9190	2006
				ST	860016	3373
				AVT	9391	4554
				SC	318	4553
AW1229-1	63° 59.6'S	14.04.96	5180	ACM-CTD	1388	4552
	00° 00.3'W	11:05		ULS	07	159
				AVTP	11888	209
				SIC	1973	210
				TC250	1570	240
				TC250	1572	515
				AVTPC	9786	778
				SC	319	779
				AVT	9770	2005
				ACM-CTD	1400	5136
AW1230-1	66° 00.2'S	19.04.96	3449	ULS	25	51
	00° 09.5'W	16:00		AVTPC	9765	91
				SC	1166	92
				TC250	1426	123
				TC250	1427	399
				AVTPC	9215	664
				SC	1167	665
				AVT	10498	1671
		ACM-CTD	1411	3406		

Mooring	Latitude	Date	Water Depth (m)	Type	SN	Depth (m)
	Longitude	Time (UTC)				
AW1231 -1	66° 30.0'S	20.04.96	4513	ULS	26	160
	00° 00.4'W	11:15		AVTPC	9213	209
				SC	1976	210
				TC250	1453	236
				TC250	1569	512
				AVTP	9212	778
				SC	630	779
				AVT	9561	1805
				ACM-CTD	1390	4466
AW1232-1	69° 00.0'S	22.04.96	3361	ULS	24	147
	00° 00.0'W	09:50		AVTP	11889	248
				AVTPC	10491	754
				AVT	10496	1960
				ACM-CTD	1404	3317
AW1233-1	69° 24.2'S	22.04.96	2001	ULS	6	149
	00° 00.7'E	15:40		AVTP	10492	255
				AVTPC	9214	751
				AVT	10499	1956

Table 2: Moorings recovered during ANT X111/4.

Mooring	Latitude	Date	Water Depth (m)	Type	SN	Depth (m)	Record length (days)
	Longitude	Time (UTC) (1. Record)					
AW1227-2	59° 27.5'S	26-12.94	5096	AVTP	10002	250	424
	03° 11.2'W	16:00		AVTP	9998	514	424
				AVT	9179	1604	424
				AVT	10531	3650	424
				AVT	10532	5058	424
B05	54° 20.6'S	28.12.94	2674	AVTP	9766	215	425
	03° 17.6'W	01:00		AVTPC	8037	425	425
				AVT	9188	1520	425
				AVT	9184	2627	425
PF8	50° 11.1'S	30.12.94	3868	AVTP	10541	301	426
	05° 53.7'E	00:00		AVTPC	7727	799	426
				AVT	10534	1594	426
				AVT	10495	3100	426
				AVT	10497	3815	426

Table 3: Moorings deployed in the western Weddell Sea.

Mooring	Latitude	Date	Water Depth (m)	Type	SN	Depth (m)
	Longitude	Time (UTC)				
AW1216-2	63° 57.6'S	06.05.96	3520	AVTIP	11926	262
	49° 08.8'W	16:54		ACM-CT	1403	573
				AVT	11885	2549
				AVT	11886	3474
				SC	631	3475
AW1207-4	63° 43.3'S	07.05.96	2510	ULS	08	174
	50° 49.2'W	20:45		AVTPC	9207	270
				TC250	2299	506
				ACM-CT	1402	762
				AVT	9767	2187
				TC250	2371	2199
				AVT	9206	2454
				SC	1979	2455
AW1236-1	63° 34.3'S	08.05.96	1803	ACM-CT	1401	1648
	51° 37.0'W	10:49		ACM-CT	1410	1759
AW1206-4	63° 29.6'S	08.05.96	960	ULS	09	157
	52° 06.1'W	15:23		AVTIP	11890	254
				ACM-CT	1409	499
				AVT	9401	914
			SC	1977	915	
AW1215-3	63° 19.6'S	08.09.96	450	AVTIP	11892	244
	52° 46.9'W	22:58		AVT	9402	444
				WLR	1154	450
AW1234-1	62° 51.4'S	09.05.96	287	ADCP	378	278
	53° 40.3'W	16:52		SC	1975	283

Abbreviations:

- ACM-CT Falmouth Scientific 3-dimension acoustic current meter with CTD sensor head (CTD=Conductivity, Temperature, Depth)
- ADCP RDI Inc. acoustic doppler current profiler
- AVTPC Aanderaa current meter with temperature, pressure, and conductivity sensor
- AVTP Aanderaa current meter with temperature and pressure sensor
- AVT Aanderaa current meter with temperature sensor
- SC SeaBird Inc. self contained CTD, type: SeaCat
- ST Sediment trap
- TC250 Aanderaa thermistor cable, 250 m length, 11 sensors 25 m spacing
- ULS Upward looking sonar Christian Michelsen Research Inc.

The hydrographical work was carried out using CTD-probes and water bottle release mechanism built by Falmouth Scientific Instruments (FSI). Two instruments of the type Triton ICTD, SN 1347 and SN 1360 were used. The water bottle rosettes used were a 24-

(12-l)-bottle rosette from General Oceanics Inc. and a 36-bottle rosette from FSI. It turned out however that to obtain a steady sink rate for the 36-bottle sampler, such a high extra weighting was required that safe handling of the rosette was no longer possible and there was the fear of breaking the winch cable. Thus only the 24-bottle sampler could be used. However, due to the intense swell 120 kg of extra weight were needed as well to avoid wire problems. The additional weights were removed once the instrument was on deck to facilitate moving the rosette to the sampling room.

CTD MEASUREMENTS during 06AQANTXIII/4

Instruments: Falmouth Scientific ICTD, Sn: 3060 and Sn: 1347

Falmouth Scientific Reference Grade
Platinum Resistance Thermometer
range : -2 - 32 deg C
accuracy : +/- 0.003 deg C
stability : +/- 0.0005 deg C/month
resolution : 0.0001 deg C

Falmouth Scientific Thermistor Sensor
range : -2 - 32 deg C
accuracy : +/- 0.010 deg C
stability : +/- 0.001 deg C / month
resolution : 0.0001 deg C

Falmouth Scientific Titanium Pressure Sensor
range : 0 - 7000 dbar
accuracy : +/- 2.1 dbar
stability : +/- 0.7 dbar/month
resolution : 0.08 dbar

Falmouth Scientific Inductive Conductivity Sensor
range : 0 - 65 mmho/cm
accuracy : +/- 0.003 mmho/cm
stability : +/- 0.0005 mmho/cm/month
resolution : 0.0002 mmho/cm

Each CTD has two Platinum Resistance Thermometer

Software: FSI Software for data aquisition
CTD postprocessing in analogy to Version 1.12

Time lag: 0.10 s

Despite these precautions, the CTD wire was damaged several times. During the comparatively long time taken to repair the wire, the CTD was deployed with the Aframe

aft of the ship. The extreme pitching of the ship however put such strain on the rosette, that the water bottles were broken loose. This led to the loss of 23 water bottles, 9 electronic pressure sensors and 7 electronic thermometers. In addition, the conductivity cell on the CTD was damaged. This was repaired by converting a sensor from a mooring instrument. Until this repair was fully functioning, some profiles were either unusable or in need of serious correction. The high loading had affected the electric quality of the wire also and lead to errors in the data transmission, which was noticeable in readings from depths of 2000 m to 3000 m. In addition, electronic adjustment problems of the new CTDs lead to some profiles being noisy. These issues have resulted in a unexpected noisy data set which has to be cleaned with care. The noise affects all parameters. The removal is thus done for each profile separately, using an interactive graphic programme, which analyses the properties of the noise. Particular priority is given to obtaining reliable CTD values at the points where bottles were closed, so that a quality calibration correction can be made.

The accuracy of the dataset is determined from laboratory calibrations both before and after the cruise. Since each CTD is equipped with two temperature sensors, the stability of the sensors can be controlled from a comparison of these readings. For instrument no. 1347, the calibrations before and after the cruise were performed by the Scripps Institution of Oceanography and FSI. For both sensors, the temperature drift in the relevant temperature range was less than 1 mK. Thus the pre-cruise calibration coefficients were used. For instrument no. 1360, where the conductivity sensor was repaired, only a post-cruise calibration at Scripps was possible. One of the sensors shows a jump in calibration values. Thus the post-cruise calibration was used. In addition, calibration on-board ship was performed using 13 electronic thermometers until they were lost and subsequently mercury reversing thermometers, calibrated by the Institut für Ostseeforschung in Warnemünde were used. Deviations from the sensor readings occurred due to the scatter in the thermometer readings, so the accuracy of the laboratory calibration can be assumed to be the relevant error. When noise is also taken into account, this gives a final accuracy of 2 to 3 mK.

```
ICTD-SN 1347; Cal_date: DEZ.95  
Calibration: pre-cruise no post calibration used
```

```
#PT1  
a1 = -0.000699749  
a2 = 0.000354949  
a3 = -9.7419E-06  
a4 = -8.44638E-07  
a5 = 2.71068E-08
```

```
#PT2  
a1 = 0.000359662  
a2 = 0.000225676  
a3 = -5.66405E-06  
a4 = -4.91609E-07  
a5 = 1.53814E-08
```

temperature pre-cruise calibration
the temperature data are used only from PT1
 $T(\text{corrected}) = T(\text{reading}) + dT$
with $dT = a1 + a2*T + a3*T**2 + a4*T**3 + a5*T**4$
ai : $T(\text{calibrated}) - T(\text{reading})$

#PRES

a1 = 1.02684
a2 = 0.000760568
a3 = -1.69817E-07
a4 = -6.67453E-11
a5 = 1.02023E-14

#UNLOAD PRES

0.0

pressure pre-cruise calibration
 $p(\text{corrected}) = p(\text{reading}) + dp$
with $dp = a1 + a2*p + a3*p**2 + a4*p**3 + a5*p**4$
ai : $p(\text{calibrated}) - p(\text{reading})$

ICTD-SN 1360; Cal_date: JUN.96
Calibration: post-cruise no pre-calibration used

#PT1

a1 = 9.40529E-05
a2 = 0.000256106
a3 = -7.04533E-06

#PT2

a1 = -0.00549481
a2 = -2.76548E-05
a3 = 3.05434E-07

temperature post-cruise calibration
the temperature data are used only from PT1
 $T(\text{corrected}) = T(\text{reading}) + dT$
with $dT = a1 + a2*T + a3*T**2$
ai : $T(\text{calibrated}) - T(\text{reading})$

#PRES

a1 = 1.08715
a2 = -0.000460084
a3 = 1.32763E-07
a4 = 1.35645E-11
a5 = -1.05971E-14
a6 = 9.25015E-19

#UNLOAD PRES

0.0

Pressure post-cruise calibration
 $p(\text{corrected}) = p(\text{reading}) + dp$
with $dp = a1 + a2*p + a3*p**2 + a4*p**3 + a5*p**4 + a6*p**5$
ai : $p(\text{calibrated}) - p(\text{reading})$

after calibration the platinum temperature is summed with the fast thermistor as follows:

$F(t) = F(t-dt)*W2+Fi(t)*(1-W2)$ filtered fast thermistor
 $F'(t) = Fi(t)-F(t)$ high pass filtered fast temperature
 $T(t) = Ti(t)+F'(t)$ summed platinum and fast thermistor

with $W2 = \exp(-dt/TtauF)$ dt is the CTD observations intervall in seconds

dt = 48ms

TtauF is the Platinum thermometer time

constand

in seconds relative to the fast thermistor

TtauF = 100 ms

Ti is the unfiltered platinum temperature = T(corrected)

Fi is the unfiltered fast thermistor

The CTD-temperature is IPTS-68

Correction of the CTD-conductivity data with the bottle-samples

$COND(\text{corrected}) = COND(\text{CTD}) - COND(\text{delta})$

with $COND(\text{delta}) = \text{average}(COND(\text{CTD}) - COND(\text{WATERSAMPLE}))$

Station/Cast	COND(delta)
00201	-0.0200
00202	-0.0107
00301	-0.0107
00401	-0.0200
00501 to 01303	-0.0107
01403	-0.0179
01502 to 01601	+0.0088
01701	+0.0080
01903	+0.0005
02201 to 02301	-0.0065
02401 to 02601	+0.0082
02701 to 03403	-0.0108
03404	+0.0020
03501 to 07201	-0.0108
07301	+0.0082
07402 to 08201	-0.0133
08302	-0.0026
08401 to 10301	-0.0133

The following 71 stations are filtered between around 2000 to 3000 dbar. In these stations was a noise in 2500 dbar which was estimated as an hardware error.

00201 to 00601
01201
01303
01403
01601
01701
01903
02203 to 02401
02503
02601
02901
03104
03201
03804 to 04401
05403
05501
05604
06004 to 06502
07001
07201 to 07801
07903 to 08901
09004 to 09301
09403 to 09801
10001

CTD station 01801 wrong conductivity data
CTD station 01901 wrong conductivity data
CTD station 02001 wrong conductivity data
CTD station 02101 wrong conductivity data
CTD station 07201 from 2604 dbar to bottom no conductivity data

CTD Files column 5 : transmissiometer raw data
range between 0 and 5 Volt
these data are not controlled

The *.SEA file is not ready. It will be send later.

For CTD no. 1347, a pressure calibration was performed before and after the cruise at Scripps and at FSI. No change was recorded. For CTD no. 1360, a calibration at FSI was performed before and at Scripps after the cruise. The correction was of order 2db. The calibration of the pressure sensors is good to better than 2db.

The conductivity was corrected using salinity measurements from water samples. IAPSO Standard Seawater from the P-series P127 was used. A total of 2477 water samples were measured using a Guildline Autosol 8400B. For stations 18, 19, 20, 21, the CTD conductivity profile was unusable, so a salinity profile was reconstructed from water

sample values. On the basis of the water sample correction, salinity is measured to an accuracy of 0.003.

In addition, the CTD also carried an altimeter from Benthos Undersea Systems Technology Inc. to determine distance above the sea floor and a transmissometer with a 25 cm light path from SeaTech Inc..

At all stations, oxygen samples were taken from the entire water column, (in total 2400 samples). The determination of oxygen was carried out in line with WOCE standards for O₂-measurement, as per Carpenter, 1965. Two radiation counters from SIS were used. For more than 10% of the samples, doubles, covering the entire range of O₂-values (180-350 µmol/l), were also measured. Using this data, a percentage error of 0.2% was obtained. This is below the WOCE-standard of reproducibility of 0.5%. Oxygen profiles were not measured as oxygen sensors fail under freezing conditions.

To measure the stable isotope ¹⁸⁰, 1713 samples were taken at 83 stations. For paleoceanographic investigations, 1350 samples for later analysis for ⁶¹³C were taken at 67 stations.

Preliminary Results

The section from 390 to 4°41'E along 54°S reached from the foot of the Conrad Rise to the Southwest Indian Ridge (Figure 5). In this area, the Antarctic Circumpolar Current has a strong southward component. This can be clearly seen in the distinct core layers of the Upper and Lower Circumpolar Deep Water (Figure 6). The Southern Circumpolar Current Front is found at station 13 at 27°23'E. The near-bottom layer, which reaches from the western slope to the Southwest Indian Ridge, is relatively cold due to the influence of Bottom Water, which flows out of the western Weddell Sea along the mid-ocean ridge to the east. As this core is not to be found on the slope of the Conrad Rise, it must exit into the Indian Ocean. The structure of the surface layers is resolved at the mesoscale from the XBT-section (Figure 11).

The section from the Greenwich Meridian to the east (Figure 7) follows the eastward current in the north of the Weddell gyre. At the depth of the Warm Deep Water, relatively cold temperatures, less than 0.3°C, show the cold regime. The boundary of the Weddell gyre, the Weddell Front, lies between stations 18 and 19. The temperature of the Weddell Sea Bottom Water of less than -0.7°C increases from west to east, reflecting the entrainment of surrounding water. The circulation perpendicular to the section is also evident from a doming of the isolines. This is caused by a northwards extension of the abyssal plain between 10 and 15°E (Figure 5), and appears as a northwards current in the west of the section and a southward one in the east.

The section along the Greenwich Meridian (Figure 8) cuts the cyclonic Weddell gyre meridionally. In the south, a deepening of the surface layer towards the continent and the onset of winter temperatures is observed. This part of the section was already covered with sea-ice and can be counted as the Antarctic Coastal Current. The warm regime occurs to the north, with temperatures in the Warm Deep Water of more than 1°C, caused

by the proximity of the inflow of the Antarctic Circumpolar Current. This warm regime is disturbed by Maud Rise, where noticeably colder temperatures are measured in the Warm Deep Water. The decrease in temperature further to the north signifies the cold regime, in which the eastward current is found. Near the bottom, cold temperatures show the flow of Bottom Water moving east out of the western Weddell Sea, leaning against the mid-ocean ridge. The Weddell Front lies at 55°30'S, between stations 36 and 37.

The southern part of the Weddell gyre, in which the major water mass transformations occur, is separated from the inflow and outflow regimes by the section from Kapp Norvegia to Joinville Island (Figure 9). The surface layer already shows winter conditions with temperatures around the freezing point. The deepening of the surface layer towards the coast, due to on-coastal Ekman transport and convection in the coastal polynya, is clearly visible on both sides of the section. The inflow of relatively warm Warm Deep Water can be seen in the east. The outflow in the west is noticeably colder. On the western slope, a layer of newly formed bottom water flows to the north.

The sections form part of the WOCE "Repeat sections" Programme. Comparison with the data of 1992 on the Greenwich Meridian Section and the 1989/1990/1992 sections through the western Weddell Sea show a clear change in the deeper layers. In the bottom water of the western Weddell Basin, a continual warming over this 6 year period is observed. This trend is confirmed by results from moored instruments. The warming is of order 0.01 K per year. The investigation of the cause of this warming is still on-going. However, the increase in temperature in the Warm Deep Water regime suggests a change in the inflow of water from the circumpolar current.

2.2.2 Tracer measurements

(Klaus Bulsiewicz, Gerhard Fraas, Malte Runge, Björn Schlenker, Hiltrud Sieverding/IUPB)

Objectives and methods

Along the sections, the CFCs Freon-11, Freon-12, Freon-113 and CCl₄ were measured on board by ECD gas chromatography. This is the first time F113 and CCl₄ have been measured in this region over a complete section. F113 has been released into the atmosphere at a known rate since the early sixties and has been taken up by the oceans by the surface transfers. Therefore it can be used to characterize the younger water. Similarly CCl₄ has been released into the atmosphere since about 1920, so that it characterizes the older water. In addition to the analysis done on board, water samples for CFC measurements were stored in flame-sealed ampoules which will be analysed ashore and will provide reference measurements for the analysis carried out on board. Water samples for tritium and helium were taken also. They will be extracted after the cruise and analysed with a mass spectrometer. All gases will be extracted from the tritium samples which will then be stored for half a year. After this time, a sufficient amount of tritium will have decayed to ³He so that it can be measured by the mass spectrometer. The data sets provide important information about circulation and renewal pathways for all relevant subsurface water masses.

Work at Sea

The water samples were taken from the rosette water sampler using flow-through containers consisting of a glass ampoule (CFMs), copper tubes (helium) and glass bottles (tritium). In total, 104 stations were sampled and 2016 water samples for the CFMs were analyzed during this cruise. In addition, 785 standard gas and blank measurements were taken periodically. In total, 1418 water samples were collected for analyses ashore, including 200 water samples for CFC, 623 water samples for helium (collected at 62 stations) and 595 samples for tritium (at 60 stations).

A special calibration cast was made in the Drake Passage in which all water bottles were closed at a depth of 3000 m. The water obtained is supposed to be free of CFCs, so that the overall blank can be checked. Apart from the apparatus blank, the blank of each individual water bottle is important for the evaluation of the data. On the cruise Meteor 11/5 In 1990 the CFMs F11 and F12 were not found. Now however, these CFMs could be detected in concentrations of 0.04 pmol/kg (F11) and 0.02 pmol/kg (F12). Only Freon-113 could not be detected (limit of detection: 0.001-0.002 pmol/kg) and therefore it can be concluded that the water bottles have not yet been contaminated with Freon-113.

Preliminary results

Preliminary data for Freon-11 are presented in [Figures 14](#) and [15](#). A quasi-zonal section from 35' E to the Greenwich Meridian is shown in [Figure 14](#). Between stations 12 and 18 the transition from the Circumpolar to the Weddell regime occurs. In the centre of the Circumpolar Deep Water (2000 m), the lowest concentrations (<0.17 pmol/kg) is measured, values which also occur in the Warm Deep Water at 1000 m depth and indicate older water with little renewal. The section from 55' S to Antarctica along the Greenwich Meridian is presented in [Figure 15 \(top\)](#). This section can be compared with results from a previous cruise (ANT X/4, 1992). For example, the 0.2-pmol/kg isoline in the centre of the gyre at 62' S now reaches up to 2500 m, whereas in 1992 it occurred at a depth of up to 4000 m. The increase of the tracer concentration in the interior is consistent with upwelling in the Weddell gyre. On the slope of the North Weddell Ridge, bottom water with F11 > 0.5 pmol/kg is advected from the Antarctic Peninsula. [Figure 15 \(bottom\)](#) shows the section across the southern Weddell gyre from Kapp Norvegia to the Antarctic Peninsula (Joinville Island). Along the slope of the Antarctic Peninsula, the newly formed bottom water is obvious from the high concentrations. Between 500 and 2000 m depth, a CFC-11 - minimum (<0.15 pmol/kg) is indicative of relatively old water. In the depth range 300 to 1500 m, an inflow of Warm Deep Water in the Weddell basin occurs at Kapp Norvegia and the outflow of this water mass is obvious on the western side. At 3000 m, a tongue of fresh water stretches from the eastern slope into the central basin. This is an indication that the centre of the Weddell basin is also ventilated from the east. On the eastern continental slope, a core of young water (>0.5 pmol/kg) occurs at 4000 m. A similar core is present on the Greenwich Meridian section in 3000 m. This indicates that the source of this water is in the Enderby basin or even further to the east.

2.3 Marine chemistry

2.3.1 The carbon dioxide system in Antarctic waters

(Mario Hoppema (AWI) and Michel Stoll/NIOZ)

Objectives

Modifications of the global carbon cycle, by the burning of fossil fuel and changes in land use, have led to an increase in atmospheric carbon dioxide (CO₂) which has the potential to increase the greenhouse effect of the atmosphere. The deep oceans are, in principle, able to take up almost all of this excess CO₂, but only on a time scale which is much longer than the one associated with the anthropogenic perturbations. This is related to the typical mixing and residence times of the deep and bottom waters of the oceans, which are of the order of 1000 years. Thus studies in areas where interactions between the deep and the surface ocean occur, such as the Weddell Sea, are vital for the study of CO₂ uptake and its distribution.

An objective of this project is to gain knowledge of the CO₂ distribution in the Weddell Sea, where the initial properties of a major part of the abyssal world oceans are generated. Another objective is to determine the potential of Antarctic waters to take up atmospheric CO₂. This is especially important for the frontal regions of the Antarctic Circumpolar Current (ACC) and for the regions with seasonal ice cover. Data from this cruise will be combined with data of previous cruises to address those questions

The ensuing CO₂ database of the Weddell Sea and the Antarctic Circumpolar Current may also be used in a modelling effort in which carbon transport and air-sea gas exchanges are calculated.

Work at sea

The CO₂ system has been investigated along four sections. Section I ran from Cape Town (SA) to 55°S 39°E, section II across the northeastern Weddell gyre from 39°E to OOE, section III along 0°E and section IV from Kapp Norvegia to Joinville Island the western Weddell gyre.

Measurements of the CO₂ system in the entire water column were performed. TCO₂ (total inorganic carbon content) was determined by a high-precision coulometric method and automated sample stripping system. Briefly, the method is as follows. A sample of seawater is acidified with phosphoric acid and stripped with high purity N₂ gas. The carrier gas plus extracted CO₂ is passed through a solution containing ethanolamine and an indicator. This solution is electrochemically back-titrated to its original colour and the amount of Coulombs used is equivalent to the amount of CO₂ in the sample. Data obtained were processed onboard and calibrated against an internationally recognized TCO₂ standard (Dickson).

Continuous measurements of the partial pressure of CO₂ (PCO₂) in water and marine air were done using an infrared analyzer (Li-Cor). A continuous water supply is passed through an equilibrator where approximately every 4 to 5 minutes the headspace gas is

analyzed for its CO₂ content, thus giving PCO₂ in the surface water. Marine air was pumped continuously from the crow's nest into the laboratory and subsampled after every fourth equilibrator reading. The equipment was calibrated with reference gases, traceable against NOAA standard gases. The data obtained were processed onboard. Final data will be available pending recalibration of the reference gases ashore.

Preliminary results

Total carbon dioxide

In [Figure 16](#), the section on the Greenwich Meridian is shown for TCO₂. The boundary between the Antarctic Circumpolar Current and the Weddell gyre regime lies at approximately 55-56°S.

Generally, TCO₂ is low in the surface layer due to phytoplankton which utilizes CO₂. Below the thermocline, a TCO₂-maximum is found, associated with the temperature maximum of the Warm Deep Water. Near the bottom, where Weddell Sea Bottom Water is present, relatively low TCO₂ values were measured. This water mass originates partly from the shelf waters of the Weddell Sea, which are low in TCO₂. The large water volume of Weddell Sea Deep Water, which lies between the bottom water and the Warm Deep Water, is merely a mixture of these two source waters with corresponding TCO₂ values.

The TCO₂ maximum is higher in the north (58-63°S) than in the south (66-69°S) and in addition is shallower in the former region. This division coincides with the cold and warm regions of the Weddell gyre, which are defined by the value of the temperature maximum. In the southern warm regime, the Warm Deep Water present has entered the Weddell gyre relatively recently. In its source area, the Antarctic Circumpolar Current, TCO₂ increases with depth. In the deep Weddell Sea, on the other hand, TCO₂ decreases with depth and thus a TCO₂ maximum is formed at the depth where the new Warm Deep Water meets the deep Weddell water. This deep TCO₂ maximum is observed at about 1500 m (66-69°S). In the northern, warm regime, Warm Deep Water is found which has already been circulating for a longer time in the Weddell gyre. The observed TCO₂ concentration is higher than in all waters of the warm regime and, since the Warm Deep Water is essentially the only source of water of the Weddell gyre, this implies that CO₂ enrichment has occurred in the Weddell Sea.

In the bottom layer at 60-63°S, a TCO₂ minimum was observed. This is probably due to the meeting of spatially separated bottom water masses with different TCO₂ content. Over the flanks and the crest of Maud Rise, TCO₂ values were different than to the north and south. For example, the 2255-ppm isoline, which normally occurs near the bottom of the thermocline, reaches much deeper to about 800 m. The deep TCO₂ maximum, characteristic for the warm regime, is also less pronounced over Maud Rise.

Toward the Antarctic continent (about 69°S) the isolines fall precipitously indicating a sharp frontal structure. This front separates the warm regime from the coastal regime.

Partial pressure Of CO₂

The measurement Of PCO₂ along the four sections resulted in a large, high spatial resolution data set. Along Section 1, near-saturation values are generally observed, somewhat modified by the local hydrographic variations with a slight oversaturation in the south. Section 11 starts with an oversaturation and decreases to undersaturation. On crossing the frontal system between Antarctic Circumpolar Current and the Weddell Sea, an increase of about 15 ppm is observed.

The section along 0°E (111) is discussed in more detail (Figure 17, top). A slight undersaturation is observed between 50 and 52°S. Then, going southwards, a sharp increase in the PCO₂ (about 10 ppm relative to atmospheric value) occurs, accompanied by a pronounced decrease in sea water temperature. Further south (about 56°S), the Weddell Front is characterized by a further increase in PCO₂ to values of 375 ppm. Regional hydrographic variations in the cold water regime of the Weddell Sea are reflected in the PCO₂ signal. In some areas the chlorophyll content is relatively high (65°S), which may be reflected in the PCO₂ signal (Figure 17, bottom). However, the major influence on the observed signal appears to be water temperature (Figure 17, top).

The cold water regime is generally characterized by oversaturation. The subsequent decrease in PCO₂ concentration, to equilibrium values and below, is correlated with crossing into the warm water regime. On the flanks and the crest of Maud Rise, the water column is different in structure. This might be reflected in the PCO₂ as shown by the steep gradients over the flanks. Generally, the warm water regime is characterized by undersaturation.

For the first time, the PCO₂ was measured on a long transect with ice-covered water (section IV: Kapp Norvegia - Joinville island). The newly designed water inlet on the box-keel ("Kasten kiel") made a fairly uninterrupted water supply possible. Also a slight modification to the equilibrator shower head was necessary. The observed undersaturation in PCO₂ (-10 to -15 ppm) is very likely caused by rapid cooling of the water which, after freezing, is prevented from equilibrating with the atmosphere. Only on nearing Joinville Island, where multi-year ice is found, oversaturation with higher values is observed (+20 ppm and over). This is caused by the upwelling of deep water, which is enriched in CO₂, into the surface water. During the next spring, when the ice cover retreats, phytoplankton will most likely use this excess CO₂ for growing.

2.3.2 Nutrient distributions in Antarctic waters

(Karl Bakker/NIOZ, Michel Stoll/NIOZ and Mario Hoppner/AWI)

Nutrient concentrations of silicate, phosphate, nitrite and nitrate were determined in all samples taken from the rosette. They were analyzed by a standard colorimetric method on a rapid flow "TRAACS" autoanalyzer (60 samples/hr) manufactured by Technicon. A standard range was used for all measurements (Table 4), while daily diluted stock standards were used for calibration. As a reference standard a so-called "cocktail" (100 fold diluted) containing a mixture of phosphate, silicate and nitrate was used. This

standard was measured for statistical purposes and corrections on the data. The precision for the different properties are given in Table 4.

Table 4: Standard measuring ranges used for Si, P04, N02 and N03 and standard deviations.

	Range ($\mu\text{mol/l}$)	STD
Silicate	0-145	0.5
Phosphate	0-3	0.03
Nitrite	0-2	0.01
Nitrate	0-40	0.21

Preliminary results

As an example for the nutrient data obtained, four silicated sections are presented (Figures 6 to 9). Generally, the nutrients are relatively low in the surface layer because of biological activity. In the Warm Deep Water below, phosphate and nitrate show a maximum, associated with the temperature maximum. Both decrease towards the bottom. The silicate maximum occurs deeper than the phosphate and nitrate maxima. It originates from the dissolution of biogenic silica, which takes place at a lower rate than the remineralisation of soft tissue, by which phosphate and nitrate are released.

In the eastern part of the section, the Warm Deep Water that entered the Weddell gyre relatively recently is recognizable by a phosphate maximum at 1000-1500 m. This structure is a continuation of the same structure on the Greenwich Meridian. Remnants of it can also be seen in the very west of the basin (200-400 km), indicating that the Warm Deep Water crosses the entire basin.

In the centre and west, the phosphate maximum is shallower and has a higher value. This area is comparable with the cold regime on the Greenwich Meridian. High phosphate and nitrate values are caused by sub-surface remineralization of biological material that sinks down. For silicate (Figures 6 to 9) some specific features can be observed which cannot be detected in other tracer distributions. In the easternmost part of the section, the highest silicate values are found in the bottom layer. This may be due to an inflow of bottom water from the Enderby basin in the east, where silicate enrichment of the bottom layers is known to occur. In the central and western basin, bottom silicate values are much lower due to the presence of bottom water recently produced in the southern and western Weddell Sea. On the western slope, some young bottom water is identified by its very low silicate, phosphate and nitrate values. Earlier data showed that this band of low silicate did only reach the lower slope (until approximately 300 km of the section; Figure 9). During this cruise, another cell of young bottom water ($\text{Si} < 100 \mu\text{mol/kg}$) is found at the base of the continental rise (about 600 km), much further down the slope than during previous observations.

A very interesting new observation on this transect is the major silicate- minimum structure between 2500 and 4000 m, extending over the entire eastern part of the basin. Relatively low silicate values in the deep Weddell basin are associated with bottom water which indicates that significant ventilation of the deep Weddell Sea does not only take place via

the bottom route, but also via the deep water route. Since such a silicate minimum can only come into existence when the deeper water shows an increase of silicate, this suggests that this deep ventilation originates from the east where the bottom layer has a high silicate concentration. The western boundary of this deep ventilation area appears to be visible in the phosphate distribution as well as a sharp, deep phosphate front at 1000-1100 km.

2.3.3 Tracer-Ozeanographie

(Prof. Dr. Wolfgang Roether - Principal investigator)

Universitaet Bremen, FB1
P.O. Box 330 440
28334 Bremen
Phone: 0421 218-3511 or -4221
Fax: 0421 218-7018
Email: wroether@physik.uni-bremen.de

Dr. Birgit Klein (contact for questions about measurement and data processing)
adress as above
Phone: 0421 218-2931
Fax: 0421 218-7018
Email: bklein@physik.uni-bremen.de

2.3.3.1 CFCs:

CFC11, CFC12, CFC113 and CCL4 have been measured on the cruise. A capillary column (DBVRX) was used. A Bremen-CFC standard has been used during the measurements which has been calibrated against the SIO93 scale. CFC measurements have been assigned individual errors. During the cruise a degasing of water samples was observed during the measurement process. The outgasing was corrected for F11 and F12, F113 additionally suffered from overlapping peaks of methyl iodid in the chromatograms and could not be corrected for the degasing. A higher error has been assigned. The overall performance is described below:

Reproducibility:

F-11:	0.4%	or	0.0015 pmol/kg (whichever is greater)
F-12:	0.4%	or	0.0014 pmol/kg (whichever is greater)
F-113:	1.0%	or	0.0003 pmol/kg (whichever is greater)
CCI4:	0.8%	or	0.0056 pmol/kg (whichever is greater)

Precision:

- F11: 0.0475 pmol/kg or a relative error of 0.80% referring to conc. greater 1.0 pmol/kg and 0.0035 pmol/kg for conc. <1.0 pmol/kg
- F12: 0.0265 pmol/kg or a relative error of 0.91% referring to conc. greater 1.0 pmol/kg and 0.0030 pmol/kg for conc. <1.0 pmol/kg
- F-113: 0.0083 pmol/kg or a relative error of 2.0 % referring to conc. greater 0.05 pmol/kg and 0.0007 pmol/kg for conc. <0.05 pmol/kg
- CCI4: 0.0418 pmol/kg or a relative error of 0.7% referring to conc. greater 1.0 pmol/kg and 0.0037 pmol/kg for conc. <1.0 pmol/kg

Mean water blank, detection limit:

2.3.3.2 Helium:

Helium samples were taken in the usual manner with pinched-off copper tubes. After the gas extraction in Bremen the samples were measured in the laboratory with specialized noble gas mass spectrometer. All samples were calibrated using an air standard (regular air). Helium samples still have to be corrected for tritium decay during storage time, as soon as the tritium data become available. Because of the low tritium concentrations in the southern ocean these corrections (concerning only the $\delta^3\text{He}$) will be very small and mainly concern the surface waters. Helium, $\delta^3\text{He}$ and neon have been assigned individual errors. The general data quality is as follows:

Relative errors:

- Helium: 0.20%
- Neon: 0.20%
- $\delta^3\text{He}$: 0.22%

These errors were estimated using 10 pairs and one set of 4 duplicates.

2.3.3.3 Tritium:

Tritium samples have also been taken from our lab during the cruise. The data are still awaiting measurement and will be submitted later.

2.3.4 Marine Organic Chemistry

(Anneke Mühlebach, Andreas Zimmermann/AWI)

Objectives and methods

The organic chemistry work aimed to determine the distribution of dissolved and particulate phytosterols in the Weddell Sea (autumn situation). This study will complement earlier studies undertaken in the western Weddell Sea during the spring bloom of phytoplankton (ANT X/7). The objective is to understand the fate of phytosterols and other trace organic compounds in the ocean, starting with their biosynthesis and input into the euphotic zone and their possible deposition in the bottom sediments. By choosing some

well defined classes out of the pool of organic compounds, the processes appearing on a molecular level can be examined. This may yield further information about the stability of highly diluted dissolutions.

Water samples (20 l each) were taken along three sections and at various depths by a rosette water sampler joined to a CTD-probe. Dissolved and particulate parts were separated by filtration. Filtration was performed over glass fibre filters (GF/C, diameter 4.7 cm, retention rate 90% for particles > 1.2 µm; for larger volume samples (vol.> 20 l), diameter 15 cm). Filters were put in ampoules and test tubes respectively, covered with inert gas (argon) to prevent oxidation, sealed and stored at -30°C. After filtration, the seawater samples were spiked with Cholesterol-d6 as an internal standard. The dissolved lipophilic compounds were extracted with hexane. A volume of 20 l of sea water was shaken with 100 ml hexane. These extracts were put in ampoules, covered with argon, sealed and kept at -30°C. In Bremerhaven, further preparation and analysis of the samples will take place. Filters will then be extracted with acetone. Hexane and acetone extracts will be evaporated. After derivatisation yielding trimethylsilyethers, the phytosterols will be analysed by GC/MS. Concentrations in the lower (ng phytosterol)/ (l seawater) range are expected (for deep water).

The quality of the extraction and the further processing is checked by the addition of various internal standards (stable isotopes). Before the extraction, 200 ng Cholesterol-d6 in 1 ml ethanol were added to the water sample. Surface samples were spiked with 2000 ng, since in surface samples higher sterol concentrations are expected. The hexane used for extraction was spiked with benz(a)anthracened12 to determine the hexane recovery (200 ng/100 ml). Just before the injection into the GC/MS system, a deuterated decachlorbiphenyl standard will be added to the sample to check the performance of the instrument.

Samples taken during the cruise

Section 1 part a (stations 3 to 16) from Conrad Rise to the southwestern Indian Ridge:

Six profiles were taken, three at the slope of the Conrad Rise (stations 3,5,7), one in the centre of the basin (station 10), and two at the slope of the Southwest Indian Ridge (stations 14,15). At each station, seven samples (20 l each) were taken. Samples were taken close to the bottom, 100 m above bottom, 600 to 800 m above bottom, at about 1500 m depth, at the temperature maximum (Circumpolar Deep Water), at the temperature minimum (Winter Water), and at the surface. All samples except the surface samples were taken from the rosette water sampler. The surface sample was provided by the Klaus-pump.

Section 1 part b (stations 16 to 31) along the northern Weddell gyre:

Five profiles were taken at a separation of 180 sm, starting at station 19 (stations 19, 22, 25, 28, 31). Again, seven samples were taken at each station. Samples were taken close to the bottom, 100 m above bottom, 600 to 1000 m above bottom, at 2500 m depth, at the temperature maximum and minimum, and at the surface.

Polar and Weddell Front:

Profiles were taken at both station 33 (Weddell Frontal) and station 34 (Polar Front). These samples are not influenced by the Weddell regime and the newly formed bottom water respectively, and can serve as a reference.

Section 2 along the Greenwich Meridian (stations 35 to 67):

11 profiles (each some 7 samples) were taken along the section from 55°S to the continent. Four of the profiles were situated close to Maud Rise (one at the northern edge, one at the southern edge, two at the shallowest points we crossed). Between the North Weddell Ridge and Maud Rise, samples were taken every 120 m close to the bottom, 100 m above the bottom, at 4500 m depth, at 2500 m depth, at the temperature maximum and minimum as well as at the surface. Every 60 m, an additional surface sample was taken (Klaus-pump). On the slopes and above Maud Rise in shallower water, the station separation decreased, additional samples were taken from 1000 m depth. Profiles were taken at stations 35, 38, 44, 48, 52, 54, 56, 57, 60, 62, 66.

Section 3 western Weddell Sea (stations 69 to 103) from Kapp Norvegia to the Antarctic Peninsula:

Samples were taken at the following depths: close to bottom, 100 m above bottom, 3000 m, 1500 m, 500 m, temp. maximum, and at the surface and 40 m, respectively. Profiles were taken at stations 69, 71, 75, 79, 83, 86, 90, 94, 99, 101, 102, 103. Additionally samples were taken close to the bottom at stations 95, 96, 97, 98, 100. In the newly formed bottom water, relatively high sterol concentrations may be found depending on the contact of the water mass to the open sea and on the half life of the sterols. In addition, sterols may be extracted from the sediment into the overlying water. The data gathered on section 3 may be compared to data from a former study along this track (ANT X/7). Then, a region with very low sterol concentrations was found in the central basin (concentration of brassicasterol < 0.5 ng/l, for example). This observation will be verified by samples from this cruise.

Along each section, various surface samples with a volume of 80 l were taken (Klaus-pump). This will allow the identification and quantification of sterols present in trace amounts in seawater. In addition, various experiments were performed to improve the methods applied, especially with respect to the recovery of the internal standard Cholesterol-d6.

2.4 Marine Biology

2.4.1 Plankton investigations

(Anke Bittkau, Corinna Dubischar, Jochen Nowaczyk/AWI), Vassili Spiridonov/ZMMU)

Objectives and methods

Zooplankton and micronekton distribution in the Weddell gyre depends largely on oceanographic structures in this region. During ANT XIII/4, two main questions were addressed by our planktological studies:

1. How are horizontal and vertical distributions of zooplankton and micronekton determined by the different oceanographic regimes in the Weddell Sea (i.e.: the frontal system between the Antarctic Circumpolar Current and the Weddell Sea; the warm regime; the cold regime, and the coastal current) ?
2. How do the dominant zooplankton and micronekton organisms switch to overwintering modes in these different regimes?

To answer these questions, our studies focused mainly on phytoplankton, zooplankton and micronekton species composition, abundance and distribution as a function of oceanographic structures. For precise measurements of the vertical distribution of larger zooplankton and micronekton, an Optical Plankton Counter (OPC) was used in addition to the net catches. This OPC was attached directly to the multinet. The continuous photometric measurement of particle size and number enables us to assess particle distribution parallel to the multinet-catches with a high resolution. In the following section, the methods used, as well as some preliminary results will be described in more detail.

Phytoplankton distribution

Chlorophyll a determination:

Phytoplankton biomass in the water can be detected by fluorometric measurement of the phytoplankton pigment chlorophyll a (Chla). Two different approaches were used:

1. Underway surface (8 m water depths) fluorescence of phytoplankton pigments (expressed as chla) was recorded by means of a Turner Design JD 10 fluorometer attached to the seawater system with the ship's membrane pump. Data were obtained every 10 seconds and averaged in 5 min intervals and subsequently stored on the ship's data logging system (POLDAT) together with the appropriate ship's position and other physical, chemical and meteorological data. Every 4 hours, and also at the stations, triplicates of normally 1 l of seawater, but occasionally more (drained from a bypass to the fluorometer system), were filtered onto Whatman GF/F glassfibre filters for calibration of the instrument. The chla and phaeopigment values were obtained after extraction with 90 % acetone/water. The determination limit was 0.001 µg chla/l.
2. At stations Cchlorophyll a measurements were done from the Niskin bottles of the CTD rosette. At 49 stations, water from 20, 40, 60, 80, 100 and 200 m was taken. if OPC

measurements and multinet samples indicated high particle concentrations in deeper water layers, additional samples were taken from water depths down to 500 m. Along the transects 3 and 4, chl_a-concentrations in the < 20 µm and the >20 µm size fraction were measured separately.

To determine the chl_a-concentrations, 2 l of seawater were filtered onto Whatmann GF/F-glassfiber filters. Pigments were extracted with 10 ml 90% acetone and measured thereafter directly on board using the method by Evans et al. (1987). Parallel to the sampling for chl_a measurements, 2 l seawater per depth level were filtered onto precombusted (24 h at 500°C) Whatmann GF/F-filters for later analyses of particulate organic carbon and nitrogen (POC/PON). These filters were deepfrozen (-20°C). Measurements will be carried out at AWI using an Carlo-Erba CHN Analyzer.

For determination of phytoplankton concentration and species composition, 200 ml of seawater were taken from the same depths as for chl_a and POC/PON-measurements and fixed with hexamethylenetetramin-buffered 20% formalin (end concentration 0.6%). These samples will be processed using the Utermöhl-counting technique (1958) at the home laboratory. Additional samples were taken with an Apstein-net (mesh size 20 µm) to concentrate larger phytoplankton from the upper 10 m of the water column.

Zooplankton and micronekton distribution

Zooplankton organisms were sampled using a Multinet (Hydrobios, Kiel) with mouth opening of 0.25 M² and mesh size of 100 µm. An OPC was mounted on the net frame. The OPC photometrically records the distribution and size of particles in the water column. Each half a second, the data are transferred to the deck unit, yielding in an exact pattern of the vertical distribution of plankton organisms parallel to the multinet tow. The multinet was towed with a speed of 0.5 m sec⁻¹. At all stations, the multinet tows were conducted down to 1000 m (or in the shelf areas nearly to the bottom). Five depth strata were chosen according to the thermohaline structure of the water column.

In total, 31 successful multinet stations were performed: 3 stations on the zonal transect along 54°S (transect 2a), 6 on the transect across the Weddell cold regime (transect 2b), one station in the Polar Front, 12 on the transect along the Greenwich Meridian (transect 3), and 9 stations on the transect across the western Weddell Sea from Kapp Norwegia to the Antarctic Peninsula (transect 4).

After towing, each sample was split into 2 subsamples using a 2 l Folsom splitter. One half was immediately preserved in 4% hexamine buffered formalin, while another was used for size fractioning and subsequent preparation for biomass measurement. Before fractioning, we checked a subsample for rare or taxonomically interesting specimens. Simultaneously, several specimens of the dominant species (mostly *Calanoides acutus*, *Calanus propinquus*, and *R. gigas*) were selected for the determination of carbon and nitrogen (C,N) content and ratio, and fatty acids composition of lipids.

For biomass measurement, a subsample was screened subsequently through 2000 µm, 1000 µm, 500 µm, 200 µm, and 100 µm meshes. Each of the fractions obtained was then

filtered onto preweighted GF/C filters and dried at 500C for 24 h. In case of the presence of abundant phytoplankton, subsamples for biomass determination were not fractionated but preserved in formalin separately. Zooplankton biomass in these samples will be estimated from size spectra of major taxa using length/weight regressions. Salps from the biomass subsample were measured and dried on filters or deep frozen separately according to a size grouping.

For determination of C,N content, the organisms were identified, staged and measured under a stereomicroscope with an accuracy of 0.1 mm, rinsed in distilled water and deep frozen individually (or for young copepodite stages of large calanoids in groups of 2-3 specimens) in Eppendorf caps. Measurements will be carried out using a Carlo Erba CHN analyzer.

For the study of fatty acids composition of body lipids, we selected 3 to 5 specimens of particular developmental stage of certain species and placed them into precombusted tubes with 10 ml conserving solution (Dichlormethan/methanol in a proportion of 2:1). These tubes were then stored under -20°C.

Micronekton was collected using a Rectangular Midwater Trawl with two nets, the larger one with an mouth opening of 8m², the smaller one with an opening of 1 m² (RMT 1+8) which was towed obliquely from the depth of ca. 450 m to the surface. The volume of water filtered was estimated using flowmeters mounted in the mouth of both nets. Four RMT tows were performed on transect 2b across the Weddell cold regime waters, 7 tows were done on the Greenwich Meridian (transect 3) and one additional tow was performed in the Bransfield Strait. The fresh catch of the big (8 m²) net was sorted into major taxonomic groups, i.e. coelenterates, polychaets, pteropods, cephalopods, euphausiids, hyperiids, decapods, chaetognaths, thaliaceans and fishes, which were preserved in 4% formalin and later counted. The sample of the small (1 m²) net was preserved without sorting. Further processing of the RMT samples will be done in the AWI and the Zoological Museum of the Moscow University.

Several vertical Bongo net (200 µm and 500 µm mesh size) tows were performed in order to obtain alive animals for experiments and for further DNA/RNA analyses.

Preliminary results

In the following section, the results of the on-line chlorophyll measurements during the transects 2a, 2b and 3 are shown. Because of the permanent ice cover during transect 4, no surface chl_a data are available. Table 5 gives some general information concerning the positions etc. of the transects.

Table 5: Characterization of the transects carried out during ANT X111/4.

Date	Station	Position Start	Position End	Name
17.3 - 23.3	01-02	Cape Town	54°00.0'S	Transect 1
			38°59.8'E	
23.3 - 28.3	03-15	54°00.0'S	54°00.0'S	Transect 2a
		38°59.8'E	25°44.4'E	
28.3 - 05.4	15-32	54°00.0'S	59°27.5'S	Transect 2b
		25°44.4'E	3°10.5'W	
12.4 - 22.4	35-66	55°00.0'S	69°38.5'S	Transect 3
		0° W	0°07.4'W	
25.4 - 08.5	68-102	71°01.0'S	63°20.1'S	Transect 4
		11°36.6'W	52°47.6'W	

Transects 2a/2b:

In general, very low chl_a concentrations were measured during both transects, which was in accordance to expected values during late autumn in this area (Figures 18 and 19). Background values were between 0.1 and 0.2 µm Chl_a/l. On transect 2a, a distinct chl_a maximum was measured between 290 und 30°E, east of a significant increase of surface salinity and a decrease in surface temperature. Further to the west, an increase of the chl_a-concentration to a maximum value of about 0.5 µm/l was detected. These relatively high concentrations persisted in the connecting transect 2b between 25°E and 19°E. These positions coincide with the site of an extensive frontal system in this region. Further analyses of phytoplankton composition and detailed investigations on hydrographic conditions are needed to detect possible reasons for this higher phytoplankton biomass.

Transect 3:

Transect 3 followed the Greenwich Meridian from 55°S to the ice shelf edge. During this transect, very low chl_a-concentrations were found (Figure 20). Chlorophyll a concentrations in the north were higher than those further south. Two maxima at about 60°S are particularly noticeable. Further investigations of, for example, phytoplankton species composition are needed to explain these patterns.

Figure 21 shows some of the vertical profiles registered by the OPC attached to the multinet. The particle concentrations showed very pronounced peaks in the upper water layers (ca. upper 150 m), but varied significantly between the different profiles. Generally the particle concentrations of up to 12000 particles m⁻³ were surprisingly high. Further investigations of the multinet catches will reveal the characteristics of the particles.

Sediment traps

Some of the particles produced in the upper ocean layers, e.g. phytoplankton aggregates and faecal pellets, may reach relatively high sinking velocities, leading to their sinking out of the surface layers. Sediment traps have been attached to the following moorings to assess this particle flux qualitatively as well as quantitatively: 227/2, 227/3, BO-5, BO-6 and PF-8. These sediment traps are equipped with 20

Table 6: Recovered sediment traps:

Mooring: 227/2 at 59°27.5' S and 3°11.2' E
Deployed on 26.12.1994
recovered on 05.04.1996

Depth of the trap	565 m	3709 m
Time of deployment	27.12.1994 - 10.08.1995	27.12.94 - 11.01.96
Sampling interval	19 days	19 days
Number of samples	115	20

Mooring: BO-5 at 54°20.6' S and 03°17.6' W
Deployed on 27.12.1994
recovered on 07.04.1996

Depth of the trap	531 m	2268 m
Time of deployment	31.12.1994 - 15.01.1996	31.12.1994 - 08.12.1995
Sampling interval	19 days	19 days
Number of samples	20	18

Mooring: PF-8 at 50°11.1' S and 05°53.7' E
Deployed on 29.12.1994
recovered on 09.04.1996

Depth of the trap	687 m	3110 m
Time of deployment	31.12.1994 - 15.01.1996	31.12.1994 - 15.01.1996
Sampling interval	19 days	19 days
Number of samples	20	20

Table 7: Newly deployed sediment traps:

Mooring: 227-3 at 59°01.8' S and 0.0° E deployed on 04.04.1996

Depth of the trap	3373 m
Time of deployment	06.04.1996 - 27.03.1997
Sampling interval	14 days

Mooring: BO-6 at 54°20.6' S and 3°17.0' W deployed on 07.04.1996

Depth of the trap	2280 m
Time of deployment	08.04.1996 - 27.03.1997
Sampling interval	14 days

sampling containers and are therefore able to collect the sinking material in 20 different time intervals. To prevent degradation of the material in the sediment trap by microbial activities and zooplankton grazing, the sampling containers were poisoned with mercury dichloride. The deployed and recovered sediment traps are summarized in [Table 6](#) and [7](#).

2.4.2 Benthos investigations

(Wolf Arntz (AWI, Alexander Buschmann/AWI, Kai Horst George/FBZO, Dieter Gerdes/AWI, Matthias Gorny/AWI, Marco Antonio Lardies Carrasco/UACH, Katrin Linse/IPO, Americo Montiel/UMAG, Erika Mutschke/UMAG, Martin Rauschert/AWIP) and Carlos Rios/UMAG)

Objectives

During the second part of the cruise, the investigations carried out by RV "Victor Hensen" in October/November 1994, were continued to study the marine fauna and flora in the Magellan region to compare it with Antarctic conditions and to detect latitudinal clines in population dynamics, reproductive biology and other life strategy components from the high Antarctic to the Strait of Magellan. These two areas separated only recently in geological terms (<20 Ma) and are supposed to have had more intense interchange than other continents around the Antarctic. In addition they should have had a similar history of glaciation.

Faunistic and floristic overlaps have often been suspected between the Antarctic Peninsula and the Magellan region, which essentially comprises Patagonia and Tierra del Fuego with their vast system of channels and fjords. This view seems to hold true for some faunal groups, however it cannot be confirmed for other taxa, or at least there are major doubts. The principal reason for these uncertainties is the lack of adequate sampling in the Magellan region and on the adjacent continental slope of the Drake Passage.

In the past years major efforts have been made to improve the knowledge on both the Antarctic and Magellan fauna and flora. From recent work at the "Dallmann" laboratory, an annex to the Argentinian base Jubany, and other stations shallowwater fauna and flora in the Bransfield Strait near King George Island are fairly well known. During the "Joint Magellan 'Victor Hensen' Campaign 1994" substantial samples were taken in shallow and deep waters of the Strait of Magellan (to 650 m depth), in the northwestern branch of the Beagle Channel and south of the eastern entrance of the Beagle Channel down to Cape Horn. The preliminary result of that cruise was that the ecosystems on the two sides of the Drake Passage, despite certain coincidences in common faunal and floral groups on genus and species levels, have developed very distinct structures.

The original idea to fly the seven German and four Chilean participants plus two Chilean observers to King George Island failed because of bad weather, and "Polarstern" was ordered to Puerto Williams to pick up the participants on Navarino Island. Thus the activities had to be restricted to the northern slope of the Drake Passage (south of Nueva Island), leaving the intended work in the Bransfield Strait and the southern slope of the Drake Passage to a future cruise. With the reduced programme on the northern slope of the Drake Passage, the benthos group pursued the following objectives:

- To assess the macro- and meiofaunal zoobenthic structures on the northern slope of the Drake Passage and the south Chilean shelf, using gear that had been deployed formerly in the high Antarctic, off the Antarctic Peninsula and in the Magellan region;

- to complement existent benthos samples by material from the areas mentioned above, above all from greater depths;
- to carry out physiological, reproductive, and population dynamic investigations and ethological studies on "key species" and to compare the results with those of related species from lower and higher latitudes.

Work at sea

The original idea was to work on a transect between 1500 m depth on the Patagonian continental slope and 200 m on the shelf south of Isla Nueva, to complete the samples obtained during the "Joint Magellan 'Victor Hensen' Campaign 1994". Part of this transect should have been done during that expedition, but this had to be abandoned due to bad weather.

On ANT XIII/4, 5 working days were available to complete the work south of Nueva. "Polarstern" encountered calm weather but, quite unexpectedly, very rough bottom topography. The layer of fine sediments, if existent, was much thinner than at the stations worked with "Victor Hensen" in the eastern mouth of the Beagle Channel in 1994. For this reason the stations, originally planned on a transect between 2500 and 100 m, had to be chosen where topography, thickness of sediments and currents allowed the use of trawled gear and corers. Even so, by no means all equipments could be deployed at all stations. The final list includes 10 Agassiz trawl (AGT) catches (2 for collecting experimental material only), 3 hauls with the epibenthic sledge (EBS), 9 catches with the small Rauschert dredge (D), 3 multibox corer (MG) stations with 21 macro and 2 meiofaunal samples, 4 multicorer (MUC) stations with 30 meiofauna samples, and 380 pictures with the underwater camera at 5 stations. A CTD rosette registered temperature, salinity and dissolved oxygen between the surface and the seafloor. A large number of macrofaunal organisms were photographed alive, and fish and crustaceans were kept in the cool containers for physiological experiments.

Preliminary results

All samples obtained during this cruise, except for live experimental material, were preserved (for methods, cf. cruise report of the "Victor Hensen" Campaign, Arntz & Gorny 1996) and require detailed analysis in the laboratories of the participating institutions. Definite results will be presented during the IBMANT/97 workshop to be held at the Universidad de Magallanes in April 1997. The following preliminary faunal results, based principally on the sorting of the AGT catches on deck, can be summarized at this time:

A first look at the meiofauna obtained from the filtrate of the multicorer samples and from other gears revealed the following groups to occur (in decreasing abundance): nematodes; copepods (calanoids presumably from the water column, harpacticoids, siphonostomatoids); polychaete larvae; ostracods; and foraminiferans. Other groups are to be expected from further microscopical analysis of the samples.

The macrobenthic endofauna of the multibox corer samples from 100 to 1200 m depth showed low densities which decreased even more with depth. At the shallower stations

the seafloor was covered with a biogenic layer of shells as well as bryozoan and hydrozoan debris, and the dominant faunal elements were ophiuroids, echinoids and crustaceans. At the deeper stations, the substrate (if any) was fine sand, and the only identifiable organisms were small sedentary polychaetes.

The benthic macro and megafauna from AGT and small dredge was richest in number and biomass at medium water depths between 200 and 600 m. Total catch weights in shallow water were high but consisted mainly of dead shells. The deeper seafloor in the area of study seems to be characterized by a generally thin sediment layer which resulted in a large number of gear failures and was further reflected in the dominance of hard-bottom dwellers, in particular gorgonarians. Larger stones came aboard from all depths and were often strongly overgrown with sponges, hydrozoans, bryozoans and gorgonarians whereas bivalve molluscs and brachiopods were missing on the stones altogether.

On the northern slope of the Drake Passage, too, the result from the "Victor Hensen" expedition is valid that there are no such rich, three-dimensional epifaunal suspension feeding communities as in many parts of the Antarctic. However, the occurrence of sponges, bryozoans and gorgonarians revealed a distinct increase as compared with the Strait of Magellan, the Beagle Channel and the eastern mouth of the Beagle Channel, and crinoids (although small and brittle) were found only in this southernmost part of the Magellan area. The scarceness of colonial and solitary ascidians as compared with the Antarctic was confirmed, and actinians were also relatively scarce. Hydrozoans remained common south of Nueva despite the non-occurrence of its principal substrate, the brown alga *Macrocystis pyrifera*, due to greater water depths. Hydrocorals were found frequently on shells and stones.

Asteroids turned out to be much scarcer and smaller than in the Magellan area further to the north. Regular echinoids were at about the same level whereas irregular sea urchins were of much lesser importance than further to the north, particularly in the Beagle Channel, presumably because of the scarceness of soft substrates. The great variety and abundance of ophiuroids on the shelf was further increased by the large gorgonocephalans which contribute an important share to the echinoderm biomass. The find of crinoids has been mentioned already.

Molluscs, especially bivalves, played a minor role south of Nueva except for the scallops (*Chlamys*) which were found to be abundant at some shallower stations. The scarceness of bivalve molluscs, which resembles the conditions in the Antarctic, was unexpected after the dominance of molluscs found in the Strait of Magellan and in the eastern mouth of the Beagle Channel; however, the reason (as for the missing of scaphopods) may again be the lack of soft bottoms. Bivalve species composition was similar to the fauna further north if the taxodont soft-bottom dwellers are not considered. Among the prosobranch gastropods there were some species which had not been found in the regions further to the north. Chitons and octopods were present at a low abundance level. Brachiopods which in the Antarctic "replace" the bivalves as hard-bottom fauna, were only found in a few small specimens, contrary to our results in the Magellan Strait.

The various "worm" groups can be judged only after more thorough analysis. It seems, however, that the scarceness and small size of echiurids and sipunculids stated during the "Victor Hensen" campaign was confirmed, and priapulids were missing altogether (at least on macro level). Polychaetes were common, but always small, and often colonise gorgonarians, bryozoans and hydrocorals.

For the small crustaceans, there is as yet no information available since all material was preserved immediately after trawling. Among the larger forms, balanoids were by no means as common in shallow waters as further north. However, at the deepest stations a large barnacle was found which strongly resembled the Antarctic genus *Bathylasma*. Isopods, in particular Sphaeromatidae, were considerably less common than to the north. Arcturidae and Serolidae, dominant groups in the Antarctic, were found in low numbers but yielded some species we had not seen before. Among the amphipods which dominated the small dredge catches, all families occurred which had been registered for the Weddell Sea and the Antarctic Peninsula area, with Eusiridae, Lysianassidae and Ischyroceridae as dominant groups. Also Stilipedidae, which had never been found in the Magellan region before, were quite common. Among the amphipods and isopods there were no giant types as described for the Antarctic. The same is true for the pycnogonids, and in all three cases this is valid for the whole Magellan region. Several new types of parabioses were detected, e.g., Caprellidae among the spines of lithodid crabs and Ischyroceridae in epizoic bryozoans (*Flustra* type) on majid crabs.

Reptant decapods, in particular of the cancrid and sea spider brachyuran types, were no longer dominant in the area of study. The Galatheidae (*Munida*) still occurred regularly but were much less common than in the eastern mouth of the Beagle Channel. The palinuran lobster *Stereomastis* two specimens of which had been found in the Beagle Channel during the "Victor Hensen" campaign occurred in a single specimen. Caridean shrimps were gaining importance in relation to the reptants but never reached Antarctic levels. Dominant genera are *Campylonotus* and *Austropandalus* as well as surprisingly, at the deep stations, also the Antarctic genus *Nematocarcinus*. As rarities among the decapods first finds of two genera, *Glyphonotus* and *Pontophilus*, have to be mentioned.

Summarizing, the working area on the northern slope of the Drake Passage, south of Nueva Island, revealed a greater similarity to the Antarctic benthic fauna than the Strait of Magellan, the Beagle Channel and the area immediately south of the Beagle Channel. We might cautiously conclude that the transition to the Antarctic is rather of a gradual nature than abrupt. Despite this fact, considerable differences remain between the Antarctic and this southernmost part of the Magellan region. This indicates that 20 million years of separation and isolation, despite some glacial periods of increased interchange, have led to rather distinct separation of two neighbouring marine ecosystems which originally had an identical fauna. A closer look at these phenomena will be taken during the IBMANT/97 workshop in Punta Arenas.

3. Leg ANT XIII/5 Punta Arenas - Bremerhaven 22.05. - 21.06.1996

3.1 Summary and Itinerary

The theme of the scientific programme of the last leg of Polarstern's 13th Antarctic expedition was 'diversity of the deep-sea fauna'. Along the ship's transect (**Figure 23**) the faunistic diversity of microorganisms, zooplankton, meio- and macrobenthic organisms was investigated in order to look for any latitudinal gradients in the distribution patterns. Of special interest were the deep basins in the South Atlantic, where little work has been done to date.

On five deep-sea stations, each greater than 5000 m water depth, four different corers (multibox-corer, rotating-corer, multi- and minicorer) were deployed, providing quantitative sediment samples for analysing the distribution patterns of meio- and macrobenthos. Depth-related and latitudinal distribution patterns of zooplankton were investigated by means of multinet catches from 4 stations; CTD measurements carried out first provided immediate information about the hydrographic structure of the water column at these locations. The microbial deepsea community was studied by means of a newly developed, deep water sampler which provided enriched samples of barophilic microorganisms under collection pressure by pumping and filtering a large volume of sea water in-situ.

Between 47°S and 24°S, a bathymetric profile 1335 sm long was obtained from Parasound surveys, which provide analyses of the bottom topography and sediment structure. The data are stored on analog paper record and also in digital form.

The multibox-corer and the rotating-corer provided a total of 28 single cores from four stations for macrobenthos analysis. Some basic work on the samples has been carried out on board but detailed analyses have to be done at the home institutions. At a first glance, the macro-benthos at the four locations under study seems to be very poor in both abundance and biomass compared to Weddell Sea samples from similar depths. The mini- and multicorers provided a total of 54 sediment cores from four stations. Eight of these were used for microbiological studies and 23 are for investigation of latitudinal diversity patterns of both nematodes and copepods. From initial examinations of the samples, we formed the impression that the meiofauna appears the same compared to other deep-sea sites further north and south. The newly developed, deep-water sampler obtained concentrated water samples from 4 stations under deep-sea pressure. These samples provide data which will form the basis for a description of the composition of the benthic microbial community structure and its biomass and will allow further insights into the existence and role of a decompression- sensitive fraction of bacteria and its biomass and activity.

Temperature measurements in the mesopause of the atmosphere, accomplished with a newly developed, potassium temperature lidar system, completed the scientific work of this leg. The group from the Institut für Atmosphärenphysik in KÖhlungsborn measured profiles of temperature and potassium densities between 47°S and 45°N on 18 nights and

obtained unique and very interesting results about the thermal structure and densities of potassium atoms in the atmospheric layer between 80 to 105 km altitude.

4. Scientific programmes

4.1 Investigations of the atmosphere

4.1.1 Weather Conditions

(Joachim England, Herbert Köhler, Edmund Knuth/DWD)

During our passage through the Strait of Magellan on the night from the May 22th to 23th, the wind conditions often changed due to orographic effects. Wind strength changed on very short time periods between Force 3 to 10. During our passage, the area of the Magellan Strait lay to the rear of a storm low. Behind this disappearing low, a pronounced shallow low developed east of our cruise track, reaching far south to the Antarctic, thus keeping us away from further deep lows which came up from the west. With these conditions our passage along the Argentinian coast line took place in quite calm weather with wind strengths around Force 3 increasing occasionally towards Force 6, the main direction being west to northwest. The first station at 47°S and 55°W could thus be worked under favourable weather conditions.

Above the central South Atlantic, a strong and wide-spread high developed with a pressure of more than 1040 hPa at its centre. On the other side, an association of clouds in front of the East-Brasilian coast, formed a relatively small low pressure whirl which persisted for several days, moving slowly in a northeasterly direction. From May 27th, this low pressure dominated the weather situation. Work on the second station at 38°S and 43°W was hindered by strong wind and consequently rough sea. On May 30th, the wind decreased to Force 3 to 5 backing towards a northerly direction and remaining so for the following day.

On the western border of a wide-spread, strong high over the central South Atlantic, the relatively strong pressure gradient maintained northeasterly winds of Force 6 during June 1st and 2nd. On June 3rd, the wind decreased to Force 4 and the third station could be worked under good conditions. On June 4th and 5th, the wind increased again to Force 6 turning towards a southeasterly direction. During June 5th, heavy showers with gusts up to 36 kn occurred decreasing, however to Force 3 to 4 towards the evening. On June 6th, another station was worked at 4°S 27°W. The wind decreased further from Force 4 to 2, accompanied however by heavy rainfall. In the late afternoon of June 7th, we crossed the equator with winds of Force 1 to 3 from an easterly direction. Light southeasterly winds Force 1 to 3 also dominated in the area of the Intertropic Convergence Zone which we passed during June 8th, when it rained occasionally. On the morning of June 9th, the wind turned towards the northeast with Force 3 to 4. No further rain occurred and weather was influenced by the northeast trades.

This situation remained until June 14th. Winds of Force 3 to 4 were a regular feature from then on and the last station at 230N 24°30'W was worked under favourable meteorological conditions. Between June 15th and 20th, light winds of Force 1 to 4 from different directions dominated along the ship's track. The feared Bay of Biscay and the Channel were amazingly calm this time. Approaching Bremerhaven on June 21st wind increased again to Force 6 or 7, with northern to northeasterly directions due to a deep low over Scandinavia.

4.1.2 Temperature observations in the mesopause

(Matthias Alpers, Veit Eska, Josef Hbffner, Ulf von Zahn/IAPR)

Objectives and methods

The scientific objectives of the IAPR participation in the legs ANT XIII/4-5 have been the exploration of both the thermal structure of the atmospheric layers in the 80 to 105 km altitude, and the densities of potassium atoms residing therein. At this altitude, the atmosphere exhibits a permanent deep, local temperature minimum (the so-called mesopause). However, little is known about the precise temperatures at the mesopause and their spatial and temporal variations. This is particularly true for the southern hemisphere. The potassium atoms, present in this region, are remains from the vaporisation of micrometeorites (i.e. shooting stars) and cosmic dust. The loss processes for these atoms are unknown. Yet, there exists a permanent layer of potassium which exhibits a maximum density of about 100 atoms per cm⁻³ at approximately 90 km altitude.

For remote sensing of the air temperature and potassium density, we used for the first time, a transportable, containerized, lidar instrument ('light radar'). It operates at the resonance wavelength of potassium at 770 nm (near infrared). From a measurement of the time which passes between emission of the laser pulse and arrival of the atmospheric echo signal in the instrument's detectors, one can calculate quite accurately the altitude of the scattering air volume. By means of a tiny modulation of the wavelength of the laser light, one can also measure the temperature of the potassium atoms between 80 and 100 km altitude. This temperature is a good approximation to the air temperature.

Work at sea and preliminary results

The observational programme, the data analysis and its interpretation, for legs ANT X111/4 and ANT XIII/5, all form a scientific entity for us and therefore we summarize the results obtained in both legs here.

The first night of lidar observations was March 25th, the last the June 18th, 1996. Within this period lie a total of 31 nights with measurements of temperature and potassium density and an additional 4 nights with measurements of potassium density only. The excellent performance of the lidar and unexpectedly good weather contributed to these good observation statistics.

Observations were made from 71°S to 45°N. Seasons changed from late autumn/early winter at high southern latitudes to "deep winter" at south-tropical latitudes and then to high summer in the northern hemisphere. For our research program, this type of variation was almost ideal. Almost all measured profiles of air temperature and potassium density are characterized by high wave activity in the upper atmosphere. This general property of the upper atmosphere is well known, but makes the determination of genuine climatological mean parameters difficult. Though in fact one just needs a very large data base. We were fortunate, therefore, to be able to obtain 4 nights of continuous observations lasting more than 12 hours plus 3 nights of more than 9 hours. These long observation series will allow us to characterize and quantify the wave spectrum and to derive corrections for the shorter observation sequences. The altitude and temperature of the mesopause was measured over a rather wide range of latitudes with high temperature accuracy and altitude resolution. We obtained new and interesting results pertaining to the latitude dependence and seasonal variations of the mesopause altitude and temperature (although we acknowledge that a clean separation of the two effects in our data will be somewhat subjective). In the southern hemisphere there are, however, no other measurements available with which we could compare our newly acquired data.

Before now, potassium density profiles have been measured in the upper atmosphere in only two locations. For that reason, all of the acquired potassium data are entirely new. We observed an outstanding variation of the potassium density with latitude and a previously unobserved high occurrence rate and intensity of so-called sporadic potassium layers. An example of atmospheric wave activity showing up in the potassium profiles is given in [Figure 25](#). The 59 potassium density profiles, which we acquired on June 7th, 1996, between about 2 and 7 pm. (UT) near YS are shown. The temporal separation of the profiles is 4 min. The number density scale at the abscissa applies to the first left profile. Each following profile is offset to the right by a value of 10 atoms per cm⁻³. During this night, the normal potassium layer extended from 80 to 100 km altitude. The density profiles are modulated by the passage of waves through the background atmosphere. In addition, there are a few short-lived sporadic layers near 90 km.

4.2 Marine Biology

4.2.1 Microbiology

(Erich Dunker, Elisabeth Helmke, Ulla Klauke/AWI)

Objectives and methods

During usual sampling of sediment or water, deep-sea organisms experience decompression. The central question of the microbiological work during this leg was whether, and if so, to what extent, such decompression affects the microbial deep-sea assemblages. The results will contribute to a better understanding, as well as to a realistic quantification, of the microbial processes in the deep-sea. A prerequisite of this study was a recently developed water sampler which concentrates particulate organic matter in-situ and brings it up to the surface maintaining in-situ pressure. Subsequent subsampling on board can be conducted without pressure loss.

As well as these investigations on the existence and role of decompression-sensitive bacteria, studies of biomass, activity, and structure of the benthic microbial community from the deep sea were carried out with the decompressed sediment and water samples of the multicorer. The results will supplement our data set from the microbial flora of different deep-sea basins of the north and east Atlantic.

Work at sea

The pressure-retaining water sampler was deployed at four stations. Concentrated water samples were obtained under deep-sea pressure. They were subdivided and subjected to different experimental conditions. The final evaluation of these experiments will be done at the home laboratory. The same is true for the measurements and the experiments with the decompressed multicorer material.

Subsamples of the sediment and bottom water were fixed and preserved for total count and biomass determinations as well as for the chemical analyses. Furthermore, growth and degradation experiments were prepared under simulated deep-sea conditions. In order to describe the structure of the benthic microbial deep-sea community, MPN-cultures were conducted. Since the MPN-cultures were subjected to different pressure and temperature conditions, a differentiation of allochthonous from autochthonous deep-sea bacteria will be possible.

4.2.2 Zooplankton

(Harald Bohlmann, Birgit Strohscher/AWI)

Objectives and methods

Studies of mesozooplankton diversity and biomass of the whole water column were addressed by means of multinet hauls (150 gm mesh size) from 5 deep-sea stations at 9 depth intervals. Vertical and horizontal biodiversity, biomass distribution patterns and length/carbon -content relationships of different-sized specimens with species from different water depths will be established. Studies of gut content and reproductive condition of dominant copepod species completed the working programme.

Work at sea

CTD measurements (SEABIRD 911 plus) were carried out before the multinet was deployed in order to provide immediate information about the hydrographic structure of the water column at the sampling locations. Four profiles are displayed in **Figure 26**. The multinet was successfully deployed at 4 stations. The station data are summarized in Annex 5. Samples were taken from the following depth intervals:

St. Nos. 118 and 122:	3600 - 2600 m	2600 - 2000 m	2000 - 1500 m
	1500 - 1000 m	1000 - 0 m	with multinet No. 1
	1000 - 750 m	750 - 500 m	500 - 300 m
	300 - 100 m	100 - 0 m	with multinet No. 2
St. Nos. 119 and 121:	3000 - 2500 m	2500 - 2000 m	2000 - 1500 m
	1500 - 1000 m	1000 - 0 m	with multinet No. 1

Multinet No. 2 at these stations sampled the same depth intervals as in the first two stations.

All samples were carefully filtered through 100 µm sieves and preserved in a 4% formaldehyde solution buffered with hexamethylenetetramine. The 1000 - 0 m sample of multinet No.1 from each station was split into two halves by means of a plankton splitter. One half was frozen for estimating the biomass later in the laboratory, while from the other half, different species groups were sorted out on board for various analyses, e.g. length/carbon -content relationships and studies of gut content and maturity stage. The detailed analyses of the material obtained has to be done at the home institution.

4.2.3 Meiobenthos

(Nicola Jane Debenham/NHM, Timothy John Ferrero/NHM, Pedro Martinez-Arbizu/FBZO, Gisela Silveira Moura/FBZO)

Objectives and methods

Recent studies have indicated the importance of the deep sea as an environment of high species diversity. Latitudinal diversity gradients in the South Atlantic are poorly studied and seem to be highly influenced by interregional variation and regional/historical processes. Patterns of diversity from the North Atlantic have been mainly derived from macrofauna and nematode studies. Only a few studies deal with other groups like foraminiferans and copepods. Our planned study will give us a first indication of latitudinal deep-sea diversity patterns in the South Atlantic. Low abundances and high variability are expected in the deep-sea, therefore a high number of replicates is needed. Quantitative samples were taken with the Multicorer.

The scope of the work is to undertake a latitudinal study of meiofauna abundances, their spatial distribution and their diversity. This allows us to correlate these parameters of the benthic fauna with surface productivity at the different stations. This work provides valuable information on the Southern Atlantic and is invaluable for comparison with data from the Madeira Abyssal Plain, Porcupine Abyssal Plain, and Arctic Ocean (Barents Sea, Laptev Sea) in the North Atlantic, and some Antarctic sampling sites in the Weddell Sea. It is hoped that the data will enable an assessment of the biogeographical range and species turnover rates of abyssal meiofauna, particularly nematodes and copepods.

Work at sea

In total, four stations were successfully sampled with the Multicorer (MUC). Two of these stations were additionally sampled with the Minicorer (MIC). An overview of the sampling regime is given in **Table 8**. The area sampled by each corer covers about 25 cm². The individual corers in the MUC were numbered and their position in the gear documented, so that the relative distances between replicates can be determined.

Table 8: Material and treatment; A: for microbiology, B: sliced for meiofauna, C: homogenisation technique for meiofauna studies and biochemistry

Station No.	Depth	MUC/MIC	Treatment
40/118	5726 m	Muc 11 corers	2 x A, 9 x B
40/119	5095 m	-	
40/120	5130 m	Muc 12 corers	2 x A, 10xB
40/121	5366 m	Muc 12 corers	2 x A, 10xB
40/122	5055 m	Muc 11 corers	2 x A, 9 x B
40/121	5362 m	Mic 4 corers	2 x B, 2 x C
40/122	5102 m	Mic 4 corers	2 x B, 2 x C

For the study of the melofauna (treatment B) the cores were sliced in 6 sections. The first section includes the first centimetre of sediment (0-1 cm) and the overlying bottom water, the remaining sections were 1-2 cm, 2-3 cm, 3-4 cm, 4-5 cm and 5-10 cm. Samples were fixed with buffered 4% formaldehyde in filtered seawater.

Homogenisation technique (treatment C): Cores were sectioned to 5 cm in 1cm horizons. Each section was homogenised to a semi-liquid state with the addition of artificial seawater and the resulting homogenate divided into two equal subsamples. One subsample will be for meiofauna studies and the other for sediment biogeochemical analysis (mainly lipids and proteins) at the University of Liverpool, Dept. of Oceanography.

Preliminary results

The sediments at the four stations sampled are very different. At Station No. 40/118, in the Argentinian Basin the sediment has a significant sandy component and gravel is also observed. Station No. 40/120 is a brownish and very compact sediment, while at Station No. 40/121 (both in the Brazilian Basin) the sediment is reddish-brown, soft and with many burrows of macrofaunal organisms. The sediment at Station No. 40/122 (Cape Verde Basin) is pale, and very consistent, with a high component of Globigerina tests.

The preliminary observations of changes in sediment type along this transect, associated with likely differences in productivity and nutrient supply to the benthos, suggest that there will be detectable differences in the meiofauna. This would present similar results to those previously observed in the North Atlantic. Preliminary observations of the fauna (mainly nematodes and copepods) suggest that the greatest difference will be observed at the species level as some typical deep-sea genera have been observed. This is consistent with the concept of the deep-sea as a high diversity environment.

4.2.4 Macrobenthos

(Harald Bohlmann, Dieter Gerdes/AWI, Peter Albert Lamont/SAMS)

Objectives and methods

The cruise from Punta Arenas to Bremerhaven provided the opportunity to sample deep-sea organisms across a wide range of latitudinal gradients in the Atlantic. Over the last few decades much deep-sea benthos data has been accumulated for the North Atlantic as far south as the Madeira Abyssal Plain but data for the South Atlantic is sparse. Therefore our main objective was to get as many quantitative samples as possible from the deep basins especially those of the South Atlantic by means of a multibox-corer and a newly developed rotating-corer. These samples provide the data basis for investigation of the vertical distribution of the animals in the sediment and for determining diversity trends along latitudinal gradients. The data will form part of the basis for the BIODEEP proposal.

Work at sea

The multibox-corer (MG) with the attached underwater-video system was deployed at 4 stations. During deployment at Stn. No. 40/119, the Revolvergreifer was damaged by ship movement in the rough sea and the gear could not be used again for the duration of the cruise. The multibox-corer, was not deployed at this station due to the bad weather conditions and rough sea. The results of both corers are summarized in Table 9

Table 9: Inventory of cores taken with the multibox-corer (MG) with the attached UW-video system and the Revolvergreifer (RG).

Stn. No.	water depth (M)	MG number of cores	RG number of cores
40/118	5732	0	1
40/119	5088	-	0
40/120	5152	9	-
40/121	5374	9(*)	-
40/122	5118	9(*)	-

(*) bottom pictures via UW-video - not deployed

In total, 28 single cores were obtained from 4 stations between 47°S and 230N for analysis of the macrofauna. The mean core length was 38 cm. Part of the MG cores from Stn. Nos. 40/120 and 40/121 had disturbed surfaces, because the cores were very full due to the soft sediments at these locations. All cores were treated according to the following procedure:

Each core was divided vertically by syphoning off the top water and removing the top centimetre, approximately, of sediment. The remainder of the core was then divided into ten centimetre slices and the sediment placed directly into five litre tubes containing 2 litres of 4% formaldehyde cooled to 4°C. As soon as possible after immediate processing of the cores, the sediment was gently manipulated by hand to mix in the formalin. Sieving

through 500 and 300 μm mesh was carried out at least 3 days after collection to allow time for preservation. After sieving, samples were stored in 4 % formaldehyde prior to sorting. It is considered that this procedure improves the condition of more vulnerable fauna such as polychaetes, which are often damaged on sieves when freshly collected.

Preliminary results

The main work on the samples has to be carried out at home institutions. The basis for our preliminary impression given here is due to the careful sample treatment described above and first microscopic sorting of some core fractions on board ship, especially those from the Revolvergreifer core of Stn. No. 40/118.

The dominant elements of the small, deep-sea macrofauna in our samples are polychaetes (sabellids, spionids, cirratulids, nephthyids, ophelids, and ampharetids plus a number of undetermined worms in tubes), bivalves, sipunculids and a few crustaceans. It appears that highest organism numbers occur at the southernmost station 40/118, followed by the northern station 40/122, whereas abundance values at the other two stations seemed to be lower.

The sediment at Stn. No. 40/120 is especially fine and for all 9 MG cores obtained there is virtually no material, including organisms, remaining on the 500 μm sieve, and only a few mineral grains were retained on the 300 μm sieve. Macrofauna abundance at this station appears to be very low. Samples from Stn. No. 40/121 have burrows extending the full depth of the core. Some of these burrows are up to 6 mm in diameter and 1 sipunculid worm about 40 mm in length was recovered from the base of a core at about 25 cm depth.

5. Acknowledgement

The achievements during both legs were to a large extent due to the effective and heartfelt cooperation between the ship's crews and the participating scientific personal. We are grateful to the Masters Pahl and Keil and their crews for the active support which helped us to overcome difficult situations and resulted not only in a scientific success, but as well in a cheerful experience. We are grateful as well to all those who were involved in the different levels of the preparations for cruise and built up the basis for our success.

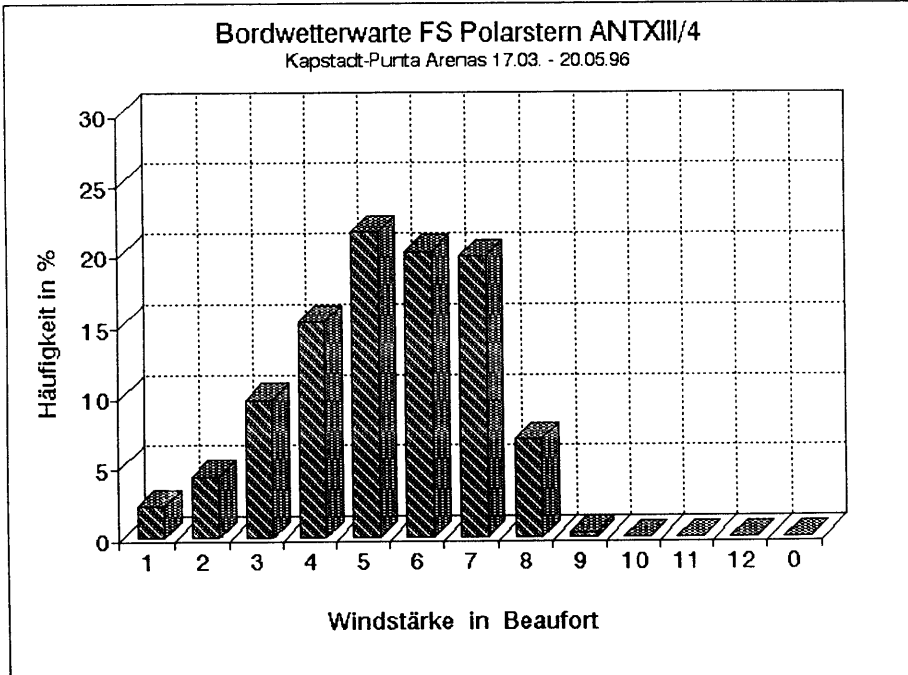
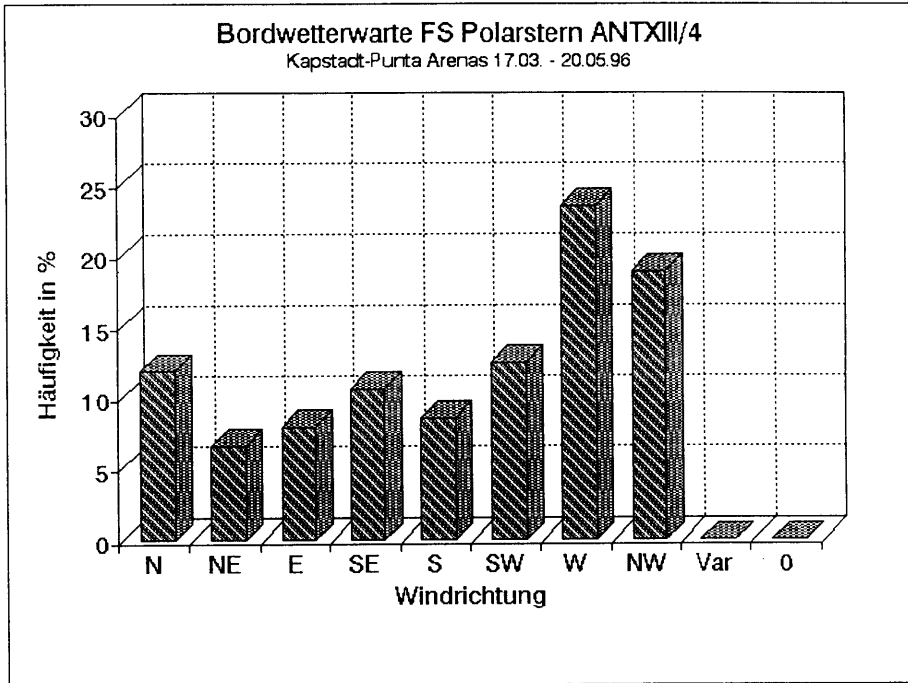


Figure 2: Frequency distribution of wind speed and direction

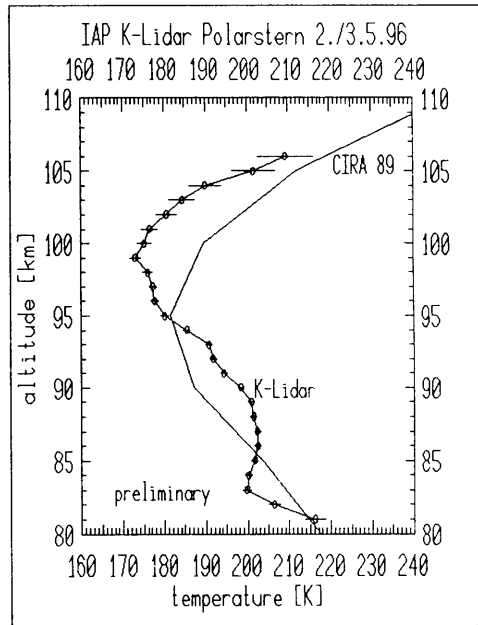
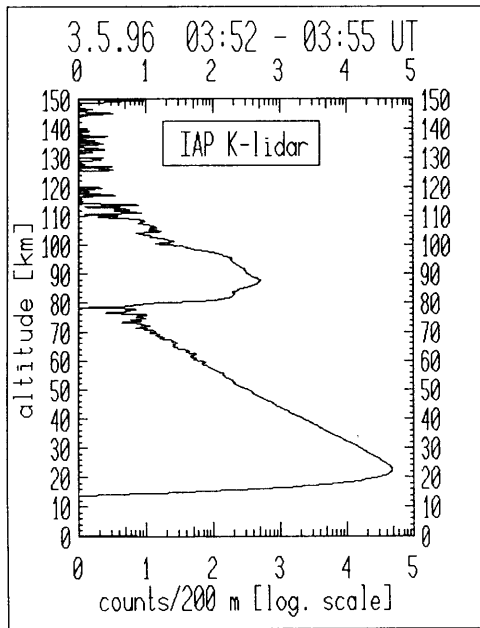


Figure 3: Backscattered profile (4000 laser pulses) and temperature profile up to 106 km at the night from May 2/3

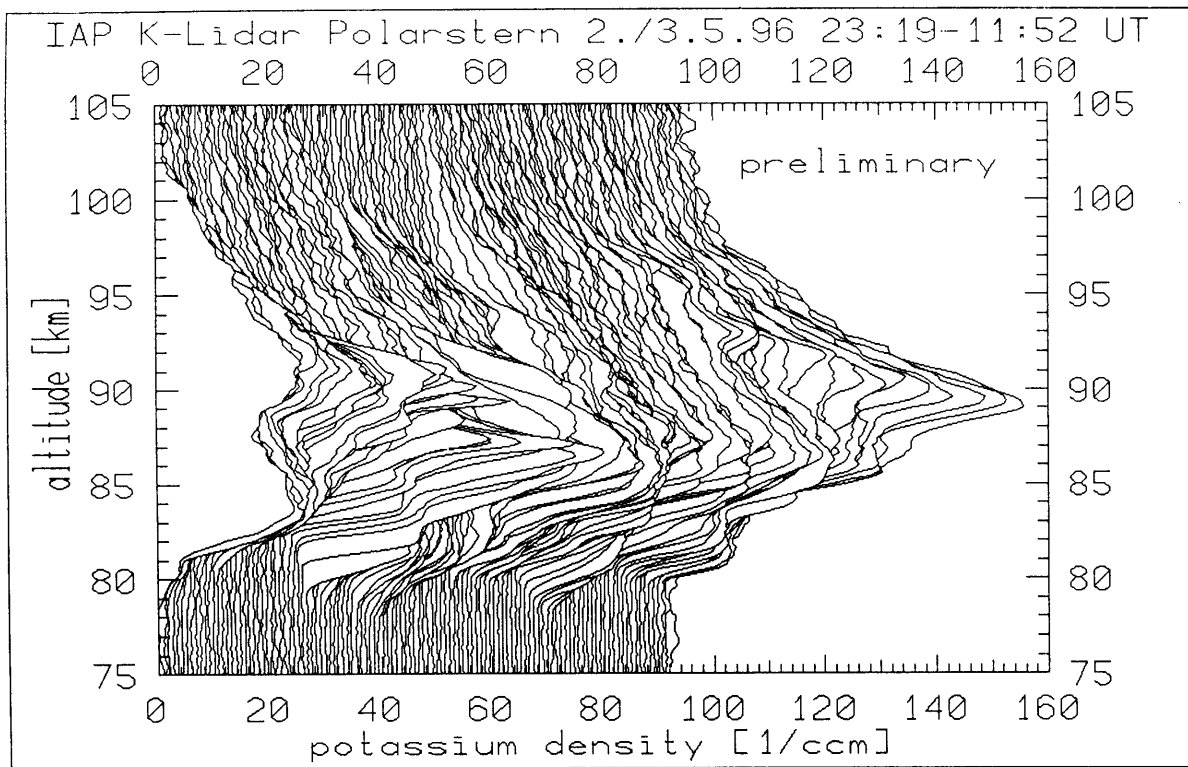


Figure 4: Density profiles of the potassium layer measured in the night from May 2/3, (23:19-11:52 UT).

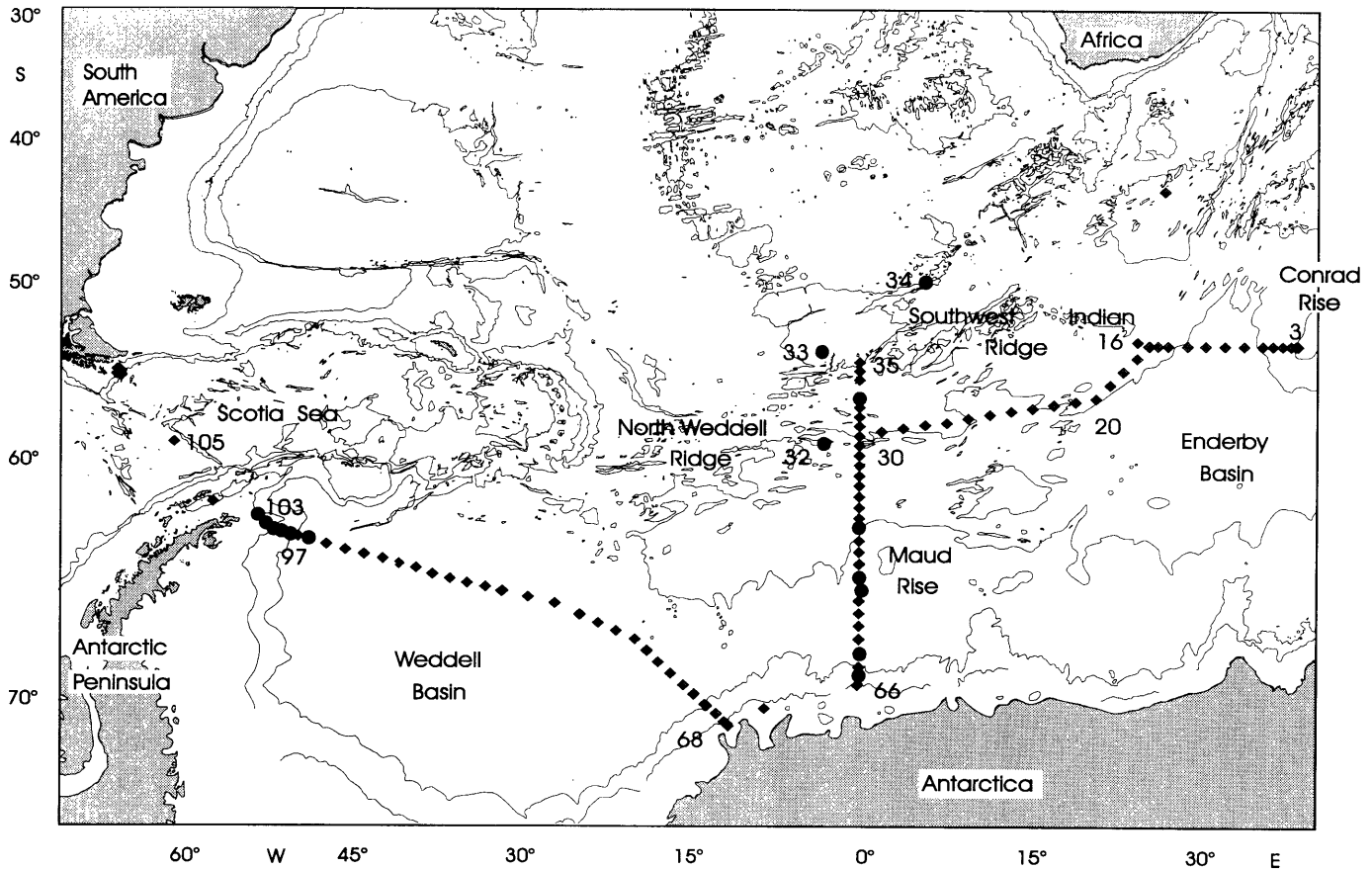


Abb. 5: Lage der hydrographischen Stationen (Quadrate) und der Verankerungen (Kreise) im Weddellmeer.
 Figure 5: Location of the hydrographical stations (squares) and mooring positions (dots) in the Weddell Sea.

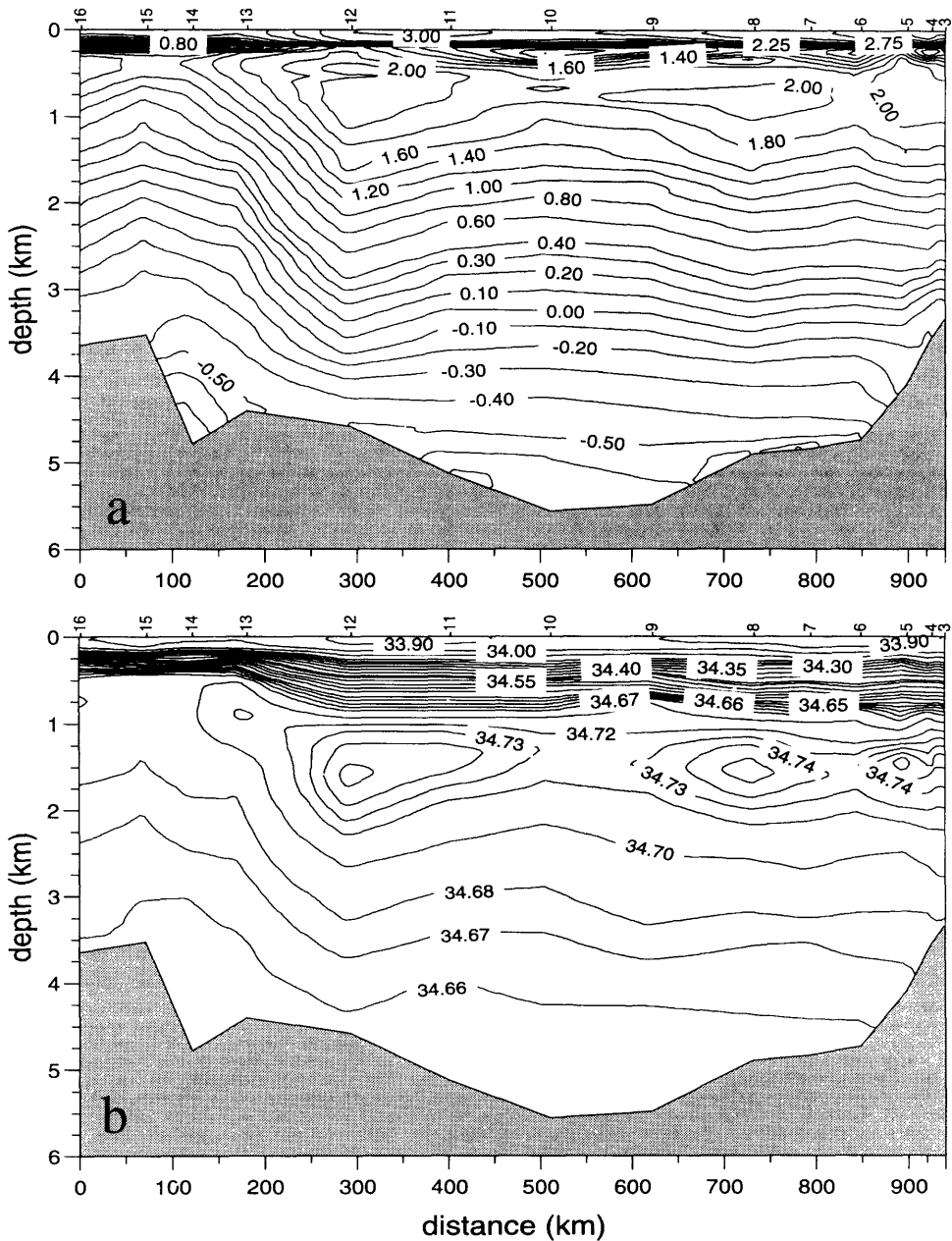


Abb. 6: Vertikalschnitt der potentiellen Temperatur (a), des Salzgehalts (b), des Sauerstoffs in $\mu\text{mol/kg}$
 Figure 6: Vertical section of potential temperature (a), salinity (b), oxygen in $\mu\text{mol/kg}$

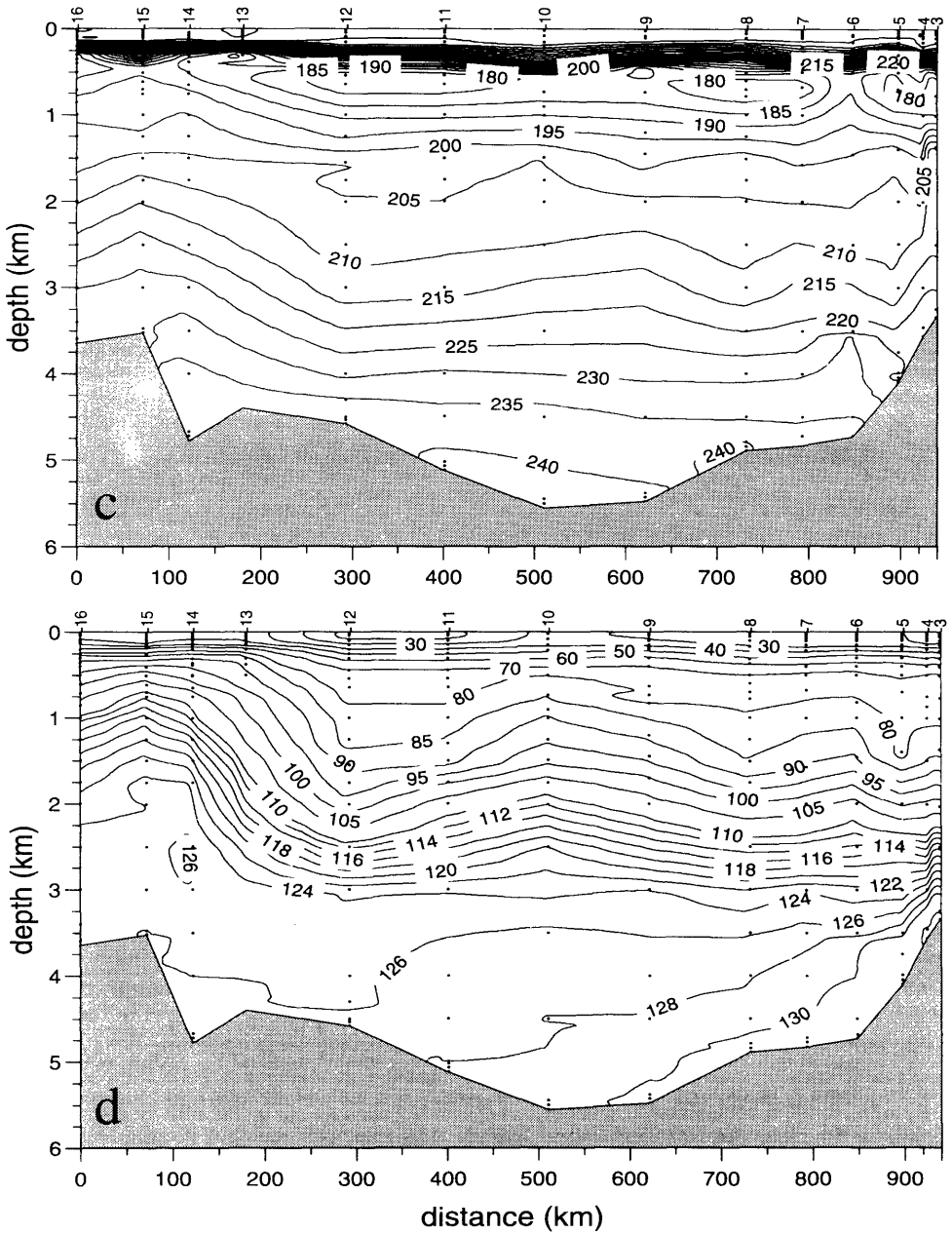


Abb. 6: Vertikalschnitt der potentiellen Temperatur (c) und des Silikats in $\mu\text{mol/kg}$ (d) durch den östlichen Rand des Weddellmeers entlang 54°S von $24^\circ 41'\text{E}$ bis 39°E .

Figure 6: Vertical section of potential temperature (c) and silicate in $\mu\text{mol/kg}$ (d) across the eastern boundary of the Weddell Sea along 54°S from $24^\circ 41'\text{E}$ to 39°E .

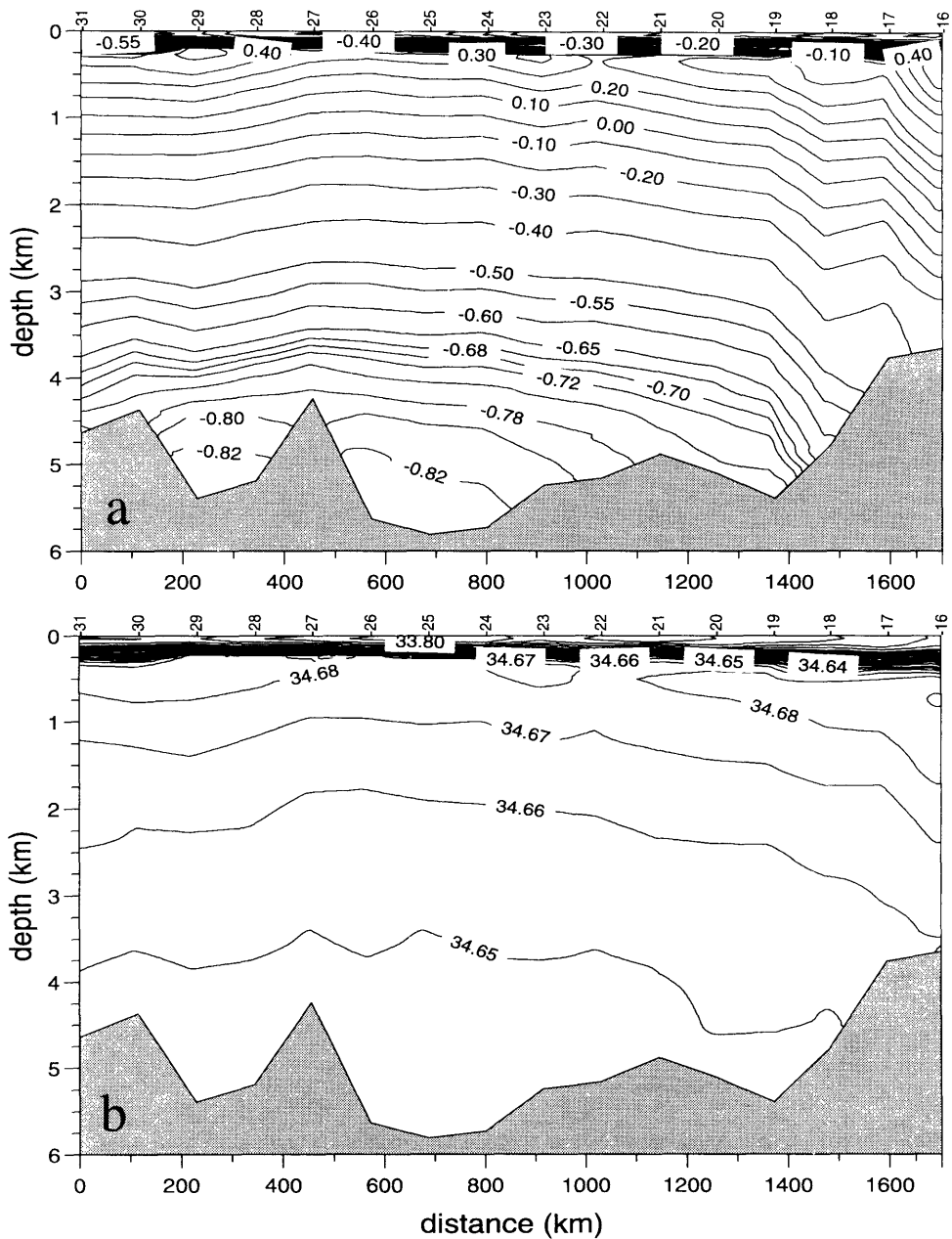


Abb. 7: Vertikalschnitt der potentiellen Temperatur (a), des Salzgehalts (b), des Sauerstoffs in $\mu\text{mol/kg}$
 Figure 7: Vertical section of potential temperature (a), salinity (b), oxygen in $\mu\text{mol/kg}$

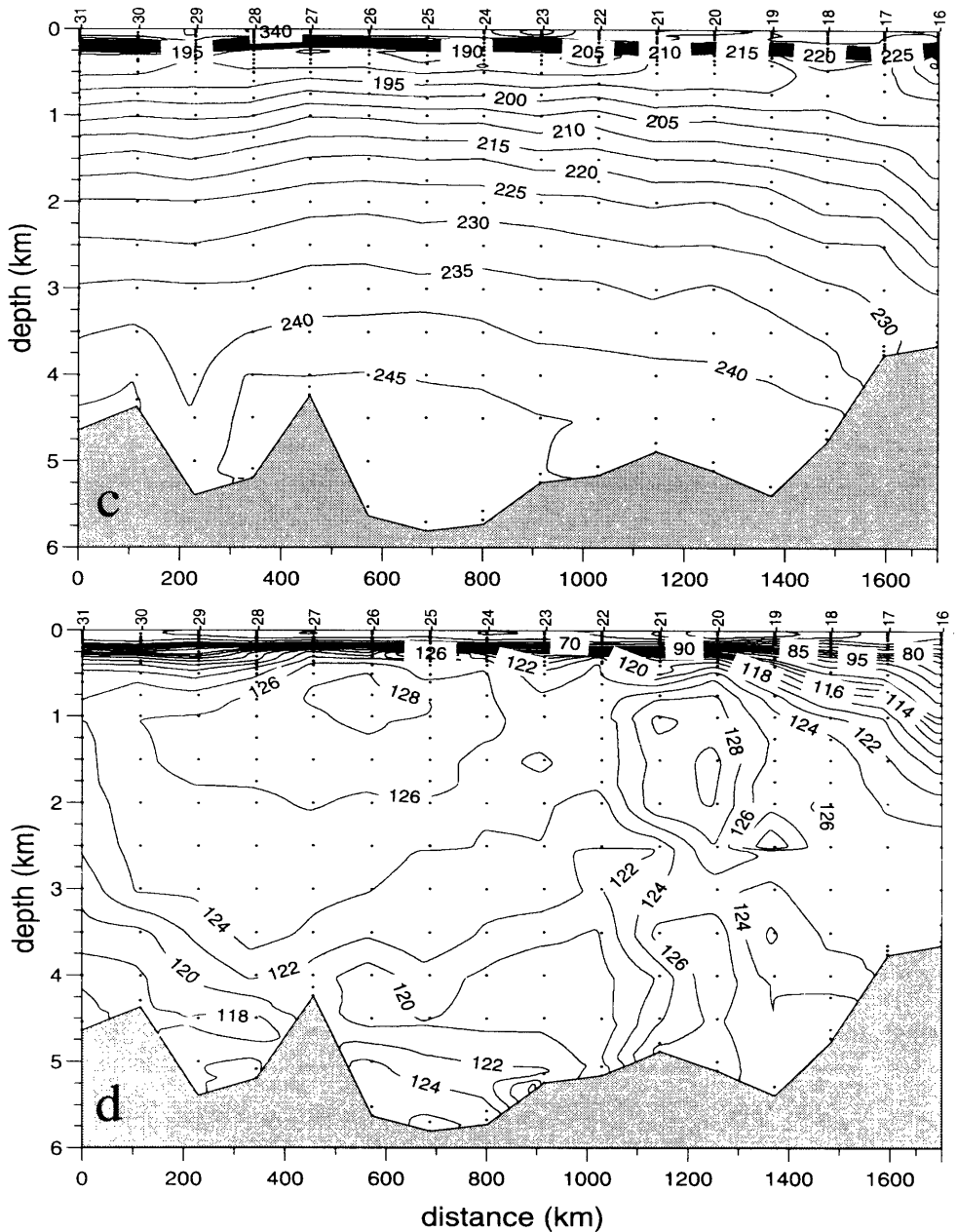


Abb. 7: Vertikalschnitt der potentiellen Temperatur (c) und des Silikats in $\mu\text{mol/kg}$ (d) durch das östliche Weddellmeer von $59^{\circ}30'S$ 0° bis $54^{\circ}S$ $24^{\circ}41'E$.
 Figure 7: Vertical section of potential temperature (c) and silicate in $\mu\text{mol/kg}$ (d) across the eastern Weddell Sea from $59^{\circ}30'S$ 0° to $54^{\circ}S$ $24^{\circ}41'E$.

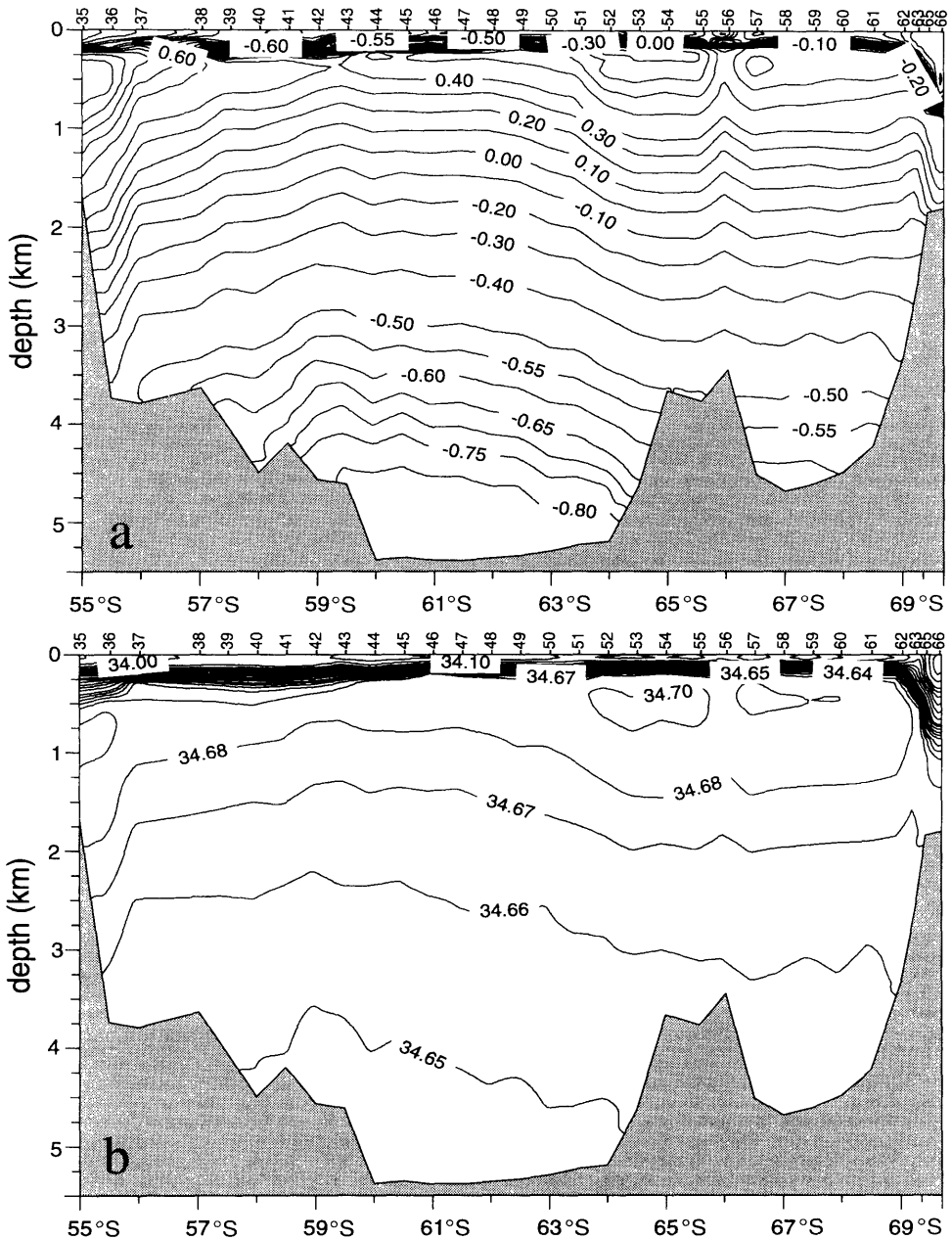


Abb. 8: Vertikalschnitt der potentiellen Temperatur
 (a), des Salzgehalts (b), des Sauerstoffs in $\mu\text{mol/kg}$
 Figure 8: Vertical section of potential temperature
 (a), salinity (b), oxygen in $\mu\text{mol/kg}$

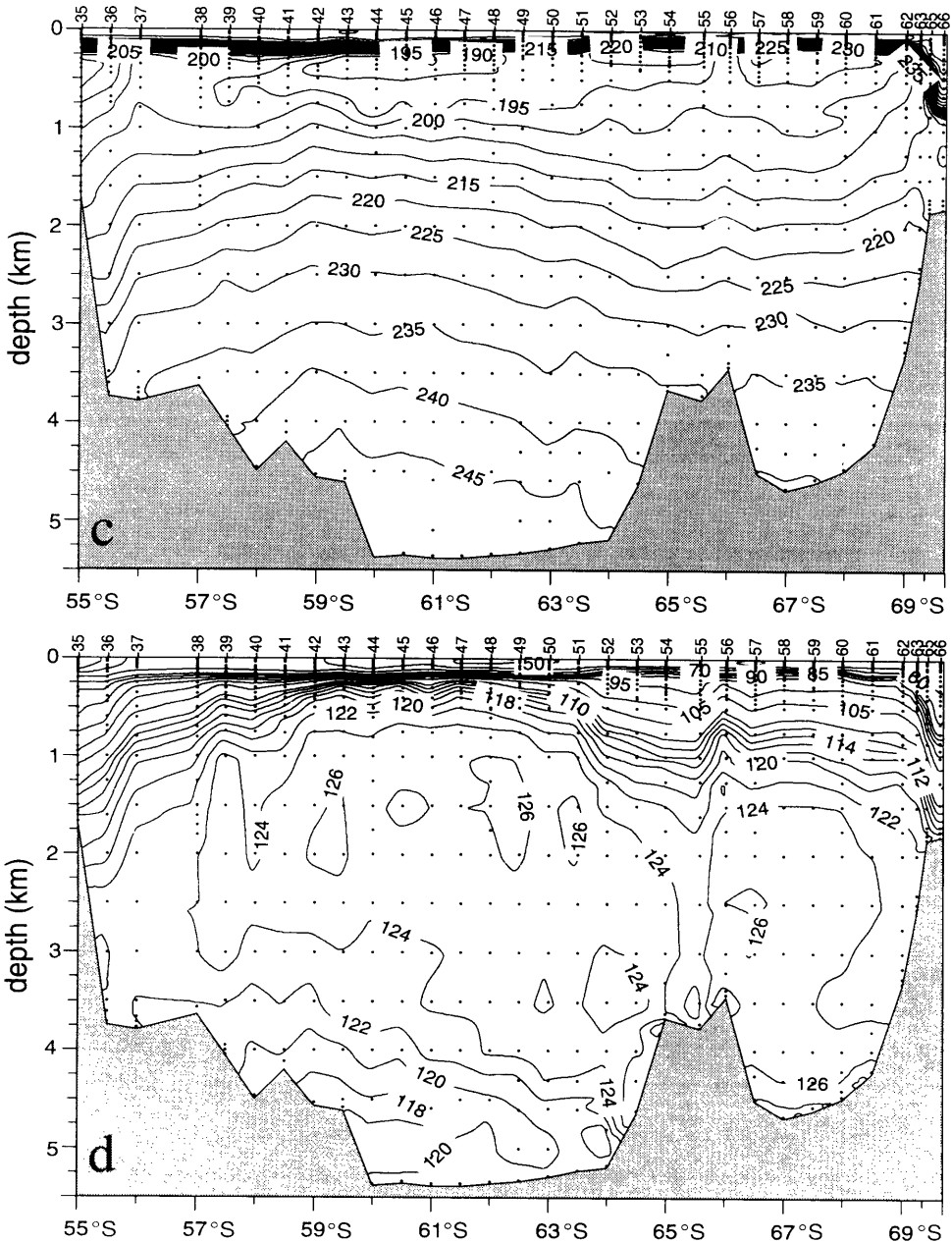


Abb. 8: Vertikalschnitt der potentiellen Temperatur (c) und des Silikats in $\mu\text{mol/kg}$ (d) durch das Weddellmeer entlang dem Nullmeridian von 55°S bis 69°38.5'S.

Figure 8: Vertical section of potential temperature (c) and silicate in $\mu\text{mol/kg}$ (d) across the Weddell Sea along the Greenwich Meridian from 55°S to 69°38.5'S.

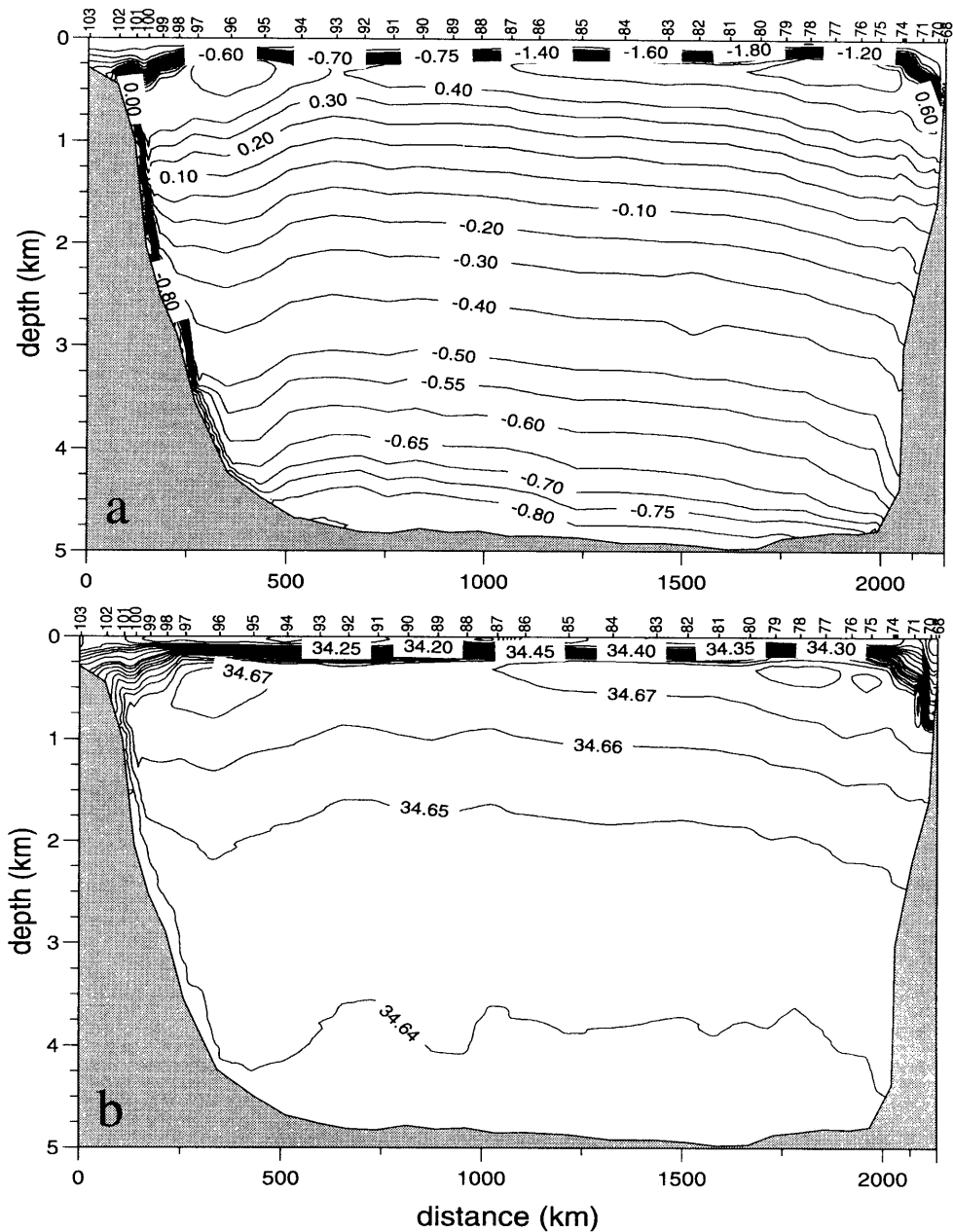


Abb. 9: Vertikalschnitt der potentiellen Temperatur
 (a), des Salzgehalts
 (b), des Sauerstoffs in $\mu\text{mol/kg}$
 Figure 9: Vertical section of potential temperature
 (a), salinity
 (b), oxygen in $\mu\text{mol/kg}$

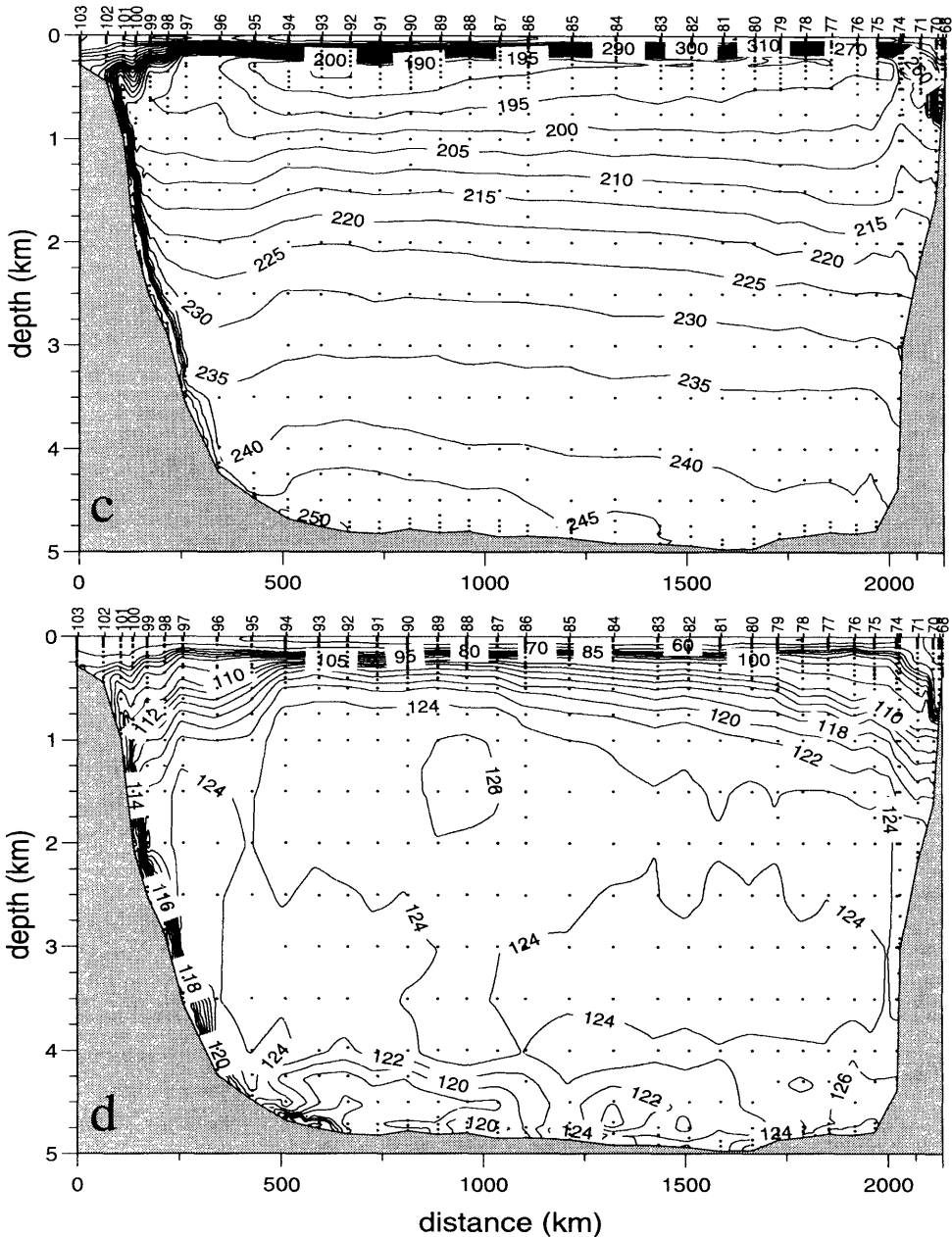


Abb. 9: Vertikalschnitt der potentiellen Temperatur (c) und des Silikats in $\mu\text{mol/kg}$ (d) durch das südliche Weddellmeer von Joinville Island nach Kapp Norvegia.

Figure 9: Vertical section of potential temperature (c) and silicate in $\mu\text{mol/kg}$ (d) across the southern Weddell Sea from Joinville Island to Kapp Norvegia.

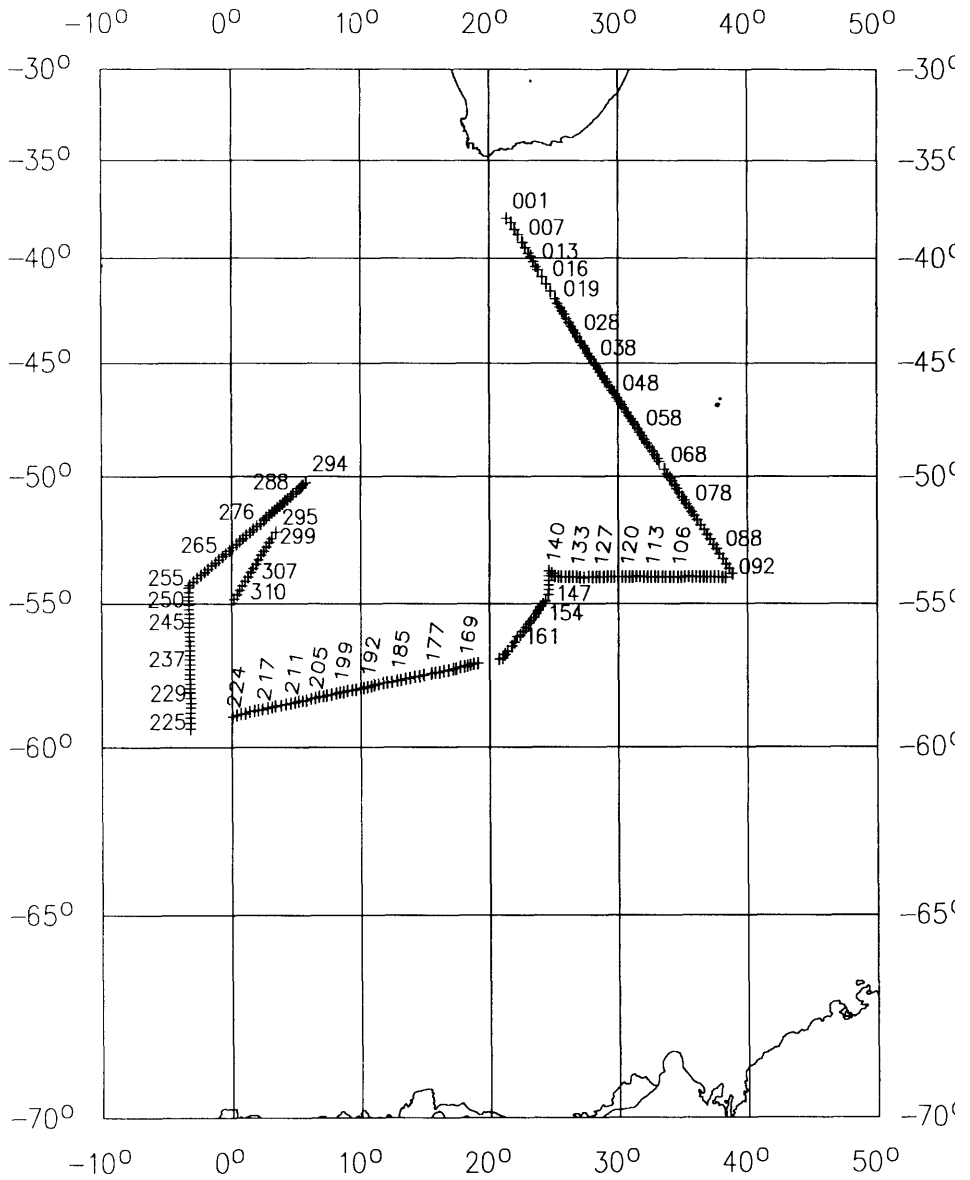


Abb. 10: Lage der XBT-Schnitte.

Figure 10: Location of the XBT-sections.

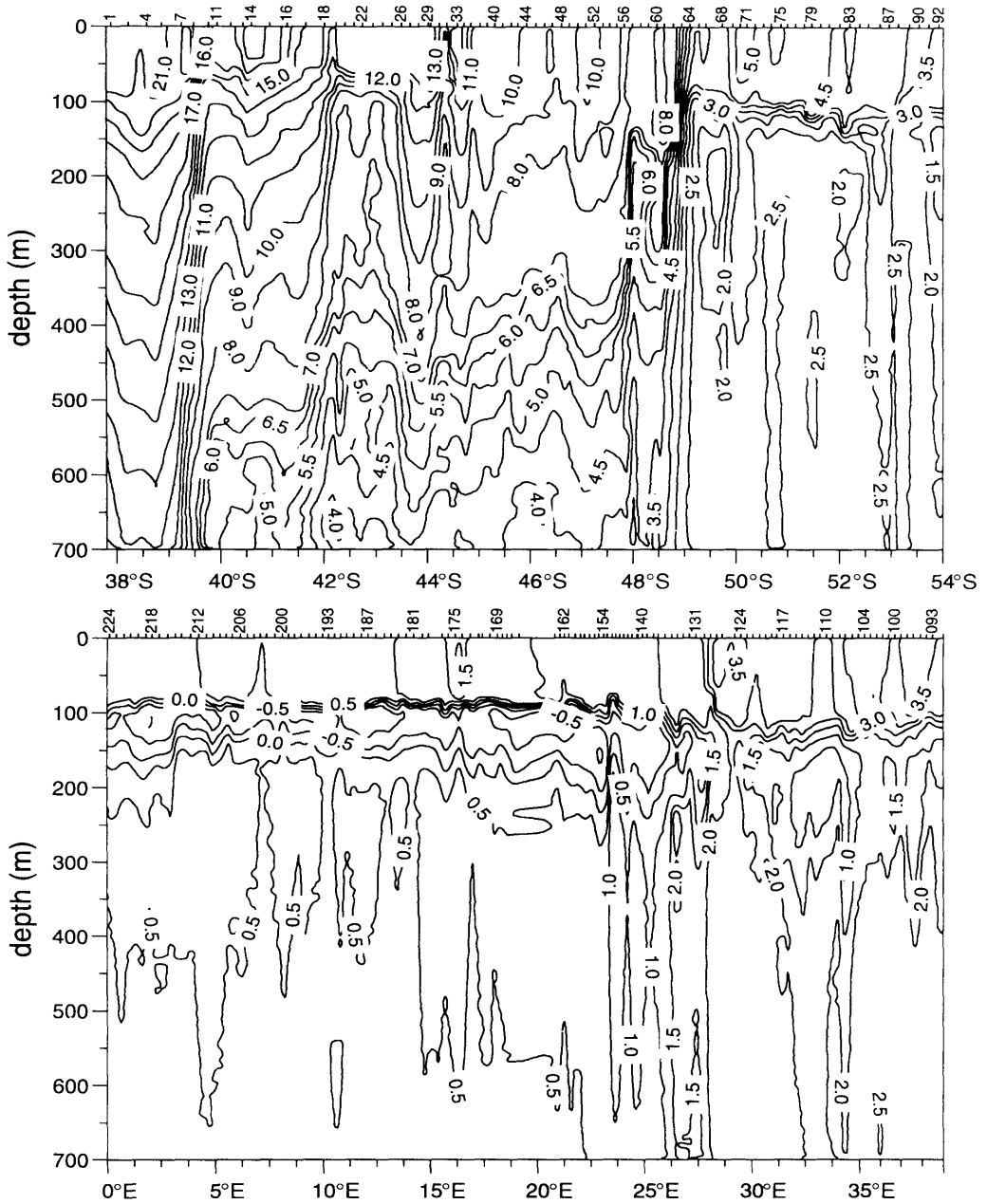


Abb. 11: XBT-Schnitt durch den Antarktischen Zirkumpolarstrom (oben) und den östlichen Weddellwirbel (unten).
 Figure 11: XBT-section across the Antarctic Circumpolar Current (top) and the eastern Weddell gyre (bottom).

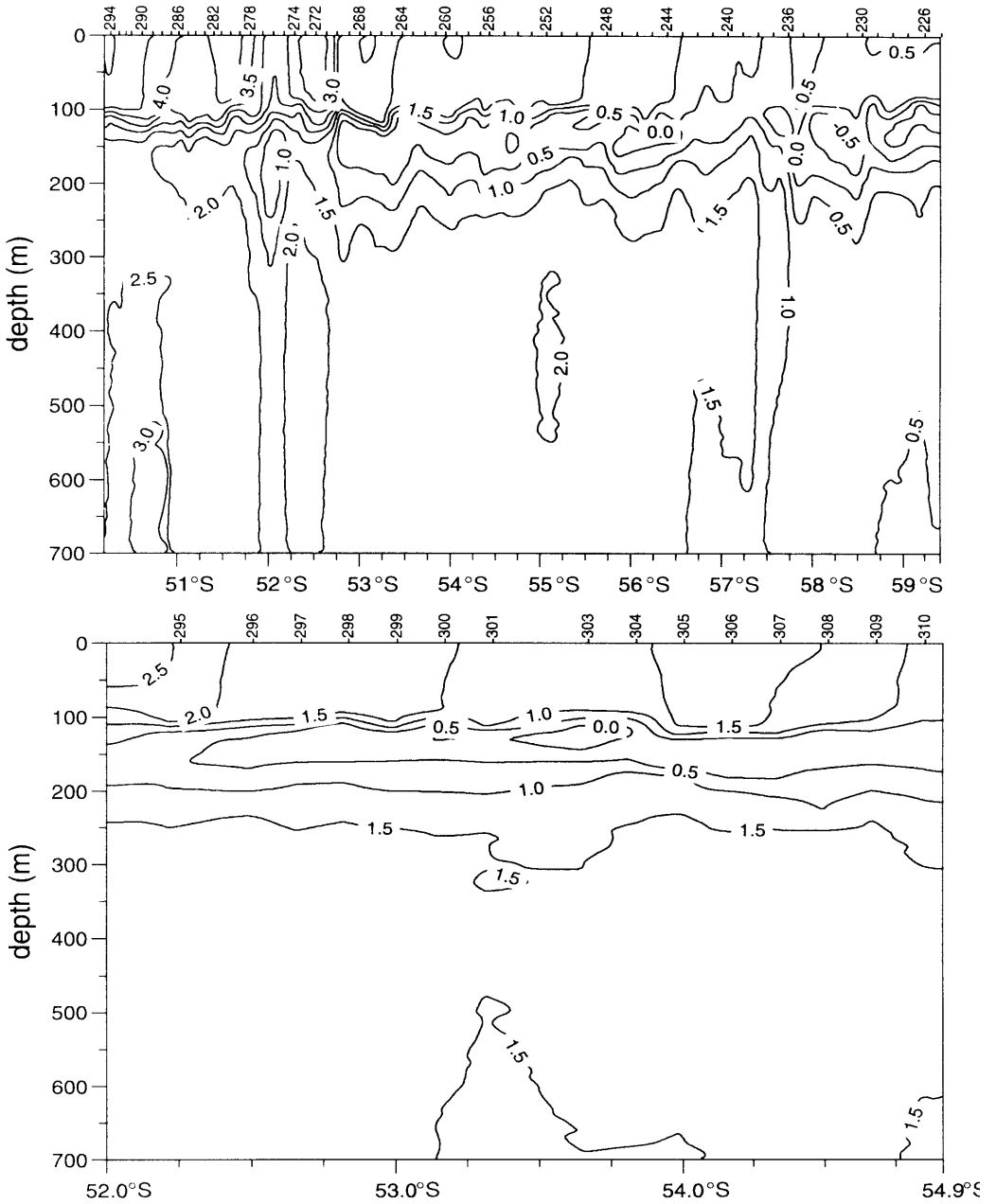


Abb. 12: XBT-Schnitt vom Weddellwirbel zum Antarktischen Zirkumpolarstrom (oben) und durch den südlichen Antarktischen Zirkumpolarstrom (unten).

Figure 12: XBT-section from the northern Weddell gyre to the Antarctic Circumpola. Current (top) and across the southern Antarctic Circumpolar Current (bottom).

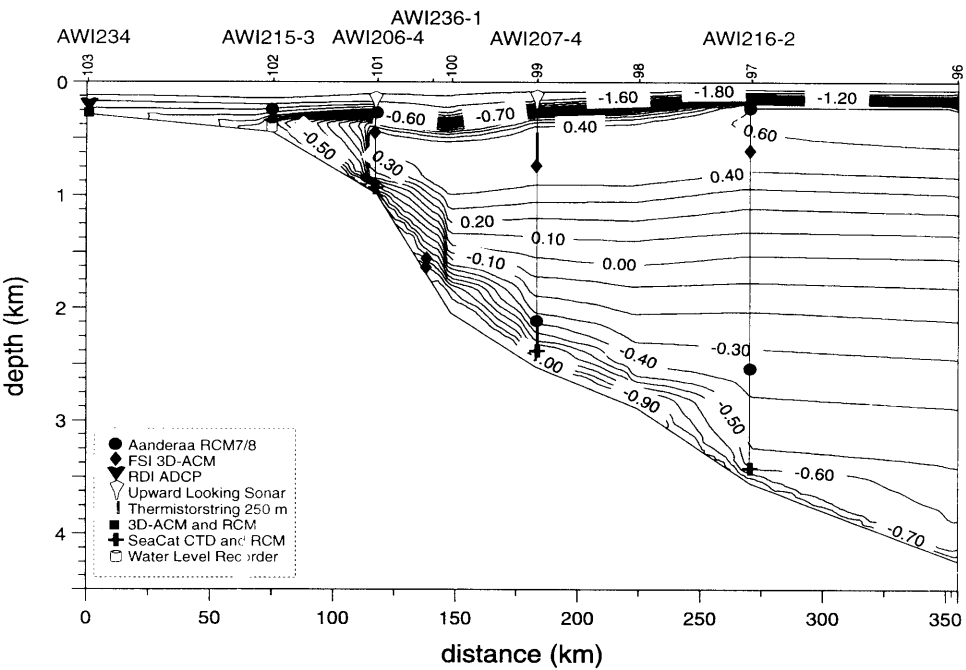
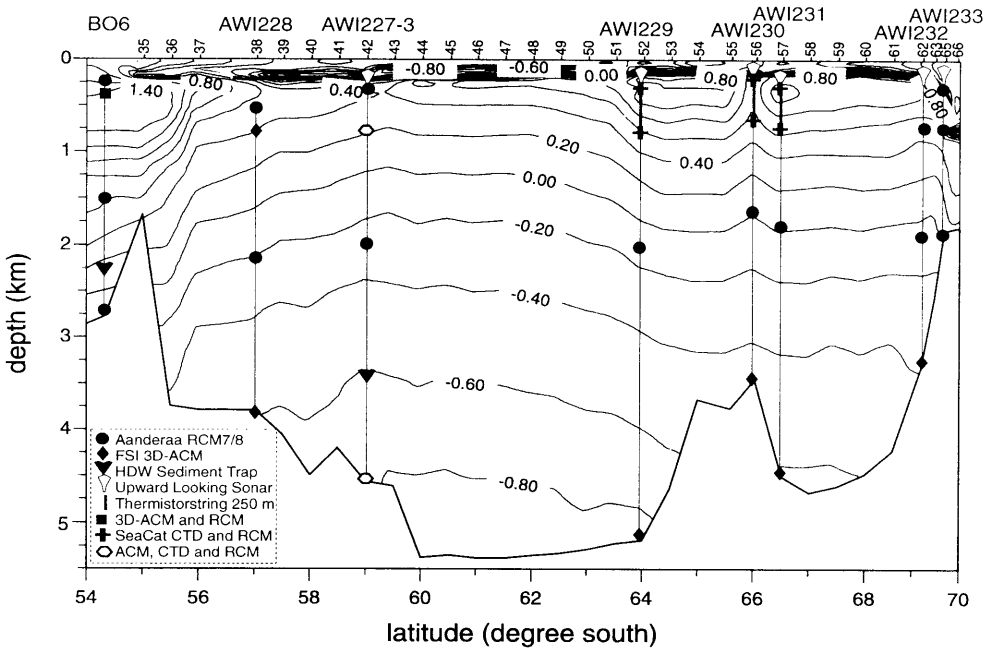


Abb. 13: Vertikalschnitt der potentiellen Temperatur durch das Weddellmeer entlang dem Nullmeridian von 55°S bis 69°38.5'S (oben) und durch das südliche Weddellmeer bei Joinville Island (unten) mit den ausgelegten Verankerungen.

Figure 13: Vertical section of potential temperature across the Weddell Sea along the Greenwich Meridian from 55°S to 69°38.5'S (top) and across the southern Weddell Sea off Joinville Island (bottom) with the deployed moorings.

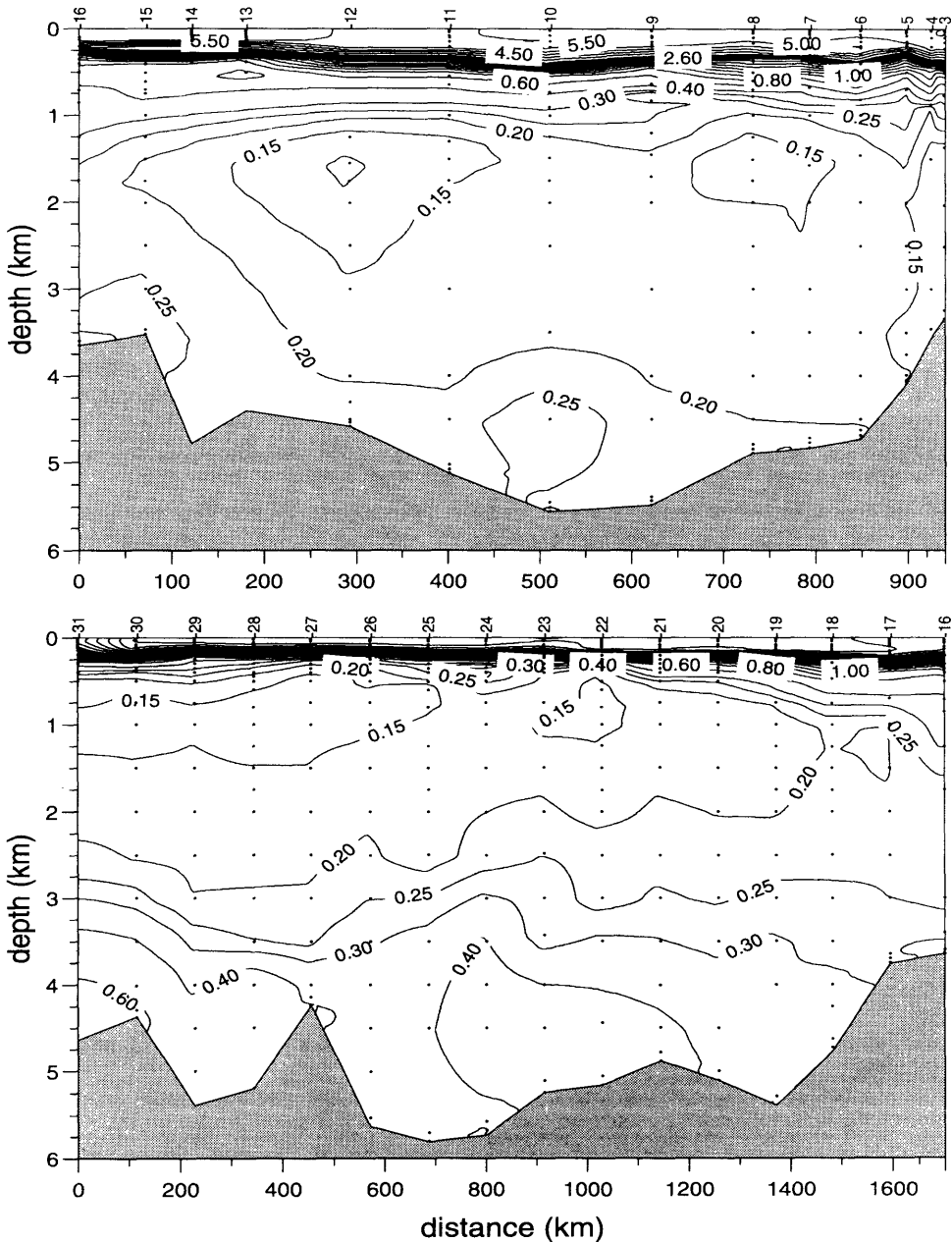


Abb. 14: Vertikalschnitt des Spurenstoffs F11 in $\mu\text{mol/kg}$ durch den östlichen Rand des Weddellmeers entlang 54°S von $24^\circ41'\text{E}$ bis 39°E (oben) und von $59^\circ30'\text{S } 0^\circ$ bis $54^\circ\text{S } 24^\circ41'\text{E}$ (unten).

Figure 14: Vertical section of the tracer CFCs F11 in $\mu\text{mol/kg}$ across the eastern boundary of the Weddell Sea along 54°S from $24^\circ41'\text{E}$ to 39°E (top) and from $59^\circ30'\text{S } 0^\circ$ to $54^\circ\text{S } 24^\circ41'\text{E}$ (bottom).

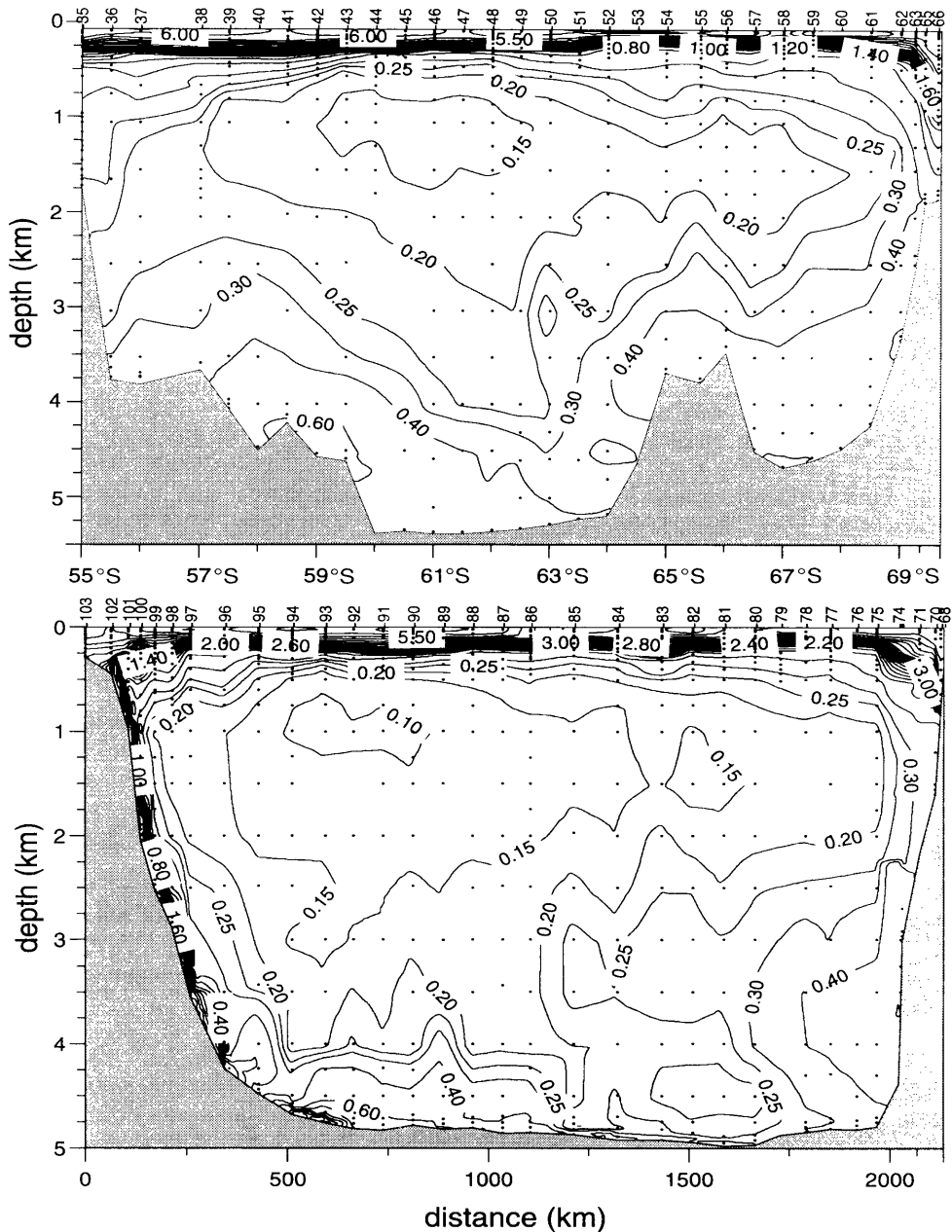


Abb. 15: Vertikalschnitt des Spurenstoffs F11 in $\mu\text{mol/kg}$ durch das Weddellmeer entlang dem Nullmeridian von 55°S bis $69^\circ 38.5'\text{S}$ (oben) und durch das südliche Weddellmeer von Joinville Island nach Kapp Norvegia (unten).
 Figure 15: Vertical section of the tracer CFC F11 in pmol/kg across the Weddell Sea along the Greenwich Meridian from 55°S to $69^\circ 38.5'\text{S}$ (top) and across the southern Weddell Sea from Joinville Island to Kapp Norvegia (bottom).

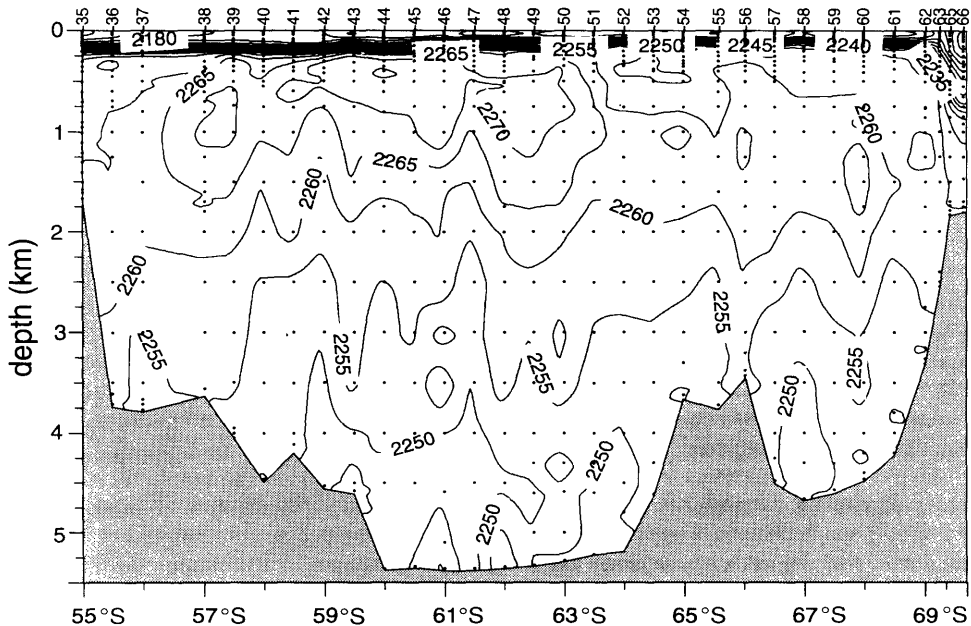


Abb. 16: Vertikalschnitt des TCO₂ in $\mu\text{mol/kg}$ entlang dem Greenwich-Meridian.
 Fig. 16: TCO₂ section along the Greenwich Meridian

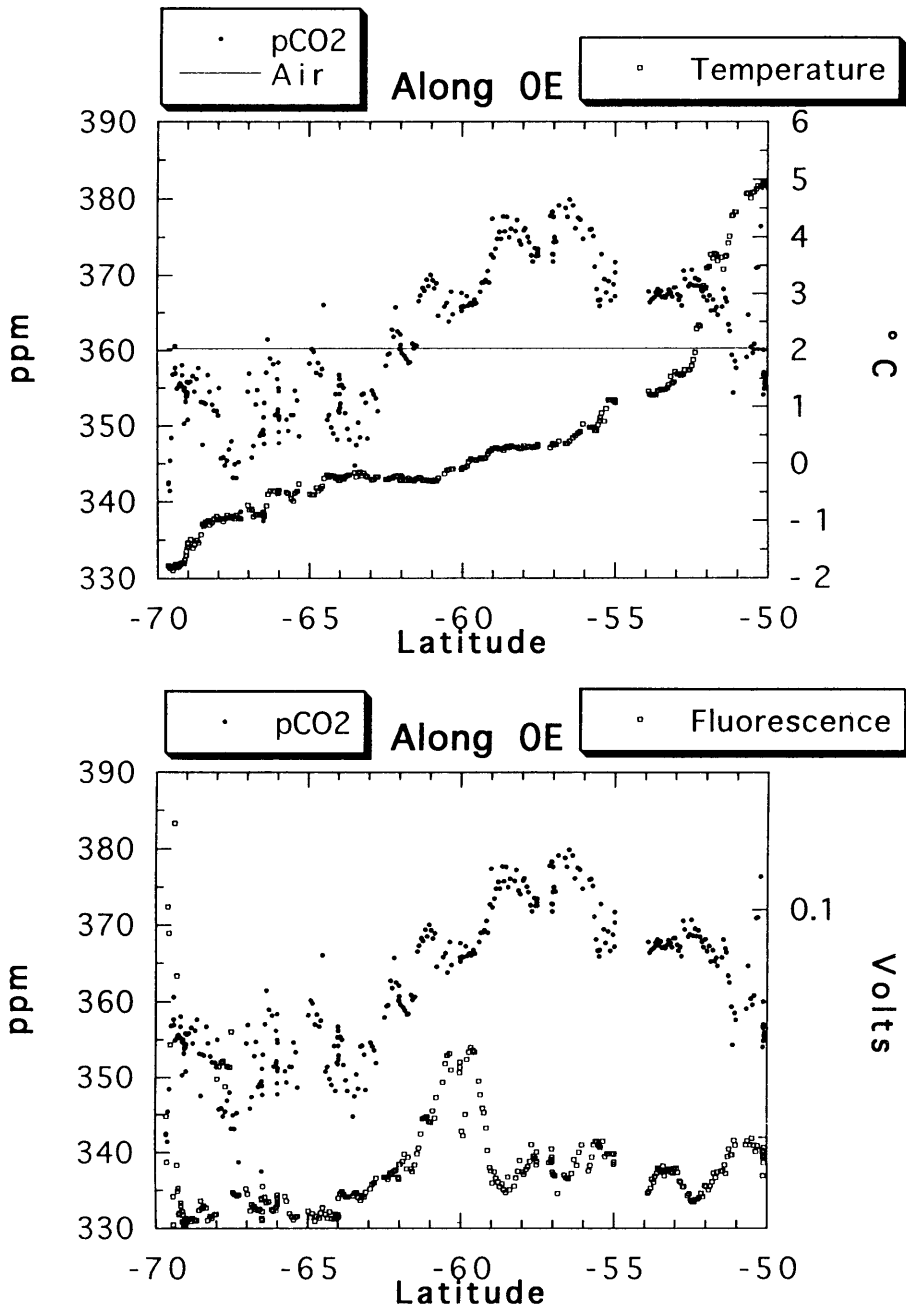


Abb. 17: Oberflächenwerte des CO₂-Partialdrucks entlang dem Meridian von Greenwich im Wasser und der Luft mit der Wassertemperatur vom Thermosalinographen am Kiel des Schiffes (oben) und mit der kontinuierlich gemessenen Fluoreszenz zur Bestimmung der Chlorophyll-Konzentration (unten).

Figure 17: Measurements of the partial pressure Of CO₂ in the surface water and the marine air along the Greenwich Meridian combined with the sea surface temperature from the thermosalinograph at the ship's keel (top) and combined with the continuously measured fluorescence for chlorophyll determination (bottom).

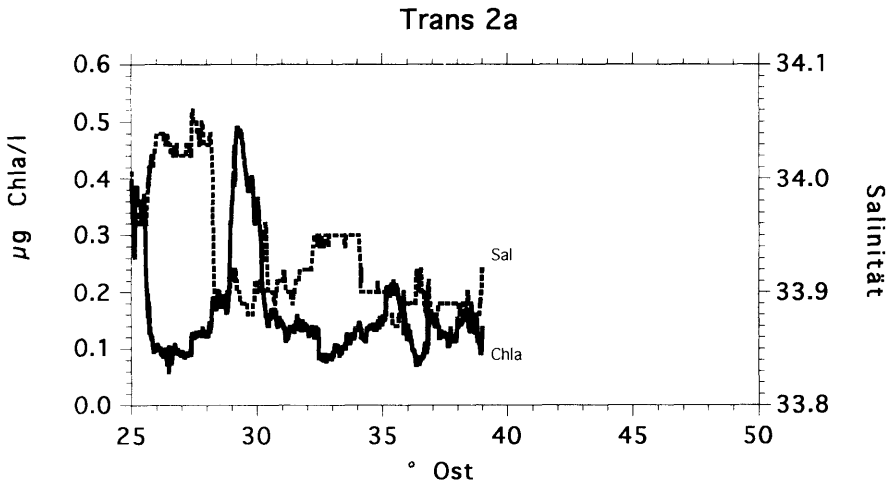
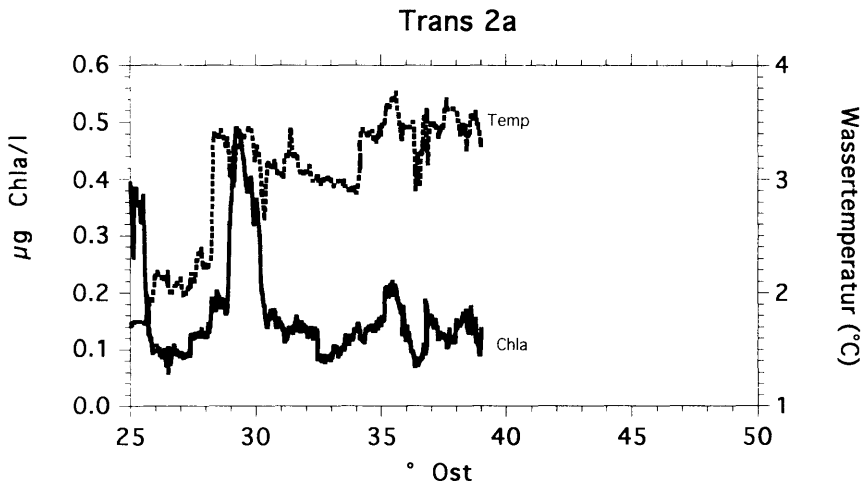


Abb. 18: Verteilung von Chlorophyll a ($\mu\text{g Chla/l}$) in 8 m Tiefe entlang Transekt 2a mit der Wassertemperatur in $^{\circ}\text{C}$ (oben) und dem Salzgehalt (unten).

Figure 18: Distribution of chlorophyll a ($\mu\text{g Chla/l}$) at 8 m depth along transect 2a together with the water temperature in $^{\circ}\text{C}$ (top) and salinity (bottom).

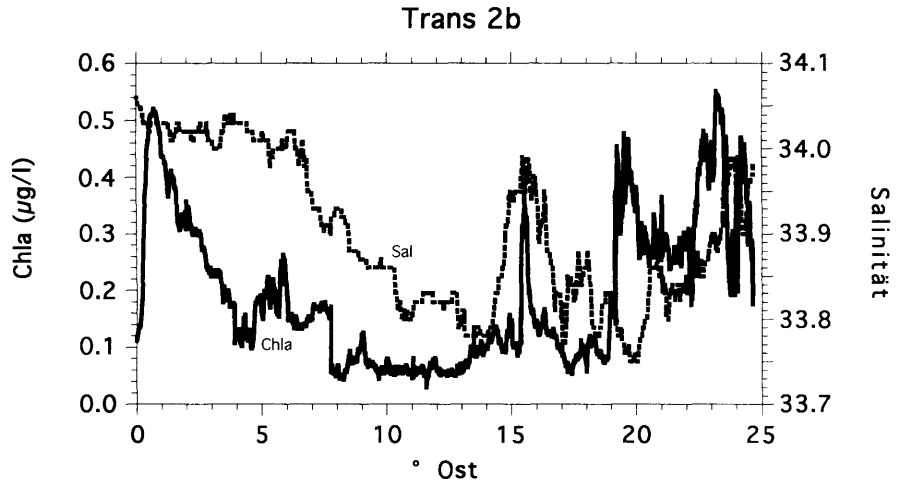
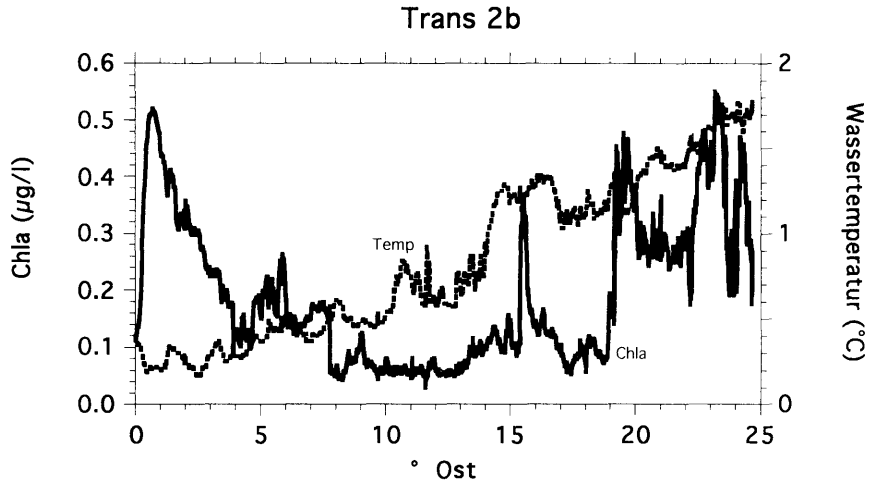


Abb. 19: Verteilung von Chlorophyll a ($\mu\text{g Chla/l}$) in 8 m Tiefe entlang Transekt 2b mit der Wassertemperatur in $^{\circ}\text{C}$ (oben) und dem Salzgehalt (unten).
 Figure 19: Distribution of chlorophyll a ($\mu\text{g Chla/l}$) at 8 m depth along transect 2 together with the water temperature in $^{\circ}\text{C}$ (top) and salinity (bottom).

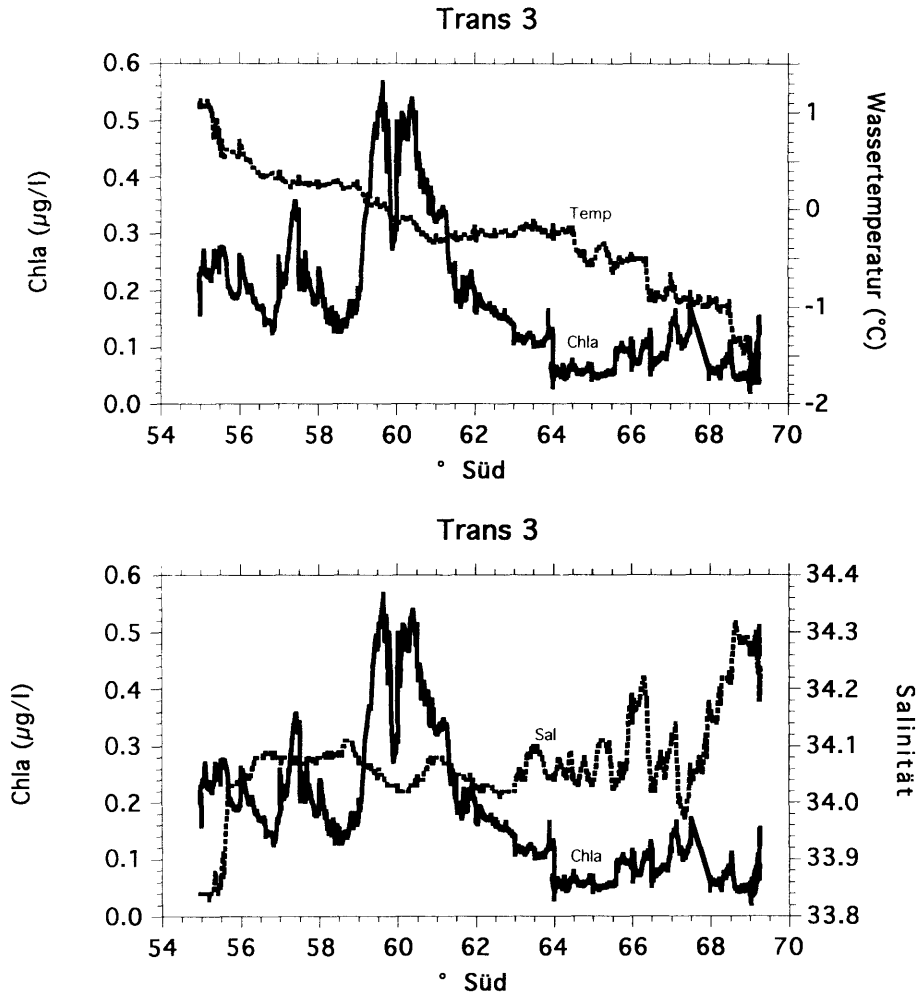


Abb. 20: Verteilung von Chlorophyll a ($\mu\text{g Chla/l}$) in 8 m Tiefe entlang Transekt 3 mit der Wassertemperatur in $^{\circ}\text{C}$ (oben) und dem Salzgehalt (unten).
 Figure 20: Distribution of chlorophyll a ($\mu\text{g Chla/l}$) at 8 m depth along transect 3 together with the water temperature in $^{\circ}\text{C}$ (top) and salinity (bottom).

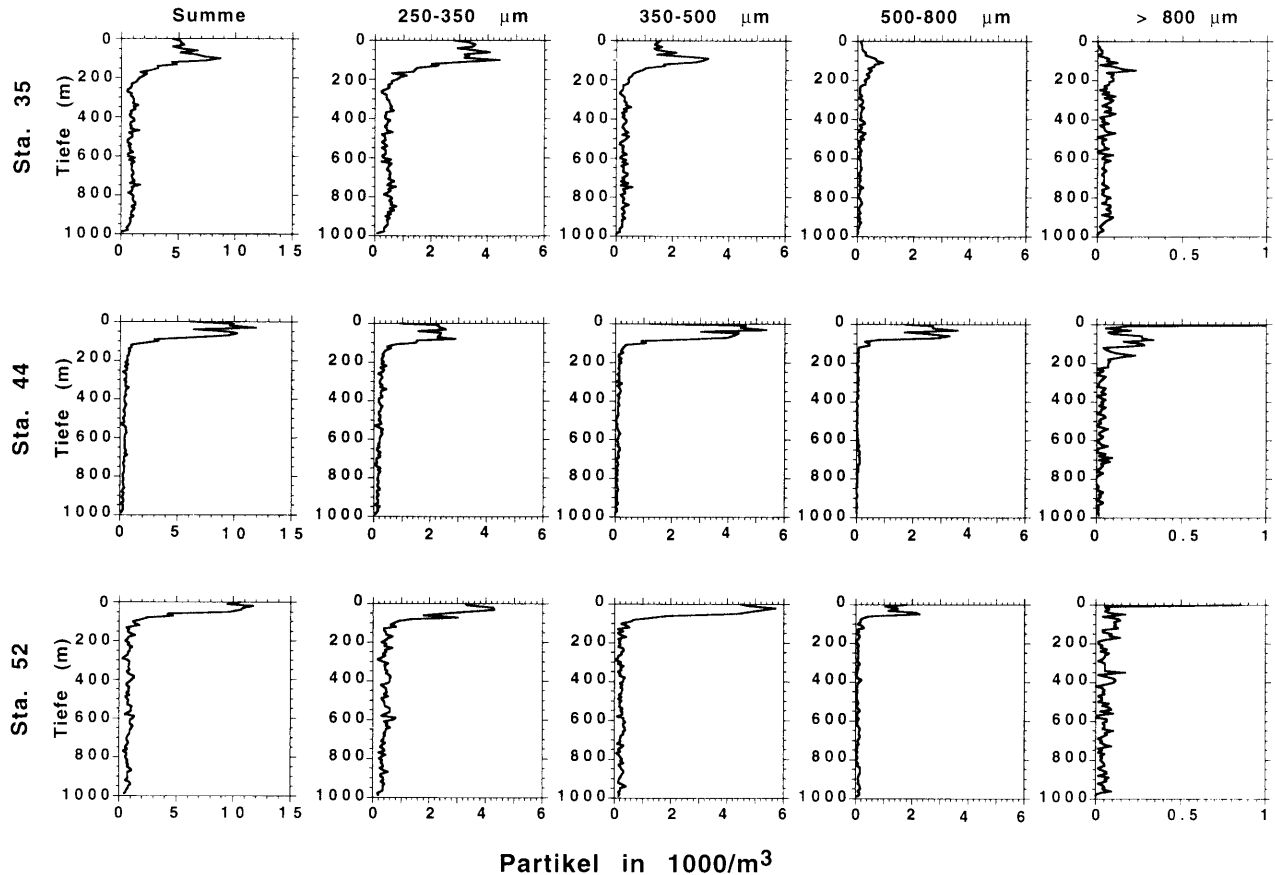


Abb. 21: Vertikalprofile der Partikel-Konzentrationen in verschiedenen Größenklassen, aufgenommen mit dem Optical Plankton Counter (OPC) am Multinetz.

Figure 21: Vertical profiles of particle concentrations obtained with the Optical Plankton Counter (OPC) mounted on the multinet.1

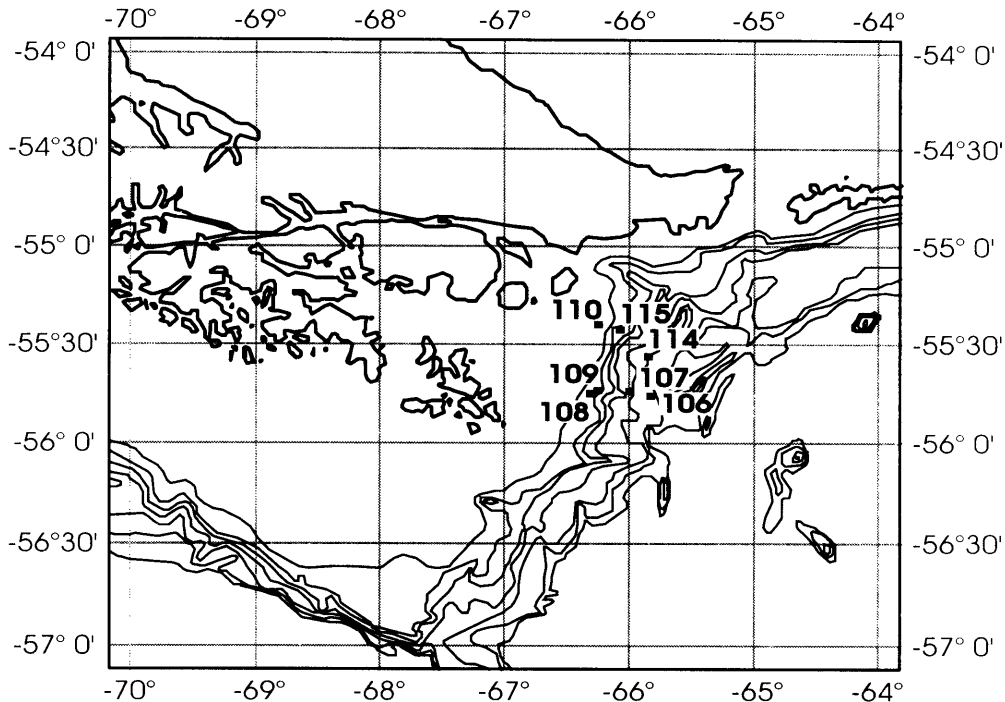


Abb. 22: Untersuchungsgebiet und Stationen des Benthosprogramms.
Figure. 22: Observation site and stations of the benthos programme.

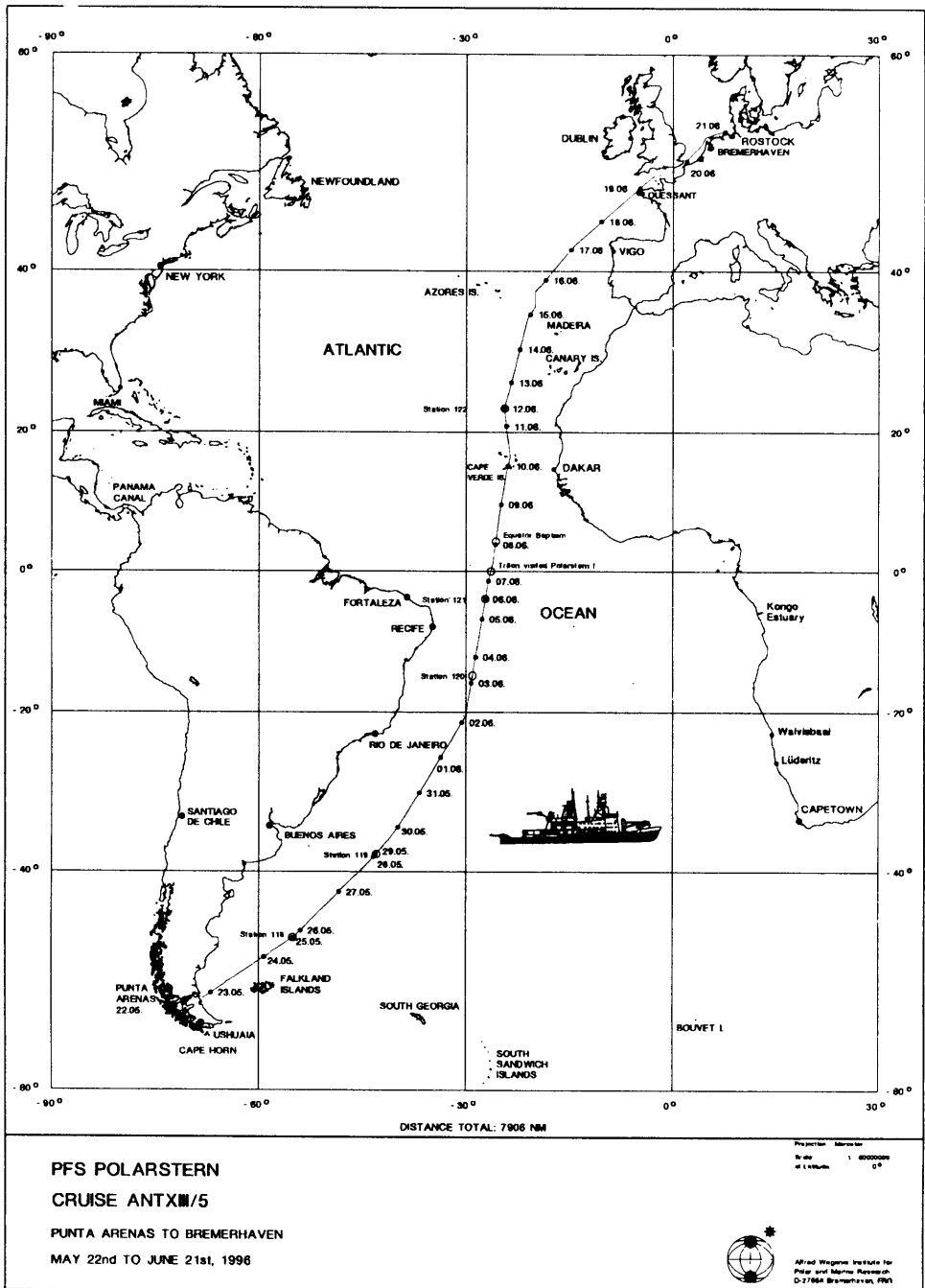


Abb. 23: Fahrtroute während des Fahrtabschnitts ANT X111/5.
 Figure. 23: Cruise track during leg ANT X111/5.

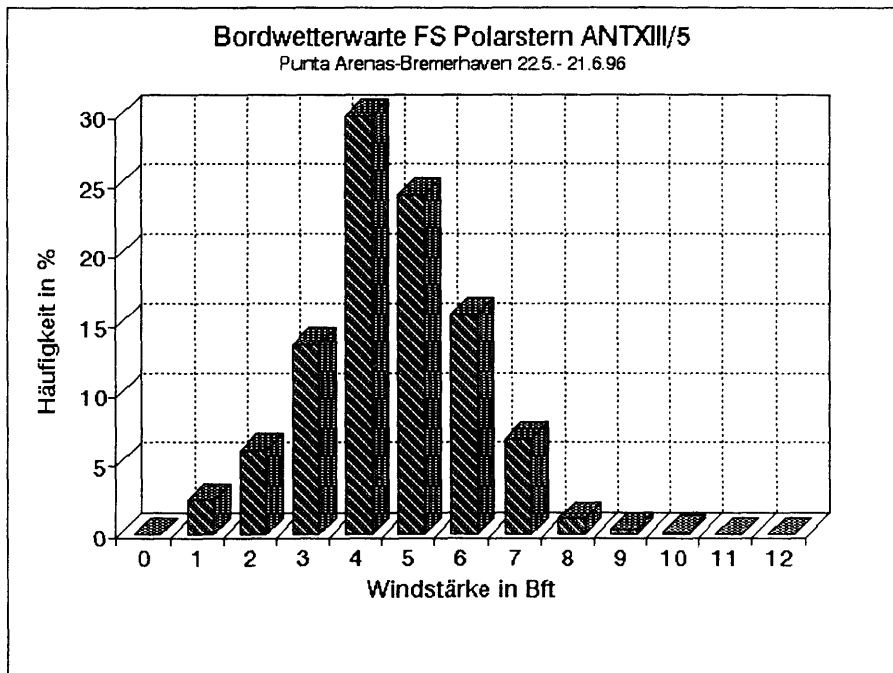
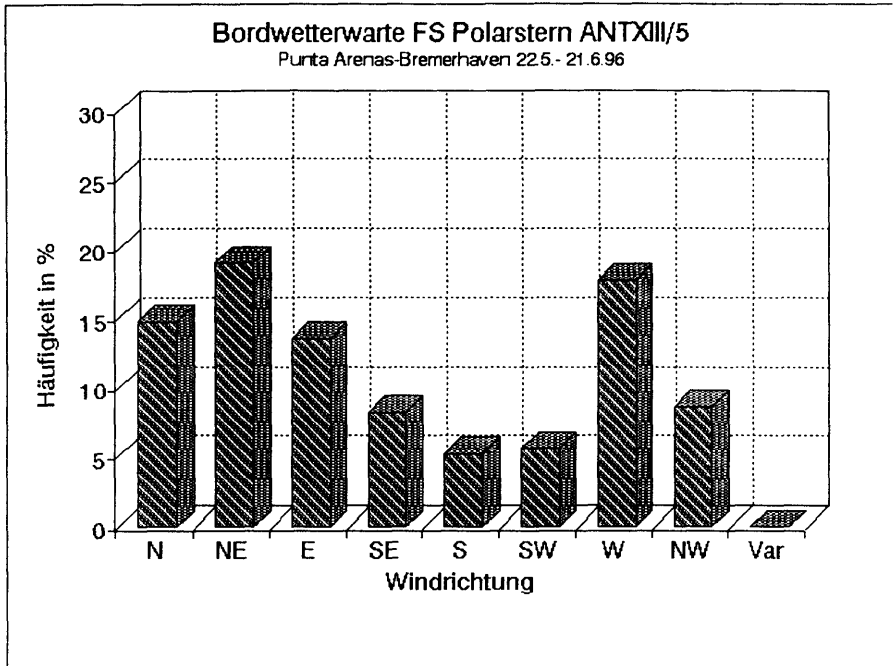


Abb. 24: Hau Figurekeitsverteilung der Windrichtung und -stärke
Figure 24: Frequency distribution of wind speed and direction

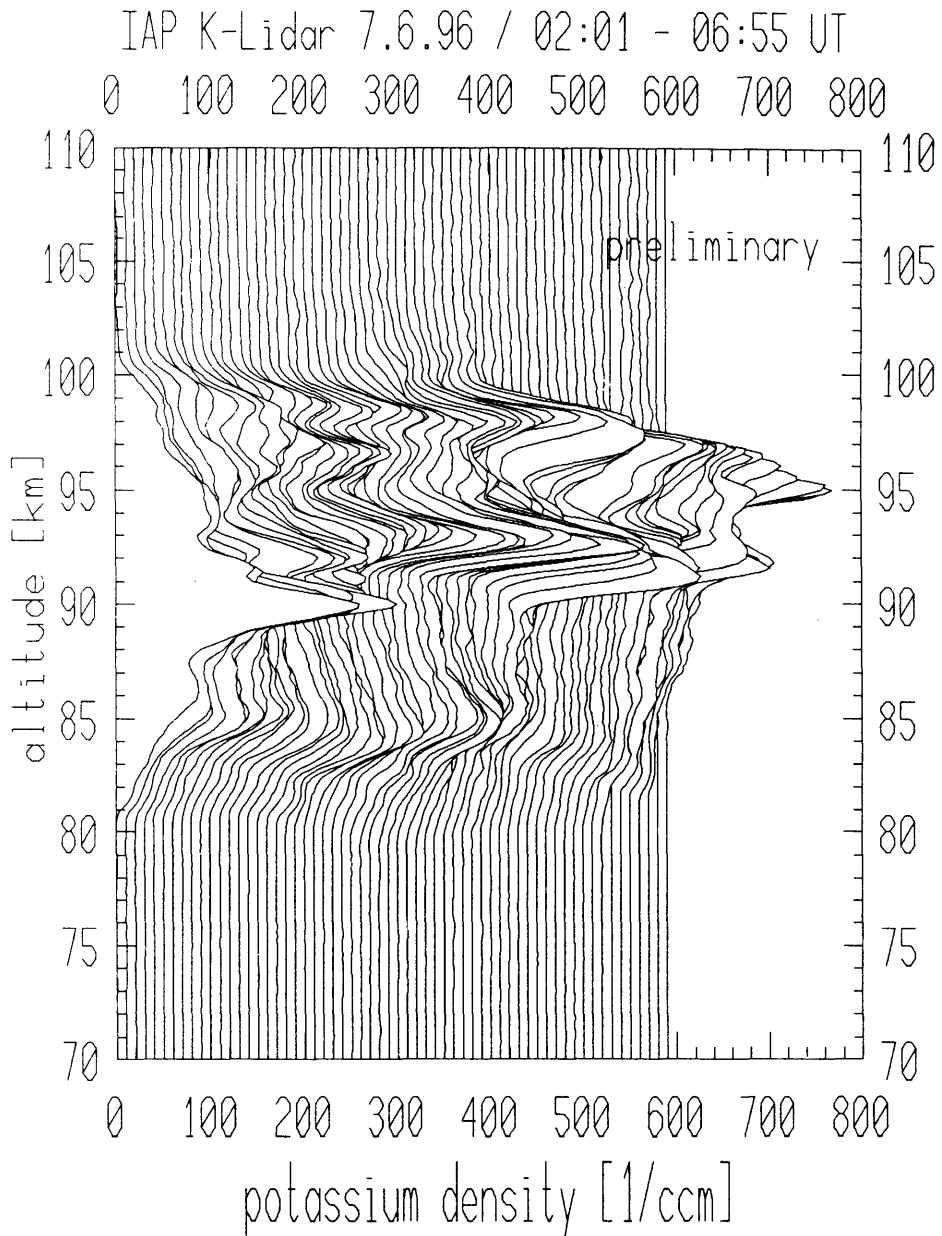


Abb. 25: Kali umlichteprof ile, die am 7. Juni 1996 bei 3°S beobachtet wurden.
Der zeitliche Abstand beträgt rund 4 min.

Figure 25: Potassium density profiles measured on 7 June 1996 at about 3°S.

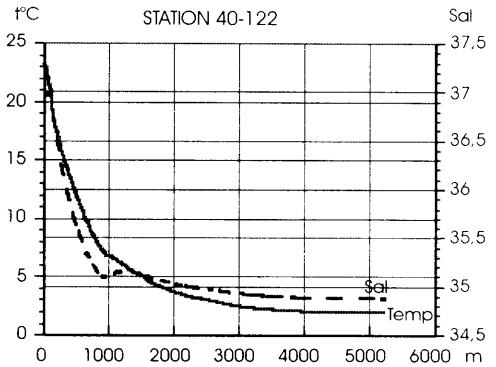
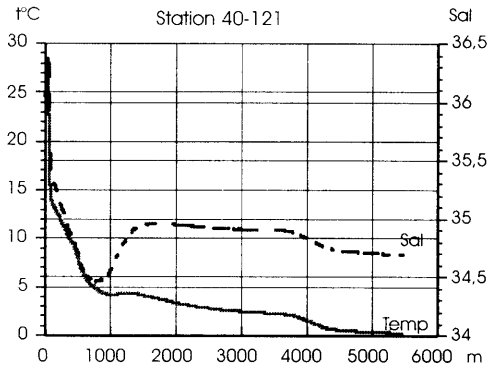
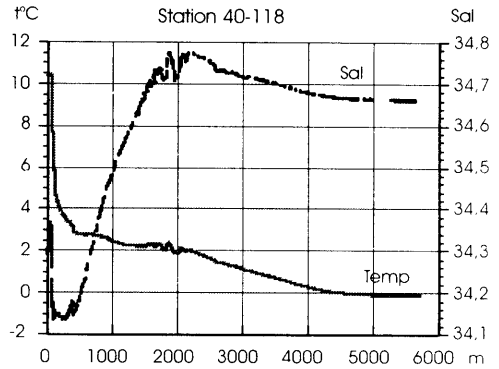
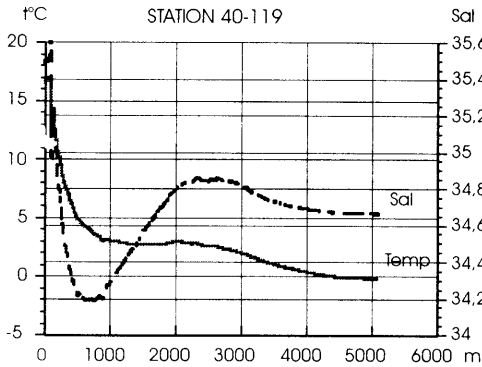


Abb.26: CTD-Profil, die an den Tiefseestationen gemessen wurden
 Figure 26: CTD-profiles measured at the deep sea stations

6. Principal Investigators

Inst	Scientist	#	Unit	Type of measurements	Data in DOD
AWI	Arntz, W.	11	stations	B18 Zoobenthos	no
AWI	Fahrbach, E.	17	stations	D01 Current meters 8 stat.: moorings deployed on the Greenwich Meridian, 3 stat.: moorings recover red during ANT III/4, 6 stat.: moorings deployed in the western Weddell Sea	no
AWI	Fahrbach, E.	5000	N miles	D71 Current profiler (e.g. ADCP)	no
AWI	Fahrbach, E.	112	stations	H09 Water bottle stations GO-Rosette 24x12l	no
AWI	Fahrbach, E.	112	stations	H10 CTD-Stations	yes
AWI	Fahrbach, E.	310	stations	H13 Bathythermograph drops XBT with T/ probes, most traces transmitted over GTS	yes
AWI	Fahrbach, E.	112	stations	H21 Oxygen	no
AWI	Fahrbach, E.	5000	N miles	H71 Surface measurements underway (T, S) Thermosalinograph, does not work in ice	no
AWI	Hoppema, M.	112	stations	H22 Phosphates Samples were analysed with a Technicon TRAACS autoanalyzer	no
AWI	Hoppema, M.	112	stations	H24 Nitrates Samples were analysed with a Technicon TRAACS autoanalyzer	no
AWI	Hoppema, M.	112	stations	H25 Nitrites Samples were analysed with a Technicon TRAACS autoanalyzer	no
AWI	Hoppema, M.	112	stations	H26 Silicates Samples were analysed with a Technicon TRAACS autoanalyzer	no
AWI	Hoppema, M.	112	stations	H27 Alkalinity	no
AWI	Hoppema, M.	112	stations	H74 Carbon dioxide Prctical pressure GF CO ₂ , total CO ₂	no
AWI	Hoppema, M.	112	stations	H76 Ammonia Samples were analysed with a Technicon TRAACS autoanalyzer	no
AWI	Mühlebach, A.	36	stations	H90 Other chemical oceanographic measurements Organic chemistry, dissolved and particulate phytosterols	no
AWI	Smetacek, V.	31	stations	B08 Phytoplankton	no
AWI	Smetacek, V.	8	No unit	B09 Zooplankton	no
AWI	Smetacek, V.	8	No unit	B11 Nekton	no
DWDSWA	Müller, H.J.	0	day(s)	M01 Upper air observations Synoptic met obs and radiosondes	no
DWDSWA	Müller, H.J.	0	day(s)	M06 Routine standard measurements Synoptic met obs and radiosondes	no
GUHB	Roether, W.	104	stations	H73 Geochemical tracers (e.g. freons) Freon-11, -12, -113, CCL ₄ , tritium, helium	no
IAPR	Höffner, J.	16	No unit	M01 Upper air observations Potassium temperature lidar profiles (nights)	no

aktualisiert am: 08.07.2002

7. Beteiligte Institutionen / Participating Institutions

	Address	Participants	Leg
Chile			
UACH	Instituto de Zoologia Universidad Austral de Chile Valdivia	1	4
UCV	Esc. de Cs. del Mar Universidad Catolica de Valparaiso Valparaiso	1	4
UMAG	Instituto de la Patagonia Universidad de Magallanes Avenida Bulnes Punta Arenas	3	4
Federal Republic of Germany			
AWI	Alfred-Wegener-Institut für Polar- und Meeresforschung Columbusstraße D-27568 Bremerhaven	26, 8	4, 5
AWIP	Alfred-Wegener-Institut für Polar- und Meeresforschung Forschungsstelle Potsdam c/o Zoologisches Museum Berlin Invalidenstr. 43 D-1 0115 Berlin	1	4
DWID	Deutscher Wetterdienst Seewetteramt Postfach 301190 D-20304 Hamburg	2, 3	4, 5
FBZO	FB/7AG Zoomorphologie Carl-von-Ossietzky-Universität D-261 11 Oldenburg	1, 2	4, 5
HSW	Helicopter-Service Wasserthal GmbH; K5tnerweg 43 D-22393 Hamburg	4	4
IAPR	Institut für Atmosphärenphysik Schloßstr. 4-6 D-18221 Köhlsbörn	2, 4	4, 5
IPO	Institut für Polarökologie Universität Kiel Wischofstr. 1-3, Geb. 12 D-24148 Kiel	1	4

	Address	Participants	Leg
IUPB	IUP - Institut für Umweltphysik Abt. Tracer-Ozeanographie Universität Bremen, FB 1 Postfach 330 440 D-28334 Bremen	5	4
The Netherlands			
NIOZ	Netherlands Institute for Sea Research P.O. Box 59 1790 Ab den Burg Texel	2	4
UK			
NHM	The Natural History Museum Department of Zoology Cromwell Road London, SW7B 5BD	2	5
SAMS	The Scottish Association for Marine Science P.O. Box 3 Oban, Argyll PA34 4AD, Scotland	1	5
Russia			
ZMMU	Zoological Museum of the Moscow University Bolshaya Nikitskaya 6 Moscow, 103009	1	4

8. Fahrtteilnehmer/Cruise participants

ANT XIII/4

Last Name	First Name	Inst.	Last Name	First Name	Inst.
Arntz	Wolf	AWI	Meyer	Ralf	AWI
Bakker	Karel	NIOZ	Möller	Hans-Joachim	DWD
Bittkau	Anke	AWI	Montiel	Americo	UMAG
Böhm	Joachim	HSW	Mühlebach	Anneke	AWI
BOchner	JOrgen	HSW	Mutschke	Erika	UMAG
Bulsiewicz	Klaus	IUPB	Nowaczyk	Jochen	AWI
Buschmann	Alexander	AWI	Rauschert	Martin	AWIP
Dubischar	Corinna	AWI	Riewesell	Christian	HSW
Eska	Veit	IAPR	Rios	Carlos	UMAG
Fahrbach	Eberhard	AWI	Rohardt	Gerd	AWI
Fraas	Gerhard	IUPB	Rohr	Harald	AWI
George	Kai Horst	FBZO	Runge	Maite	IUPB
Gerdes	Dieter	AWI	San Miguel	Esteban	Armada de Chile
Gorny	Janja	AWI	Schlenker	Björn	IUPB
Gorny	Matthias	AWI	Schneider	Hans	HSW
Hansjosten	Andreas	AWI	Schröder	Michael	AWI
Heras De las	Miriam	AWI	Sieverding	Hiltrud	IUPB
Höffner	Josef	IAPR	Splridonov	Vassili	ZMMU
Hopperna	Mario	AWI	Stoll	Michel	NIOZ
Horstmann	Uta	AWI	Tan	GiokNlo	AWI
Jochum	Markus	AWI	Winterrath	Tanja	AWI
Köhler	Herbert	DWD	Wisotzkl	Andreas	AWI
Kolb	Leif	AWI	Witte	Hannelore	AWI
Lardies Carrasco	Marco Antonio	UACH	Woodgate	Rebecca	AWI
Linse	Katrin	IPO	Zimmermann	Andreas	AWI
Maturnana	Jenny	UCV			

ANT XIII/5

Last Name	First Name	Inst.	Last Name	First Name	Inst.
Alpers	Matthias	IAPR	Klauke	Ulla	AWI
Bohlmann	Harald	AN	Knuth	Edmund	DWD
Debenham	Nicola Jane	NHM	Kbhler	Herbert	DWD
Dunker	Erich	AWI	Lamont	Peter Albert	SAMS
England	Joachim	DWD	Martinez-Arbizu	Pedro	FBZO
Eska	Veit	IAPR	MenBen	Klaus	AWI
Ferrero	Timothy John	NHM	Schröder	Sabine	AWI
Gerdes	Dieter	AWI	Silvelra Moura	Gisela	FBZO
Helmke	Elisabeth	AWI	Strohscher	Birgit	AWI
Höffner	Josef	IAPR	Zahn von	Ulf	IAPR

8. Schiffspersonall/Ship's Crew

	ANT XIII/4	ANT XIII/5
Kapitän	Pahl	Keil
1. nautischer Offizier	Keil	Rodewald
Leitender techn. Offizier	Schulz	Schulz
2. nautischer Offizier	Block	Block
2. nautischer Offizier	Schwarze	Schwarze
2. nautischer Offizier	Spielke	
Arzt	Schuster	Schuster
Funffizier	Koch	Hecht
2. technischer Offizier	Delff	Delff
2. technischer Offizier	Folta	Folta
2. technischer Offizier	Simon	Simon
Elektroniker	Dimmler	
Elektroniker	Fröb	Fröb
Elektroniker	Holtz	Holtz
Elektroniker	Pabst	Pabst
Elektroniker	Piskorzynski	
Schiffbetriebsmeister	Loidl	Loidl
Zimmermann	Neisner	Neisner
Facharbeiter/Deck	Bdcker	Bdcker
Facharbeiter/Deck	Bohne	
Facharbeiter/Deck	Burzan	
Facharbeiter/Deck	Hagemann	
Facharbeiter/Deck	Hartwig	Hartwig
Facharbeiter/Deck	Kreis	
Facharbeiter/Deck	Moser	Moser
Facharbeiter/Deck	Schmidt	Schmidt
Storekeeper	Renner	Renner
Facharbeiter/Maschine	Dinse	Dinse
Facharbeiter/Maschine	Fritz	Fritz
Facharbeiter/Maschine	Hartmann	Arias Iglesias
Facharbeiter/Maschine	Krösche	Krösche
Facharbeiter/Maschine	Schade	Schade
Koch	Silinski	Silinski
Kochsmaat	HOnecke	
Kochsmaat	Tupy	Tupy
1. Stewardess	Dinse	Dinse
Stewardess/Krankenschwester	Lehmbecker	Lehmbecker
2. Stewardess	Klomet	Klomet
2. Stewardess	Schmidt	Schmidt
2. Stewardess	Silinski	Silinski
2. Steward	Tu	Huang
2. Steward	Wu	Mui
Wäscher	Yu	Yu

9. **Appendix 1, Stationsliste/Station list ANT XIII/4**
(see .sum file)

10. **Appendix 2, XBT Data ANT XIII/4**

No.		Date	Time (GMT)	Latitude	Longitude	Depth (m)
001		18.03.1996	17.54	37°52'S	21°23'E	5074
002			20.03	38°12'S	21°41'E	5205
004			22.06	38°33'S	21°59'E	5119
005			23.55	38°50'S	22°15'E	4988
006	f	19.03.1996	02.09	39°12'S	22°34'E	5165
007			02.18	39°13'S	22°36'E	5156
008			03.59	39°27'S	22°49'E	5128
009	f		05.59	39°44'S	23°03'E	5126
010			06.09	39°44'S	23°03'E	5139
011			08.02	39°54'S	23°15'E	5041
012			11.19	40°10'S	23°27'E	4791
013			13.44	40°24'S	23°39'E	4460
014			17.58	40°34'S	23°48'E	4348
015			20.00	40°55'S	24°08'E	4327
016			21.59	41°15'S	24°27'E	4008
017			23.58	41°37'S	24°47'E	2714
018		20.03.1996	01.59	41°59'S	25°09'E	3534
019			03.02	42°12'S	25°20'E	3765
020			04.00	42°22'S	25°30'E	4157
021			05.00	42°33'S	25°40'E	4469
022			05.55	42°43'S	25°50'E	4731
023			07.00	42°55'S	26°01'E	4981
024			08.02	43°06'S	26°13'E	4987
025			08.59	43°17'S	26°23'E	5376
026			09.56	43°28'S	26°33'E	5223
027			10.55	43°38'S	26°43'E	5400
028			11.57	43°48'S	26°53'E	5704
029			13.04	43°59'S	27°04'E	5270
030			17.00	44°02'S	27°08'E	5300
031			18.02	44°12'S	27°19'E	5404
032			18.59	44°21'S	27°28'E	5454
033			20.06	44°33'S	27°39'E	5414
034			20.59	44°41'S	27°48'E	5422
035			22.00	44°49'S	28°00'E	5385
036	f		23.03	44°59'S	28°10'E	5416
037	f		23.11	44°59'S	28°10'E	5420

f=probe failure with repeat

No.		Date	Time (GMT)	Latitude	Longitude	Depth (m)
038			23.14	45°00'S	28°11'E	5422
039			23.58	45°08'S	28°20'E	5180
040		21.03.1996	00.59	45°17'S	28°30'E	5829
041			02.00	45°26'S	28°40'E	5404
042			02.59	45°36'S	28°50'E	5281
043			03.59	45°44'S	29°00'E	5274
044			04.56	45°54'S	29°11'E	5354
045			06.00	46°05'S	29°23'E	4283
046			07.00	46°15'S	29°35'E	5318
047			08.00	46°24'S	29°46'E	5247
048			09.00	46°35'S	29°56'E	4991
049			09.59	46°44'S	30°07'E	5430
050			11.03	46°54'S	30°18'E	5220
051			11.58	47°03'S	30°29'E	4309
052			12.58	47°13'S	30°40'E	4135
053			14.00	47°23'S	30°51'E	4463
054			14.56	47°31'S	31°01'E	5102
055			15.55	47°39'S	31°10'E	2769
056			16.55	47°48'S	31°20'E	3697
057			17.56	47°57'S	31°31'E	4513
058			18.56	48°07'S	31°42'E	5603
059			19.57	48°16'S	31°53'E	4579
060			20.56	48°26'S	32°03'E	2648
061			21.57	48°35'S	32°15'E	3975
062			22.58	48°45'S	32°27'E	3973
063		22.03.1996	00.01	48°55'S	32°39'E	4411
064			00.59	49°04'S	32°50'E	4066
065	f		01.59	49°14'S	33°01'E	4003
066			02.07	49°15'S	33°03'E	3966
067			02.57	49°23'S	33°12'E	4975
069			04.55	49°42'S	33°35'E	4074
069			06.03	49°54'S	33°49'E	5237
070			06.59	50°03'S	34°00'E	4733
071			07.58	50°11'S	34°12'E	4610
072			08.59	50°20'S	34°23'E	4566
073			09.58	50°30'S	34°34'E	5163
074			10.57	50°39'S	34°44'E	5235
075			12.04	50°50'S	34°58'E	5185
076			12.58	50°58'S	35°07'E	4880
077			13.53	51°07'S	35°18'E	4775
078			14.57	51°17'S	35°31'E	4901

f=probe failure with repeat

No.	Date	Time (GMT)	Latitude	Longitude	Depth (m)
079		15.55	51°26'S	35°42'E	5198
080		16.55	51°36'S	35°55'E	4261
081		17.57	51°46'S	36°08'E	4875
082		19.00	51°58'S	36°23'E	4596
083		20.08	52°10'S	36°39'E	4237
084		21.01	52°21'S	36°52'E	4516
085		22.01	52°32'S	37°07'E	4508
086		23.06	52°45'S	37°22'E	4492
087	23.03.1996	00.00	52°55'S	37°36'E	4459
088		00.57	53°06'S	37°50'E	4412
089		02.02	53°19'S	38°06'E	4296
090		03.00	53°30'S	38°21'E	4271
091		03.59	53°41'S	38°35'E	4185
092		04.58	53°53'S	38°50'E	3500
093		18.46	54°01'S	38°20'E	4129
094		19.55	54°01'S	38°03'E	4314
095		21.04	54°00'S	37°46'E	4622
096	24.03.1996	02.02	54°00'S	37°26'E	4710
097		02.53	54°00'S	37°10'E	4736
098		03.50	54°00'S	36°53'E	4772
099		11.09	54°00'S	36°36'E	4560
100		12.17	54°00'S	36°19'E	4844
101		13.23	54°00'S	36°02'E	4701
102		18.18	54°00'S	35°45'E	4724
103		19.32	53°59'S	35°28'E	4822
104		20.42	54°00'S	35°11'E	5034
105		21.52	54°01'S	34°54'E	4778
106		22.58	54°00'S	34°37'E	5310
107	25.03.1996	00.05	54°00'S	34°17'E	5327
108		04.32	54°00'S	34°02'E	5432
109		05.40	54°00'S	33°42'E	5440
110		06.37	54°00'S	33°25'E	4571
111		07.40	54°00'S	33°07'E	5448
112		08.32	54°00'S	32°51'E	5433
113		09.29	54°00'S	32°34'E	5296
114		14.00	54°00'S	32°17'E	5470
115		14.57	54°00'S	32°00'E	4630
116		16.12	53°59'S	31°43'E	5483
117		17.20	53°59'S	31°25'E	5514
118		18.31	54°00'S	31°07'E	5483
119		19.29	54°00'S	30°52'E	4981
120	26.03.1996	00.06	54°00'S	30°36'E	5272

No.		Date	Time (GMT)	Latitude	Longitude	Depth (m)
121			01.09	54°00'S	30°19'E	5510
122			02.28	54°00'S	30°01'E	5044
123			03.39	54°00'S	29°44'E	5510
124			04.51	54°00'S	29°27'E	5227
125			06.04	54°00'S	29°10'E	4603
126			13.51	54°00'S	28°54'E	5294
127			14.59	54°00'S	28°34'E	4871
128			15.53	54°00'S	28°19'E	5173
129			16.56	54°00'S	28°02'E	4053
130			18.06	54°00'S	27°45'E	5297
131		27.03.1996	01.49	54°02'S	27°21'E	4185
132			02.58	54°01'S	27°03'E	4544
133			04.46	54°00'S	26°46'E	4896
134			14.02	54°00'S	26°29'E	4779
135			15.05	54°00'S	26°13'E	3302
136			16.04	54°00'S	25°55'E	3318
137			23.54	54°00'S	25°35'E	4179
138		28.03.1996	00.42	54°00'S	25°22'E	4147
139			01.43	53°58'S	25°04'E	4534
140			02.41	53°52'S	24°51'E	4844
141			06.15	53°46'S	24°37'E	3294
142			07.21	53°58'S	24°38'E	4132
143			08.13	54°08'S	24°38'E	4935
144			09.13	54°19'S	24°37'E	4518
145			10.08	54°29'S	24°37'E	4186
146			11.16	54°41'S	24°36'E	4449
147			16.38	54°54'S	24°22'E	3823
148			17.38	55°01'S	24°11'E	4141
149			18.36	55°08'S	23°59'E	3870
150			19.36	55°16'S	23°48'E	3961
151			20.33	55°23'S	23°37'E	4685
152		29.03.1996	01.05	55°32'S	23°26'E	4668
153			02.07	55°38'S	23°12'E	4657
154			03.02	55°46'S	23°02'E	5115
155			04.05	55°54'S	22°49'E	5237
156			05.02	56°02'S	22°37'E	5113
157			06.05	56°10'S	22°23'E	5088
158			13.57	56°14'S	22°09'E	5222
159			15.03	56°26'S	21°57'E	4805
160			16.01	56°34'S	21°44'E	5116
161			17.19	56°45'S	21°25'E	5023
162			18.09	56°52'S	21°13'E	5009

No.		Date	Time (GMT)	Latitude	Longitude	Depth (m)
163			22.22	57°00'S	21°01'E	4738
164			23.20	57°01'S	20°46'E	5213
165		30.03.1996	10.34	57°11'S	19°06'E	4824
166			11.53	57°12'S	18°46'E	4878
167			12.51	57°14'S	18°32'E	4994
168			13.49	57°16'S	18°19'E	4941
169			14.52	57°17'S	18°04'E	5318
170			16.23	57°19'S	17°44'E	3850
171			17.57	57°21'S	17°23'E	5396
172		31.03.1996	00.14	57°23'S	17°12'E	4803
173			02.01	57°25'S	16°48'E	5327
174			03.34	57°27'S	16°26'E	5116
175			04.59	57°29'S	16°06'E	5351
176			06.33	57°30'S	15°46'E	5232
177			07.59	57°32'S	15°29'E	4965
178			12.20	57°32'S	15°29'E	5345
179			13.46	57°35'S	14°52'E	5655
180			14.56	57°37'S	14°34'E	4955
181			16.30	57°39'S	14°11'E	5607
182			18.00	57°41'S	13°49'E	5711
183			23.34	57°43'S	13°28'E	5513
184		01.04.1996	01.04	57°45'S	13°07'E	5655
185			02.27	57°47'S	12°48'E	5550
186			04.01	57°49'S	12°24'E	5506
187			05.38	57°51'S	12°02'E	5175
188			07.08	57°52'S	11°44'E	5609
189			15.55	57°54'S	11°22'E	5999
190			17.30	57°36'S	11°02'E	5379
191			19.01	57°58'S	10°46'E	5375
192			20.35	58°00'S	10°29'E	5570
193			22.11	58°01'S	10°12'E	5621
194			23.30	58°02'S	09°57'E	5589
195		02.04.1996	05.07	58°05'S	09°36'E	5501
196			06.24	58°06'S	09°18'E	5284
197			07.40	58°08'S	08°56'E	4947
198			08.45	58°10'S	08°38'E	4908
199			09.42	58°11'S	08°21'E	4440
200			10.42	58°13'S	08°04'E	3248
201			17.17	58°16'S	07°42'E	3998
202			18.29	58°17'S	07°20'E	4009
203			19.25	58°19'S	07°03'E	5004
204			20.31	58°20'S	06°45'E	5067

No.	Date	Time (GMT)	Latitude	Longitude	Depth (m)
205		21.56	58°22'S	06°26'E	5342
206		23.10	58°24'S	06°06'E	5143
207	03.04.1996	07.12	58°27'S	05°44'E	5172
208		08.07	58°28'S	05°27'E	5040
209		09.04	58°29'S	05°10'E	5331
210		10.00	58°31'S	04°52'E	5209
211		11.02	58°33'S	04°32'E	5445
212		12.13	58°35'S	04°10'E	5514
213		17.05	58°37'S	03°48'E	5083
214		18.14	58°39'S	03°22'E	5611
215		18.58	58°41'S	03°06'E	4722
216		19.55	58°43'S	02°45'E	4925
217		20.58	58°45'S	02°21'E	4983
218		21.55	58°47'S	02°01'E	4186
219	04.04.1996	02.38	58°48'S	01°43'E	4644
220		03.50	58°50'S	01°22'E	4734
221		04.50	58°53'S	01°02'E	5326
222		05.47	58°55'S	00°43'E	4028
223		06.47	58°57'S	00°22'E	3912
224		07.36	59°00'S	00°04'E	4459
225	05.04.1996	16.50	59°24'S	03°11'W	4765
226		18.00	59°13'S	03°11'W	4897
227		19.05	59°02'S	03°12'W	4994
228		20.18	58°52'S	03°12'W	5371
229		21.24	58°42'S	03°10'W	4017
230		22.28	58°32'S	03°09'W	4535
231		23.37	58°22'S	03°11'W	4978
232	06.04.1996	00.49	58°12'S	03°13'W	3723
233		01.00	58°10'S	03°13'W	4187
234		01.44	58°03'S	03°13'W	4656
235		02.52	57°53'S	03°13'W	3688
236		04.05	57°43'S	03°13'W	3653
237		05.04	57°33'S	03°14'W	3984
238		06.07	57°23'S	03°14'W	3788
239		07.12	57°13'S	03°14'W	3895
240		08.17	57°03'S	03°14'W	4022
241		09.26	56°53'S	03°14'W	3461
242		10.36	56°43'S	03°14'W	3325
243		13.20	56°33'S	03°14'W	3731
244		14.21	56°23'S	03°15'W	3774
245		15.26	56°13'S	03°15'W	2834
246		16.28	56°03'S	03°16'W	3616

No.		Date	Time (GMT)	Latitude	Longitude	Depth (m)
247			17.32	55°53'S	03°16'W	2812
248			18.36	55°43'S	03°16'W	4623
249			19.35	55°33'S	03°16'W	1834
250			20.42	55°23'S	03°16'W	3011
251			21.49	55°13'S	03°17'W	3154
252			22.58	55°03'S	03°17'W	3219
253		07.04.1996	00.06	54°53'S	03°17'W	2699
254			01.17	54°44'S	03°17'W	2542
255			02.22	54°35'S	03°17'W	2698
256			03.37	54°25'S	03°18'W	1812
257			13.55	54°19'S	03°13'W	2520
258			15.00	54°11'S	02°55'W	2302
259			16.01	54°03'S	02°38'W	2592
260			17.05	53°56'S	02°21'W	2157
261			18.03	53°49'S	02°04'W	2405
262			19.01	53°42'S	01°48'W	2457
263			20.03	53°34'S	01°31'W	2416
264			21.04	53°27'S	01°14'W	2318
265			22.02	53°20'S	01°00'W	2378
266			23.02	53°13'S	00°43'W	2505
267		08.04.1996	00.02	53°06'S	00°28'W	2554
268			01.03	52°59'S	00°11'W	2493
269			02.04	52°52'S	00°05'E	2684
270			03.03	52°44'S	00°22'E	2825
271			04.04	52°37'S	00°38'E	2725
272			05.02	52°30'S	00°53'E	2836
273			05.59	52°23'S	01°08'E	2635
274			06.57	52°16'S	01°24'E	2706
275			08.00	52°09'S	01°40'E	2766
276			09.00	52°02'S	01°56'E	2658
277			10.07	51°55'S	02°13'E	2817
278			11.04	51°47'S	02°29'E	3122
279			11.58	51°40'S	02°42'E	2843
280			12.58	51°34'S	02°57'E	2947
281			14.04	51°28'S	03°09'E	3490
282			15.01	51°23'S	03°21'E	3323
283			16.04	51°17'S	03°34'E	3318
284			17.05	51°11'S	03°46'E	3285
285			18.04	51°06'S	03°58'E	3585
286			19.02	51°00'S	04°09'E	3612
287			20.10	50°55'S	04°21'E	3474
288			21.10	50°49'S	04°34'E	2890

No.	Date	Time (GMT)	Latitude	Longitude	Depth (m)
289		22.23	50°43'S	04°45'E	3536
290		23.45	50°36'S	05°02'E	3389
291	09.04.1996	01.11	50°29'S	05°15'E	1208
292		02.13	50°25'S	05°24'E	2691
293		03.20	50°21'S	05°33'E	3639
294		04.50	50°15'S	05°45'E	3425
295	11.04.1996	11.54	52°15'S	03°25'E	3177
296		13.37	52°30'S	03°05'E	1437
297		14.52	52°40'S	02°53'E	2736
298		16.04	52°50'S	02°42'E	2602
299		17.26	53°00'S	02°29'E	2638
300		18.35	53°10'S	02°17'E	2718
301		19.50	53°20'S	02°05'E	2659
302		20.54	53°30'S	01°54'E	2595
303		22.27	53°40'S	01°40'E	2718

Data Processing Notes

Date	Contact	Data Type	Data Status Summary
04/15/97	Diggs	CTD	Submitted
			successfully retrieved files from ftp site
04/15/97	Witte	SUM/DOC	Submitted
			CTD tar files available on their ftp site ftp.awi-bremerhaven.de (login: anonymous)
04/28/97	Fahrbach	CTD/BTL	Data are NonPublic
			please password control
02/01/99	Witte	BTL	Submitted
			File available on ftp site
02/02/99	Witte	SUM/DOC	Update Requested by sd
			could you please re-submit the SUM file? It would seem as though the time parameters are always at 3,4 or 5 minutes past the hour. This could not possibly be correct. Also, do you have a more comprehensive documentation file than the one you provided?
02/04/99	Witte	SUM/DOC	Data Update
			will update sum asap & ask colleague for doc
02/12/99	Anderson	SUM	Reformatted by WHPO
02/12/99	Witte	CTD/BTL	Status Update
			protect by a password until the 31th of December 1999
02/12/99	Witte	SUM	Data Update
			I prepared a new SUM file and put it on your ftp server in the directory INCOMING. The name is ANTXIII_4.SUM.
02/12/99	Diggs	SUM	Data Merged/OnLine
			updated with the WOCE formatted sumfile
06/07/99	Klein	CFCs/He/Neon	Submitted for DQE
			Tritium not yet ready to submit
02/29/00	Anderson	SUM	Data Update
			I have reformatted and "corrected" the station/cast problem for s04a, but that isn't the only difference in the two .sum files (sr04e and s04a, 06AQANTXIII_4). Times and positions are different in the two files for the same station and cast in some cases. Also station 14 cast 3 does not appear in s04a (this may not be the only case) and s04a has what I think is the CTD # under COMMENTS, but sr04e does not.
03/01/00	Diggs	BTL	Data Update
			Changes:
			<ul style="list-style-type: none"> • Changed 06AQANTXIII/4 to 06AQANTXIII_4 • Moved STNNBR to align with the station numbers (right justification) • Added "QUALT1" header over the quality 1 flag fields • Added date/time stamp
			All tables and related HTML files have been updated accordingly.

03/01/00	Diggs	SUM	Data Update
	<p>I found the original, updated SUM file sent by Hannelore Witte 2/12/1999. It was not in WOCE format, and Sarilee received it and reformatted it on the same day. Witte sent a file that was different from the original in that the STN# is a combination of the Station# and Cast#. In any case, Sarilee apparently split these out into their original components, making the new sumfile match the bottle data files for SR04 (there wasn't ever one for S04A, even though they're the *same line*).</p> <p>I have reformatted this sumfile (again) to change the WOCE section number to be S04 instead of SR04, for consistency's sake. I am now combining the two lines into one, even though they will have separate representation on the Southern Onetime and Repeat tables. However, the onetime designation of the cruise will take precedence as is our custom here at the WHPO. The repeat listing will simply link to the onetime section.</p>		
03/15/00	Newton	CFCs/He/Neon	Data Merged/OnLine
	<p>Notes on merging CFCs HELIUM NEON in: 06AQANTXIII_4 S04 BTLNBR in 06aqantxiii_4_data.199906.hyd.txt is really SAMPNO.</p> <p>Following sta/cast were in new cfcHeNe file, but not in existing .hyd file or .sum file:</p> <p>2/1 104/2 105/1 106/1 107/1 108/1 109/1 110/1 111/1 114/1</p> <p>but 2/1 109/1 110/1 111/1 114/1</p> <p>contained entirely missing data values. pressure sequenced file and changed DELHE3 missing from -9 to -999.</p> <p>15 Mar 2000</p>		
05/19/00	Fahrbach	CTD/BTL	Data are Public
	<p>Possible errors, see note:</p> <p>I received several messages on different sections and did notice only afterwards that this was not a repeat, but referring to a different section.</p> <p>I think I had authorized you earlier to use our WOCE data openly and repeated now. I might be that my earlier statement referred only to some sections. This is now for all.</p> <p>However, I have a problem and would like your opinion. We only recently noticed that there was a problem with our FSI-CTD which did not show up in the lab calibrations. Therefore we had to reprocess all our data observed since 1995. This is now finally finished. The changes are less than a few mK and mPSU. I can not resubmit the corrected data before 1 June because my technician is seriously ill.</p> <p>What is your opinion:</p> <ol style="list-style-type: none"> 1. Could you check if the data was resubmitted recently? 2. If not, should we resubmit at all when he will return? 3. Do you want to include in the CD-ROM the present data? 		
11/01/00	Bartolacci	CTD/BTL	Website Updated; Data are public
	<p>As per Farhbach's clarification on 19/5/00 the bottle and ctd files for this cruise have been unencrypted and made public. All references have been updated to reflect this change.</p>		

05/07/01	Witte	CTD/BTL	Update Needed
	<p>the data of our cruise ANTXIII/4 I sent to WOCE in 1997 are wrong. There are some errors in the data of EXPOCODE 06AQANTXIII/4 WHP_ID SR4 CRUISE DATE 031796 TO 052096</p> <p>1. BOTTLE data:</p> <p>We got some questions about our nutrients data and when we compare the data of us with the data I sent to WOCE we see that the WOCE data are too small. When I checked them I found that the data must changed three times from mol/l to mol/kg.</p> <p>The CTD-data in the bottle file had the same error than the CTD-data.</p> <p>2. CTD-data:</p> <p>The CTD-data are processed with the PT1 temperature sensor which had had a hardware error.</p> <p>The new CTD data are processed with the PT2 temperature sensor.</p> <p>Please let me know what I shall do with the new cruise data and who must know about this mistake.</p>		
06/21/01	Uribe	BTL	Website Updated; CSV File Added
	Bottle exchange file was put online.		
06/27/01	Uribe	CTD	Website Updated; CSV File Added
	CTD exchange files have been put online.		
12/04/01	Diggs	CTD/BTL/SUM	Submitted
	<p>Data need to be merged, see note:</p> <p>new data submission from Hannalore Witte 06/18/2001 data need to be re-merged with existing online files.</p> <p>original/20010618.052257_WITTE_S04-SR04</p>		
12/26/01	Uribe	CTD	Website Updated; CSV File Added
	CTD has been converted to exchange using the new code and put online.		
01/03/02	Hajrasuliha	CTD	Internal DQE completed
	created *check file for this cruise.		
06/26/02	Coartney	DOC	Website Updated
	New text doc online.		
10/20/02	Kappa	DOC	Website Updated
	<p>Added complete text and pdf files of final cruise report, published by the Alfred Wegener Institute for Polar and Marine Research: D-27515 Bremerhaven - FRG. The tracer report that was previously online (submitted by Birgit Klein) is included in this final cruise report. The pdf version includes figures and links between the figures and tables and the relevant text passages.</p>		